Modelling of morphological development of the Vecht river due to changes in the weir policy

Report MSc Thesis Civil Engineering and Management

24 August 2023

A.V. (Lieke) van Haastregt

Witteveen+Bos   Drents Overijsselse Delta   UNIVERSITY OF TWENTE.

Colophon

This report contains the findings of the Master thesis research project of Lieke van Haastregt for completion of the Master Civil Engineering and Management at the University of Twente

Title	*Modelling of morphological development of the Vecht river due to changes in the weir policy*
Version	*Final*
Report size	*72 pages*
Location	*Deventer*
Date	*24 August 2023*
Author	*A.V. (Lieke) van Haastregt*
Student number	*S1938193*
Email-address	*a.v.vanhaastregt@student.utwente.nl*
	liekevanhaastregt@gmail.com
Supervisor University of Twente	*Dr. Ir. D.C.M. Augustijn*
	University of Twente
	Faculty of Engineering Technology
	Department of Coastal Systems and Nature-Based Engineering
Supervisor University of Twente	*Dr. V. Kitsikoudis*
	University of Twente
	Faculty of Engineering Technology
	Department of Coastal Systems and Nature-Based Engineering
Supervisor Witteveen+Bos	*Ir. S.J.H.A. Gradussen*
	Witteveen+Bos
	Sector Deltas, Coasts, and Rivers
	Department of Coasts, Rivers, and Land Reclamation
	Group Hydrodynamics and Morphology
Supervisor Waterschap Drents Overijsselse Delta	*Ir. G. Tromp*
	Waterschap Drents Overijsselse Delta
	Advisor Hydrology

Preface

This report marks the end of my time as an MSc student for the track River and Coastal Engineering at the University of Twente. Fitting for a thesis to mark the end of this study, is a research project into river morphology, which I have been working on for the past half year at the company Witteveen+Bos. Specifically, I have looked into the morphology of the river Vecht, and its dependence on the applied weir policy.

Although my studies have helped me to gain sufficient knowledge before the research project to get started on the thesis, actually diving into morphological modelling has made me learn a lot. Not only about the topics of modelling and morphology, but also about the complexity of the systems that we often try to mimic in the models. During this process of learning I have appreciated and enjoyed the supervision of Bas Gradussen, who did not mind spending time to help me with my modelling issues, from the side of Witteveen+Bos. Overall I enjoyed the time that I spent at Witteveen+Bos, for which I would also like to thank the other employees that were often interested in my results and that helped along the way.

Also the supervision of Gerben Tromp, from waterboard Drents Overijsselse Delta, was valuable. The Friday morning calls helped me to understand the complex river system that is the Vecht, but also the practical view and the implications of what I was doing found a place in these meetings.

Furthermore the involvement and insights of Vasilis Kitsikoudis, from the University of Twente, were helpful, often providing a theoretical background (and difficult questions at the same time) when interpreting the findings of the study. Also from the University of Twente I would like to thank Denie Augustijn, as chair of the graduation committee, who was very involved with the process. Starting from the set-up of the research project until the very end at the presentation of the thesis, his feedback and guidance were pleasant and helpful.

Lastly, I would like to thank my family and friends for the support they have given me during the past half year. Although there was not much besides this thesis that I could talk about, they have continued to listen to my findings and struggles, and they have encouraged me until I wrote these last words on paper. While my interest in the topic has not reduced during this research project (on the contrary, it has grown), I promise to talk about (modelling) river morphology a little less from now on.

However, since you are reading this report I expect there is a shared interest in the topic of (modelling) river morphology. Therefore I hope you will enjoy reading it as much as I enjoyed doing the research!

Lieke van Haastregt

August 2023

Summary

The River Vecht, located in the eastern part of the Netherlands, has previously been canalized by cutting of meanders, constructing weirs, and covering the banks with revetments. However, in the past thirty years a new vision has been formulated and measures have been taken to rebuild the Vecht into a semi-natural river as a result of river management practices focusing on the environmental wellbeing of the river system. The characteristics of such a semi-natural river include the presence of meanders and morphological activity in the sense that processes of deposition and erosion should be visible.

The current weir policy that is applied in the Vecht is based on maintaining target water levels, but this is non-fitting for a semi-natural river. The weirs block the flow of water and sediment, and a reversed seasonal water level variation is maintained where target water levels are higher in summer than in winter to prevent droughts. It was expected that an alternative discharge controlled weir policy could increase the flow through the river, and bring back appropriate seasonal water level variations. To investigate the impact of such a discharge controlled weir policy, several alternative weir policies were set up and their effect on the longitudinal morphology of the Vecht was evaluated based on morphological model simulations. These alternative weir policies consisted of opening the weir gates at a discharge of 50 m^3/s, 30 m^3/s, or always having the weir gates in the fully open position. The first two alternatives maintained a target water level if the discharge threshold (measured at one location in the river) was not met. The effect of the alternative weir policies on the morphology was compared to a reference scenario in which the current weir policy was applied.

The four scenarios (one per weir policy) were simulated for a period of 50 years with a 1D SOBEK 3 model of the Vecht. This model was adapted from a previous model of the Vecht to include the construction of several meanders and a new side channel. The bed roughness was calibrated and validated to increase and confirm the hydrodynamic accuracy of the model, as were the calibration parameter α (used in the Engelund and Hansen sediment transport formula) and the median sediment grain size for increased morphodynamic accuracy. The results of this calibration and validation process exhibit water levels that deviate less than 15 (30) cm from the corresponding measured water levels during both medium and low flow (high flow) scenarios. For the calibration and validation of the morphology a spatial validation was done, after which the simulated patterns of erosion and deposition were generally simulated well compared to observed patterns. Specifically, over a simulation period of nine years, the simulated bed levels deviated on average 40 (55) cm from the bed levels measured in the calibration (validation) section.

For all scenarios several morphological patterns were found, consisting of local deposition peaks upstream of the weirs, while both local and large-scale erosion were found downstream of the weirs. These changes were initial changes to the system, but also long-term changes were observed in the form of downstream propagating erosion and deposition waves, which were partially blocked by weirs. The magnitude of the peaks and pits was largest for the reference scenario and smallest for the scenario in which all weirs were fully open, whereas the propagation of the waves was blocked most by the former and least by the latter. A decrease in large-scale deposition upstream of the most upstream weir was found when comparing the alternatives to the reference scenario, with the fully open scenario having the largest decrease. Downstream of the weirs a large-scale decrease in erosion was found, which was again largest for the fully open weir scenario. Overall, the findings show that this last scenario leads to the most sediment transport in the Vecht.

While the local patterns and propagation of erosion/deposition waves agree with the existing literature, the large-scale change to increased deposition downstream of weirs differs from earlier research, where an overall decreased bed level was predicted. This difference can be caused by various factors, but more research is required to pinpoint what exactly causes this different outcome. Therefore it is unsure whether a discharge controlled weir policy contributes to the achievement of a semi-natural Vecht.

Table of content

1.   Introduction

The Overijsselse Vecht (hereafter called the Vecht) is a relatively small river which flows through Germany and the Netherlands. It is a river with a history of human interventions that have affected the surrounding areas on aspects such as nature, water safety, agriculture, and recreation. In the past 25 years, a paradigm shift has resulted in the aim to increase the morphological activity of the Vecht so that there is space for diverse ecological systems along the river. In this context, morphological activity has been defined as 'visible processes of erosion, deposition, and meandering' (explained in Section 1.1.2.). There are multiple interventions possible of which it is expected that they can contribute to the achievement of the above-mentioned aim, such as creating artificial meanders or increasing the flow velocity by adjusting the weir policy. However, for such interventions it is important to have at least a general idea about what their effects on the hydrodynamics and morphodynamics are before the interventions are implemented. This is because of the high societal and economic relevance of these interventions, since they impact various functions of the river.

This report presents a study into the effects of one of the possible interventions that can be done to increase the morphological activity of the Vecht. This specific intervention consists of adjustments in the weir policy that is currently maintained in the Vecht. An introduction to this intervention is provided in this chapter, after a description of the study area and the context of the research project. Furthermore, the research objective, research questions, and the scope of the study are described in this chapter. Lastly, a reading guide for the rest of the report is provided.

1.1.   Background

1.1.1.   Study area

With a length of 167 km, the Vecht flows from Rosendahl in Germany to the Zwarte Water near Zwolle in the Netherlands, draining an area of 3780 km^2 (Spruyt, 2021; Wolfert & Maas, Downstream changes of meandering styles in the lower reaches of the River Vecht, the Netherlands, 2007). For this research, the study area is limited to most of the Dutch part of the Vecht, taking the upstream boundary at Emlichheim just across the border in Germany, and the downstream boundary at the weir near Vilsteren (Figure 1.1). In this river stretch, which has a length of approximately 50 km with a bed fall of 10 m (Wolfert & Maas, Downstream changes of meandering styles in the lower reaches of the River Vecht, the Netherlands, 2007), there are five main lateral inflows with the Regge river being the largest one. From the German border until the point where the Regge flows into the Vecht, management of the river is controlled by waterboard Vechtstromen (WVS), whereas the downstream stretch is part of the area controlled by waterboard Drents Overijsselse Delta (WDOD). The median grain size of sediment in the Vecht is 0.325 mm (Wolfert et al., 1998), and most sediment is transported as suspended sediment (Lamers, 2017).
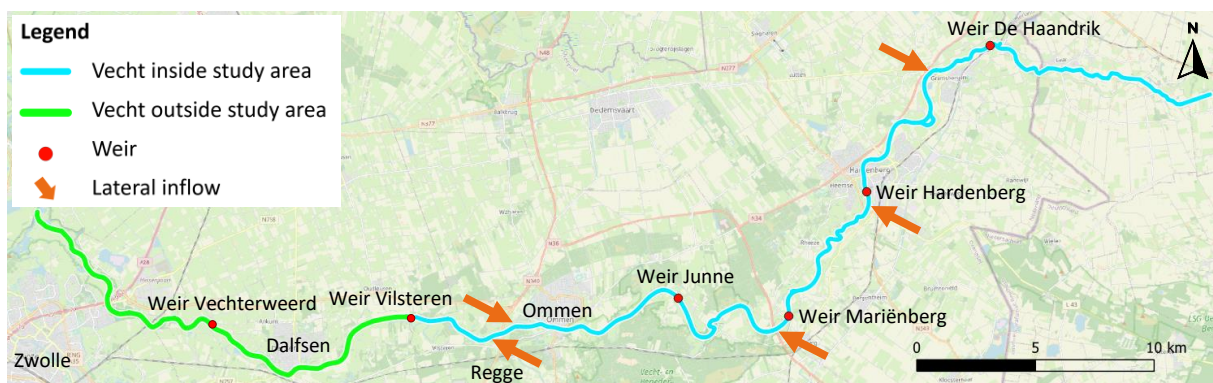

Figure 1.1. *Study area, including locations of weirs in the Vecht and main lateral inflows*

The discharge regime of the Vecht is characterized by precipitation runoff, with high discharges (100-200 m^3/s peak flow) during the winter and low discharges (<50 m^3/s peak flow) during the summer (Spruyt, 2021). The peak discharges along the river are shown in Figure 1.2 for several return periods. A discharge wave takes approximately 10 hours to travel through the entire study area, from Emlichheim to the weir near Vilsteren (Spruyt, 2021).
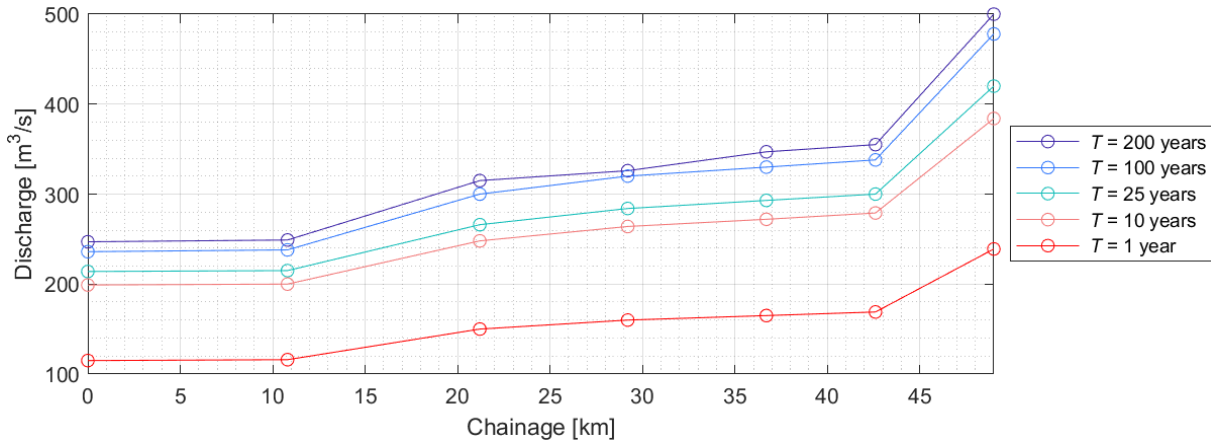

Figure 1.2. *Peak discharges at several locations along the Vecht (T = return period of discharge), adapted from Spruyt (2021)*

From the end of the 19th century until mid-20th century the Vecht was canalized, in order to discharge the water quicker so that the number of floods would reduce (Wolfert & Maas, Downstream changes of meandering styles in the lower reaches of the River Vecht, the Netherlands, 2007; Waterschap Vechtstromen, n.d.). The canalization resulted in 69 meanders that were cut off, thereby reducing the length of the river by 25 km (Wolfert & Maas, Downstream changes of meandering styles in the lower reaches of the River Vecht, the Netherlands, 2007; Spruyt, 2021). This led to a decrease in water depth along the river, which also resulted in channel degradation and lowering of the groundwater level in the surrounding areas (Wolfert & Maas, Downstream changes of meandering styles in the lower reaches of the River Vecht, the Netherlands, 2007). In order to prevent these effects of the canalization, many revetments were installed at the river banks and seven tilting gate weirs were constructed along the Vecht of which six have remained in use to date (Figure 1.3). Several characteristics of the weirs are shown in Table 1.1, which are the number and width of the weir gates, the maximum and minimum crest levels, the target water levels for winter and summer, and the weir location along the river from the most upstream point of the study area (chainage). The target water levels differ for winter and summer in order to ensure sufficient flow during dry summer periods (Helder et al., 2017). Of the six weirs that are still in the Vecht, only four are located within the study area, which are weirs De Haandrik, Hardenberg, Mariënberg, and Junne. However, for a better understanding of the Vecht as a complete system, weirs Vilsteren and Vechterweerd have been included in Figure 1.3 and Table 1.1.

Table 1.1. *Characteristics of weir gates taken from Spruyt (2021) and Duró et al. (2022). The target water level not in brackets is for the winter period, the value between brackets is the target water level for the summer period*

Weir	# of gates	Width per gate [m]	Max. crest level [m+NAP]	Min. crest level [m+NAP]	Target water level [m+NAP]	Chainage [km]
De Haandrik	2	10.5	9.17	6.96	9.10 (9.15)	10.8
Hardenberg	3	9.0	7.10	5.12	6.80 (7.10)	21.2
Mariënberg	3	9.0	5.77	3.88	5.30 (5.60)	29.2
Junne	3	9.0	4.51	2.67	4.15 (4.50)	36.7
Vilsteren	4	9.0	2.81	0.60	2.35 (2.65)	49.1
Vechterweerd	4	9.0	1.41	-0.90	1.00 (1.25)	> 49.1

Combined with the construction of locks in side channels around every weir (partially visible in Figure 1.3), the revetments and weirs have made that ships with a maximum draught of one metre can navigate the river between Zwolle and Ommen (Spruyt, 2021). Upstream of Ommen there is a maximum draught of 0.5 metre (Tromp, personal communication, 2023). Fish ladders have been constructed around the weirs, in order to limit the ecological impact of the weirs (some also visible in Figure 1.3).
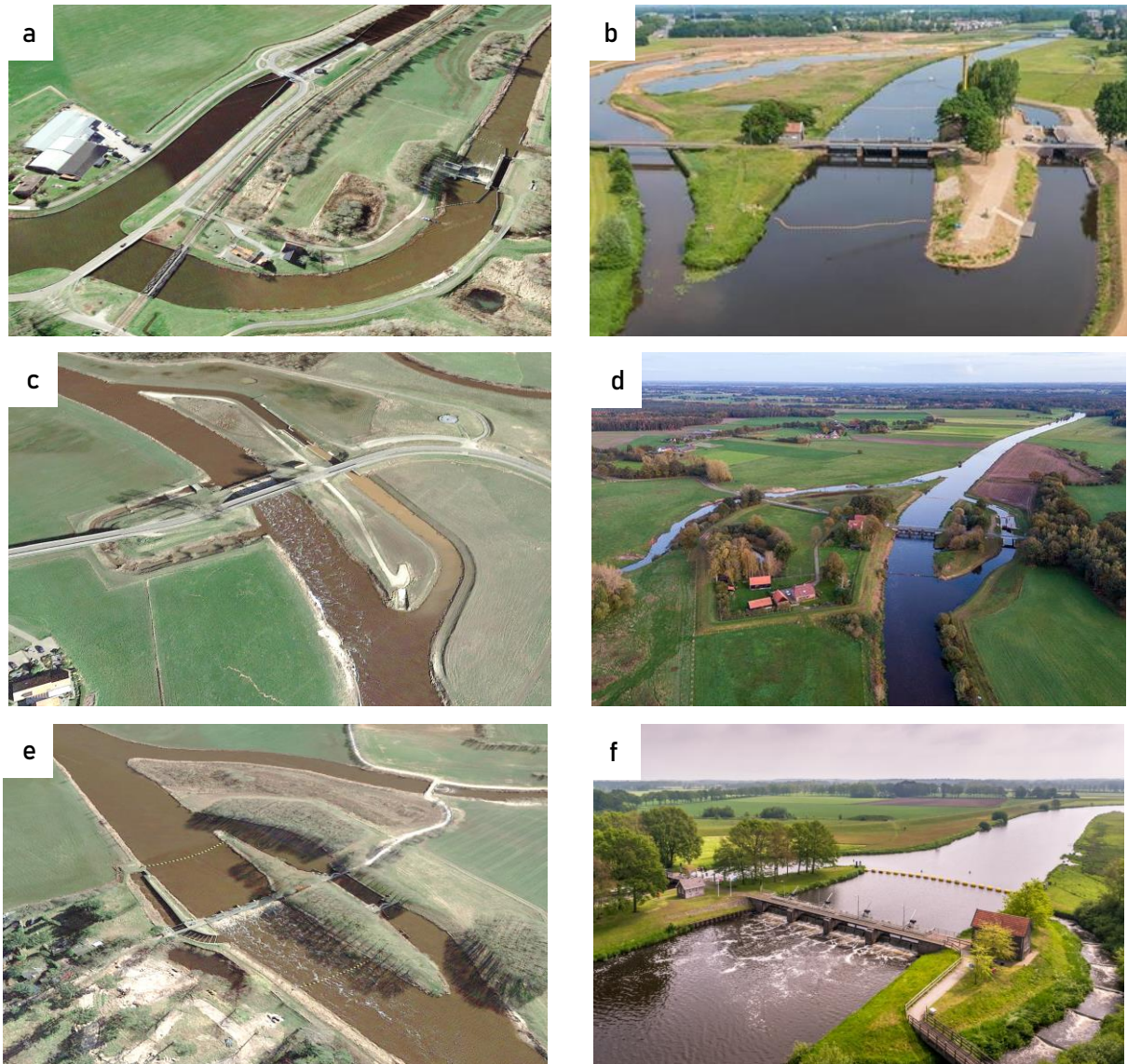
Figure 1.3. *Aerial overview of the weirs (a) De Haandrik (Google Earth, 2023), (b) Hardenberg (Waterschap Vechtstromen, 2021), (c) Mariënberg (Google Earth, 2023), (d) Junne (Bijzitter, 2019), (e) Vilsteren (Google Earth, 2023), (f) Vechterweerd (Waterschap Drents Overijsselse Delta, n.d.). All from downstream side except for (a), which is upstream side*

1.1.2. Recent developments concerning the Vecht

As mentioned at the start of this chapter there has been a paradigm shift concerning the management approach that is used for the Vecht, but also for other rivers in the Netherlands, due to the effects of climate change that have become increasingly noticeable (leading to increased peak discharges and longer periods of drought) and changing demands and wishes for the functions of river systems (DHV & NWP, 2009). For the Vecht the shift in thinking has developed in the past 30 years, resulting in many plans to reshape the river into a more natural one, to accommodate the peak flows and dry periods by creating extra space for the water during peak flows and retaining the water in this extra space for dry

periods. Instead of the canalized river with bank revetments and weirs hindering the natural flow, the aim is to get a semi-natural river, which means that it contains as few as possible man-made structures, it meanders, and it is morphologically active in the sense that there are visible processes of sedimentation and erosion (Waterschap Vechtstromen, n.d.; Helder et al., 2017). This morphological activity is desired to increase diversity in the ecosystems surrounding the Vecht, by creating a more diverse environment for flora and fauna than what is currently in place (Tromp, personal communication, 2023). This can result for example in plants settling on newly deposited sediments at an inner river bend, whereas these plants could not settle on the revetments that are currently in place at many locations. The aim is set to create a semi-natural instead of a fully natural river since complete removal of hard structures from the system (which would be required for a fully natural river) would lead to drainage of the river in the current situation (Helder et al., 2017).

Plans to elaborate on the abovementioned goals and interventions that are required to achieve them have been published and updated regularly between 1997 and 2020 (e.g. Ruimte voor de Vecht, 2020; Helder et al., 2017; DHV & NWP, 2009). Helder et al. (2017) conducted a study for WVS that assesses the visions that have been set up (more space for water combined with water safety, improvement of water quality, and adequate services for agriculture), and how these visions can/have become reality. Also it describes specific goals and conflicts for various functions and surroundings of the Vecht, such as water safety, nature, recreation, urban areas, and agricultural land, showing the societal and economic relevance of the river and interventions in it.

In total, 37 interventions have been done from 1999 until 2022 that have contributed to the transformation of the Vecht into a semi-natural river with more space for diverse ecosystems (Appendix B). These projects mainly consist of destoning river banks, construction of side channels, construction of sluices around weirs, and small-scale adaptations in floodplains (Tromp & Van der Scheer, personal communication, 2023). At the end of 2022 a (mostly) observational study was published, which looked into the effects of these interventions on the morphology in the Vecht (Duró et al., 2022). It was found that bank erosion occurs at locations where revetments have been removed and that the bed level has been increasing with one to two centimetres per year over the last fifteen years. Also a modelling study into the morphology of the Vecht and an observational study by WVS and WDOD found an average increase in bed level over time due to the many interventions (Lamers, 2017; Schmidt & Lips, 2017). It is expected that this increase in bed level will continue until a dynamic equilibrium situation is reached, which is expected to take approximately 100-500 years after the last intervention has been implemented, but only if no further interventions are done (Duró et al., 2022).

Even though the interventions contribute to visible processes of erosion and deposition in the river (Duró et al., 2022), it is important to increase the morphological activity further. If there is morphological activity, the river does not have to depend on artificial measures to increase meandering and to become a more diverse system in terms of habitat services, since there are already inherent processes of both erosion and deposition that contribute to the achievement of these things. However, currently the presence of weirs in the Vecht limits the morphological activity required for the Vecht to become a semi-natural river (Helder et al., 2017). Another aspect that is non-fitting for a (semi-)natural river is that the current weir policy results in a reversed seasonal water level, with higher water levels in summer than in winter. This is because the current weir policy is based on controlling the water levels, which means that the gates are opened or closed to maintain a constant water level, and this water level target is set higher in summer than in winter to prevent droughts (see Table 1.1) (Duró et al., 2022).

1.1.3.   Weir policies and their effect on morphology

The six weirs in the Vecht affect sediment transport through blockage of sediment, or by creating flow velocity differences between locations up- and downstream of the weir through blockage of water (thereby affecting the sediment transport capacity of the flow). Research has shown that the presence of weirs leads to increased bed levels upstream of the weirs, and decreased bed levels downstream of the weirs (Nguyen et al., 2015; Ni et al., 2021; Zhang et al., 2008; Ohmoto & Une, 2018). However, only the studies of Nguyen et al. (2015) and Ni et al. (2021) concern the effect of movable weirs instead of fixed weirs. Both studies used a 2D morphological model to find the effect of alternative weir policies on the local morphology around weirs, where Ni et al. (2021) looked at a system with cascade weirs and Nguyen et al. (2015) looked at a single weir. It was found in both studies that most change in the bed occurred when the gates where fully opened, i.e. flat on the river bed (Nguyen et al., 2015; Ni et al., 2021). In those scenarios where the weirs were fully opened, less deposition was found just upstream of the weirs, but the erosion pit downstream of the weir did not disappear. Based on these studies several alternative weir policies were thought of that could increase the morphological activity of the Vecht and thereby contribute to the transformation of the Vecht into a semi-natural river. These alternative weir policies, which were already suggested by Wolfert et al. (2009) and by Helder et al. (2017), are to remove the weirs, change the target water levels, or change to a discharge controlled weir policy.

In practice the removal of weirs is not viable, since this intervention would lead to decreased water levels and consequently detrimental effects for navigability of the river, nature, and agriculture (Helder et al., 2017; Zhang et al., 2012; Sumida et al., 2014). A limited adjustment of the target water levels is a viable option, the adjustment depending on various functions of the Vecht, but this does not increase the flow in the river to the extent that is required to increase erosion (and deposition) as much as is needed for more ecosystem diversity in the river (Helder et al., 2017). An alternative that is better suited for a semi-natural river is a discharge controlled weir policy, which means that opening of the weir gates depends on a discharge threshold, instead of a water level threshold. If the discharge threshold is not met, the water level controlled weir policy can be maintained so that the river does not drain. Although discharge is related to the water level, the implementation of a discharge controlled weir policy as proposed in this study leads to a more frequent opening of the weir gates than the current water level controlled weir policy (see Section 3.4.).

A small qualitative exploratory study into the morphological effects of applying such a discharge controlled weir policy in the Vecht has been done by Duró et al. (2022). In this study it was found that with the adapted weir policy water levels decrease along the entire river during the time the weirs are opened, and increased bank and bed erosion upstream of the weirs were predicted. The study did not use morphological simulation results, but based its qualitative analysis on the theory that removal of weirs in a hypothetical river with cascade weirs leads to a reduced water level throughout the river, which in order to maintain an equilibrium should lead to lower bed levels in the entire river (Duró et al., 2022). Due to the limited scope and the lack of morphological model results for this analysis, it was recommended to do further research into the effects of changes in the weir policy on the morphology of the Vecht with a morphological model.

1.2.   Research gap

The previous sections highlight the aim for increased morphological activity in the Vecht in the form of visible processes of sedimentation and erosion. A way to increase the morphological activity in the Vecht is to reduce the impact of the weirs on flow and sediment transport throughout the river. In order to prevent the river from draining, a weir policy should be applied that increases the flow, but

keeps sufficient water in the system. A possible weir policy could thus be a discharge controlled weir policy (Helder et al., 2017).

It is known that the presence of weirs leads to upstream bed level increase and downstream erosion pits (Zhang et al., 2008; Ohmoto & Une, 2018). It is also known that erosion occurs upstream of the weirs if the weir gates are fully opened, but the erosion pit downstream of the weirs does not necessarily disappear (Nguyen et al., 2015; Ni et al., 2021). Based on this literature it is expected that similar behaviour will be observed if a discharge controlled weir policy is implemented in the Vecht. However, for such a weir policy the exact morphological impact on the Vecht is unsure, especially since no quantitative research was done on the impact of such weir policies on the global (longitudinal) morphology in rivers (Duró et al., 2022). Therefore this research contributes to the existing literature concerning the morphological impact of movable weirs in a river system, by providing insight into the response of such a river system to various weir policies based on a morphological modelling study.

1.3.   Research objective and research questions

As explained in Section 1.1., there are currently many (potential) morphological developments in the Vecht, largely due to human interventions in the river. Since there is an aim to increase the morphological activity in the river in the sense of visible erosion and sedimentation processes, it is desired to continue doing interventions that contribute to the achievement of this aim. However, for some interventions, such as the potential alteration of the weir policy, it was unclear what the effect on morphological developments would be. Combined with the fact that an up to date model to look into morphological development was not available at the start of this research project, the aim of this research project was two-fold: first to set up a reliable and accurate morphological model of the Vecht, which could then be used to find the effect that changes in the weir policy have on the morphology of the Vecht.

In order to achieve this objective and guide the research, three research questions were set up that divide the research into two parts. Eventually, both parts contribute to the answering of the main research question, which was:

What is the expected effect of changes in the weir policy on the longitudinal morphology of the Vecht, based on morphological model simulations?

Firstly, a reliable and accurate model had to be set up to do simulations where changes in the weir policy could be taken into account. To find how reliable the results of this model are, the following sub-question was set up:

1) How well does the morphological model of the Vecht perform after it has been adjusted and recalibrated to take into account recent interventions in the Vecht?

Secondly, the simulations could be done with the model that had been set up in the first part of the research. To determine which effects are caused by the changes in weir policy and which changes are autonomous (based on recent interventions other than changing the weir policy), a reference scenario was simulated followed by simulations of various new weir policies. To guide this part of the research, the following two sub-questions were set up:

2) What is the expected short- and long-term morphology of the Vecht, taking recent interventions in the Vecht into account?
3) What is the expected short- and long-term morphology of the Vecht, taking both recent interventions and various scenarios for changes in the weir policy into account?

The methodology that was used to answer these questions is explained in chapter 3.

1.4.   Scope

This research project is an exploratory study into the longitudinal morphological development of the Vecht. Since it is an exploratory study, the choice was made to focus only on the longitudinal morphology and neglect variations in width direction.

For the spatial scale the choice was made to limit the study area from the upstream boundary in Germany (Emlichheim) to the downstream boundary at weir Vilsteren. This area is large enough to find the morphological effects of the adjusted weir policy in different sections of the river, which means that the findings in these sections provide sufficient information for an exploratory study.

For the temporal scale a period of 50 years of morphological developments was used. This period was judged to be sufficiently long to find initial changes in the system due to interventions, and also to find trends towards a (dynamic) equilibrium situation.

Lastly, several scenarios were set up in such a way that they are expected to cover the full range of possible morphological impact on the system, so that a complete picture of the morphological effects of changes in the weir policy is provided.

1.5.   Reading guide

This report is structured in seven chapters that provide an introduction to the research project (this chapter, chapter 1), detail the theoretical background of the study (chapter 2), explain the methodology that was used to do the research (chapter 3), present the results of the model calibration and validation, and the results of the long-term simulations (chapter 4 and 5), discuss the results of the research (chapter 6), and provide an overall conclusion of this study and several recommendations for further research (chapter 7).

To ease the reading process, the meaning of several abbreviations and specific terms that are used in this report are listed in Appendix A. The other appendices contain a list of interventions that have been done in the Vecht from 1998 until 2022 (Appendix B), morphological equations that are used in morphological models (Appendix C), an explanation about the set-up of the used discharge time series (Appendix D), hydrographs of the discharge time series that were used for the various model runs (Appendix E), details about the set-up of the controllers that were used to control the weir positions (Appendix F), and lastly the results of the hydrodynamic calibration runs (Appendix G).

2. Theoretical background

There is some relevant theoretical knowledge that is required to understand the methodology that is used to answer the research questions. This knowledge is explained in this chapter and concerns some general concepts regarding the topic of morphological modelling, the inclusion of movable weirs in morphological models, and knowledge about morphological modelling of the Vecht.

2.1. Basics of morphological modelling

Getting information about the morphological behaviour of river systems is difficult, due to the large temporal and spatial scales that are often involved. Observational data about such systems is therefore limited, and research is often focused on small-scale experiments and modelling studies (Wang & Wu, 2004; Sumida et al., 2014; Nguyen et al., 2015; Ohmoto & Une, 2018). While there are certain disadvantages to the use of morphological models compared to field experiments, such as the requirement of high computational power and the fact that models are always an approximation of reality, there are numerous advantages to modelling studies compared to field studies. A benefit of using morphological models over laboratory or field experiments is, for example, the opportunity to mimic the large temporal scale with the use of morphological scaling factors, which reduce the required time to generate the desired results (Nguyen et al., 2015). Besides, there are no issues with differences in spatial scale in models, while there can be issues related to this in physical experiments. Lastly, an advantage of a modelling study is the opportunity to isolate certain interventions or factors that affect the morphodynamics of a system (such as the weir policy that is used in the river), without having to set up many physical scale models.

For river modelling studies, often a numerical modelling approach is used instead of an analytical modelling approach, the difference being that numerical models solve discretized equations iteratively to approximate the behaviour of a system and analytical models solve equations directly to obtain exact solutions (Williams et al., 2016). Numerical models are often used because both the (morphological) processes that occur in the modelled systems and the systems themselves are very complex, thereby making it difficult to use an analytical model. When using a numerical approach, the choice can be made to use either a 1D, 2D, or 3D physics-based model (Williams et al., 2016). Since the choice was made to use a 1D model for this study, this chapter focuses mostly on the state of the art of 1D morphological modelling.

A physics-based 1D numerical model assumes width-averaged variations in bed level, and width- and depth-averaged flow processes over the longitudinal profile of a river stretch, contrary to a 2D model, which assumes only depth-averaged flow processes, and a 3D model, which does not average in any direction (Williams et al., 2016). When simulating morphodynamics, the 1D model first predicts water levels and flow velocities with the Saint-Venant equations (also known as the 1D shallow water equations, Equation C.1. Appendix C), then solves the sediment mass continuity equation (Equation C.2, Appendix C), updates the bed levels (often using the Exner equation, Equation C.3, Appendix C), and finally repeats the cycle for each time step (Williams et al., 2016). Equations that are often used to calculate sediment transport in physics-based morphological models are the empirical formula of Engelund and Hansen (used in this study, Equation C.4, Appendix C), the empirical formula of Meyer-Peter and Muller, and the empirical formula of Van Rijn. Since many sediment transport equations are empirical, based on lab and field experiments, they can only be used for specific sediment types that differ for example in load type (suspended - flowing across the entire water column, bed - flowing over the bed, and mixed - both suspended and bed load) or in grain size, or for certain flow conditions (Yang & Huang, 2001). For the applicability of the Engelund and Hansen sediment transport formula, a

median grain diameter of the sediment of 0.19-0.93 mm is required, as well as a Shields parameter of 0.07-6 and the main load type is suspended sediment (Kitsikoudis & Huthoff, 2021).

2.2. Movable weirs in morphological models of small–scale river systems

As mentioned in Section 1.1.3., weirs affect the morphology of a river in several ways. It is therefore important to include the presence of weirs in morphological models. There are several types of weirs, and while little research has been done into the presence or removal of fixed weirs, even less studies have included movable weirs in morphological models (Ni et al., 2021). For movable weirs the position of the gates depends on certain rules, based on e.g. the discharge or water level that is measured at a point along the river, or a given time interval during which the gates of the weir open or close. In terms of morphological effects of the weirs the difference between movable and fixed weirs is mainly that fixed weirs hinder the flow of sediment more than movable weirs. The reason for this is that the crest level of a movable weir can be reduced, while this cannot be done for a fixed weir. A lower crest level has proven to reduce flow velocities less than a higher crest level, and a lower crest level generally leads to smaller local bed forms such as deposition peaks upstream of the weir and erosion pits downstream of the weir (Zhang et al., 2008; Ohmoto & Une, 2018). Bed features caused by the presence of a weir are therefore expected to be larger around fixed weirs, compared to movable weirs with the same crest level.

For the inclusion of movable weirs in a model, a coupling needs to be made between the hydrodynamic part of the model (which simulates the water depth, flow velocity, and discharge), and the part of the model that controls the position of the weir gate. Depending on the software that is used, this coupling can be done in different ways. Aspects to take into account for this are for example which parameter(s) the gate position depends on, and the frequency of the coupling between the model parts (Deltares, 2019a). In the software that will be used for this study (SOBEK 3), the coupling is made using a Real Time Coupling (RTC) module (see Section 3.1.).

2.3. Morphological modelling of the Vecht

At the start of this research project only one morphological model of the Vecht was available, which was a 1D SOBEK 3 model. In the Netherlands, SOBEK 3 has often been used for studies into the morphology of rivers. The morphological component of SOBEK 3 can only be applied to 1D model schematisations, thereby limiting the detail of the simulated results. The available morphological model was set up by Lamers (2017) as part of a MSc thesis research project, and it built upon several existing SOBEK 2 models that were previously developed by WVS (Lamers, 2017). The schematised area is based on the Vecht as it was in 2012, and it is limited to the area shown in Figure 2.1-a, from Emlichheim (upstream) to weir Vilsteren (downstream). The schematisation is a simplification of the Vecht in the sense that it is a 1D model and several fish ladders and lateral inflows that were judged to be insignificant are not included. An RTC module is included in the model, in which the movement of the weirs is controlled by proportional-integral-derivative (PID) controllers so that a target water level is maintained (further explained in Section 3.1.4.). The sediment transport formula that is used by the morphological component is the Engelund and Hansen formula (Equation C.4, Appendix C), which was chosen based on the range of applicability of the formula (Lamers, 2017).

The water levels in the model were calibrated by adjustment of the bed roughness, and the morphology of the model was calibrated by adjustment of the calibration parameter α (which is part of the Engelund and Hansen formula, see Equation C.4, Appendix C) and the sediment inflow at the upstream boundary. For the calibration and validation data was used that consisted of discharge measurements, water level measurements, and bed level measurements from 2008 until 2013

(Lamers, 2017). The calibration and validation resulted in an approximated average error of 8 cm for simulated water levels and 38 cm for simulated bed levels. These error values are judged to be reasonable for a 1D morphological model. However, it was later found that part of the bed level measurements that were used to calibrate and validate the morphology of the model contained a systematic measurement error (Duró et al., 2022), which reduces the reliability of this model.

Besides this one morphological model, two hydrodynamic models of the Vecht exist. These are a 1D SOBEK 3 model that has been set up by Van der Mheen et al. (2015) and a 2D Delft3D FM model that has been set up by Spruyt (2021). Both of these models have schematised a larger part of the Vecht than the morphological model that was set up by Lamers (2017), since they cover the area from Emlichheim (upstream) to the Ramspolbridge (downstream) (Figure 2.1-b,-c). Both of these models have an RTC module for the weir movement, where the weir gate position is also controlled by PID rules, similar to the model that has been set up by Lamers (2017). The 1D model that was set up by Van der Mheen et al. (2015) overestimates the water levels along the river on average by approximately 30 cm during high flow conditions (Van der Mheen et al., 2015), while the 2D model that was set up by Spruyt (2021) simulates water levels with a deviation of just 1-4 cm compared to observed water levels for a wide range of flow conditions (Spruyt, 2021). One exception for the latter is found at a high water event from 1998, for which the simulated water levels deviate on average with 12.6 cm compared to the observed water levels. Based on this, it is judged that the 2D model simulates water levels along the Vecht most accurately of all three models of the Vecht.

The schematisation of the 1D model that was set up by Van der Mheen et al. (2015) is very similar to the schematisation of Lamers (2017). However, while the latter has a more detailed bed level schematisation (i.e. a higher density of profile definitions along the river), the schematisation of the first represents a more recent state of the Vecht (2014 compared to 2012). Comparing all three models, however, the 2D model that was set up by Spruyt (2021) has the most detailed and up to date schematisation (2019 state of the Vecht).
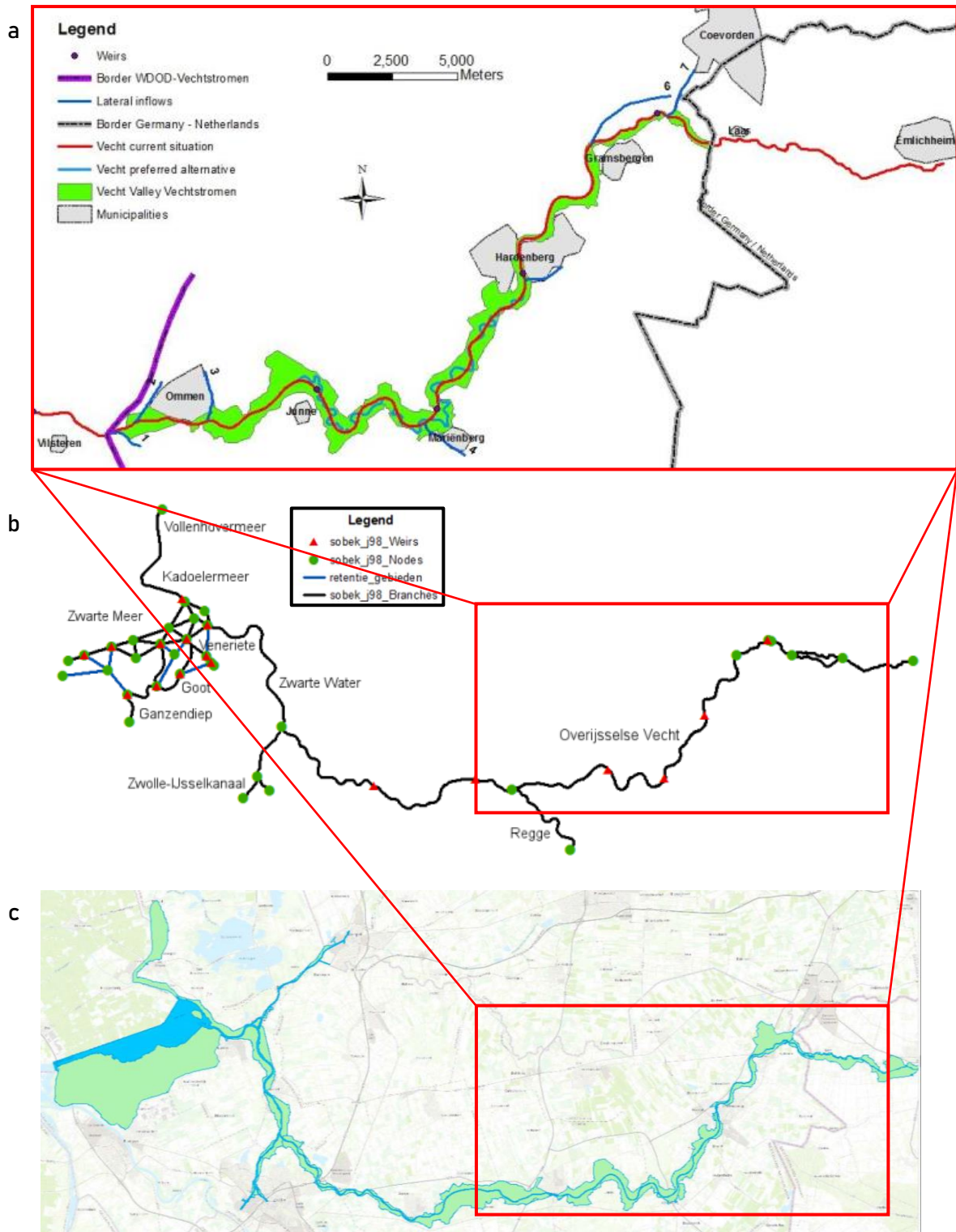
Figure 2.1. *Overview of areas covered by the (a) 1D SOBEK 3 model set up by Lamers (2017), taken from Lamers (2017), (b) 1D SOBEK 3 model set up by Van der Mheen et al. (2015), taken from Van der Mheen et al. (2015), and the (c) 2D Delft3D FM model set up by Spruyt (2021), taken from Spruyt (2021). Red boxes in (b) and (c) enclose the area schematised in (a)*

3.   Methodology

In order to answer the research questions, the methodology as schematised in Figure 3.1 has been used. Figure 3.1 has been divided into two parts, where part one focusses on the set-up of the model (research question 1), and part two focusses on simulations that are done with the model (research questions 2 and 3).

An elaboration of the schematised methodology is provided in this chapter, as well as a description of the SOBEK 3 model that has been used as a starting point for the first part of the research.
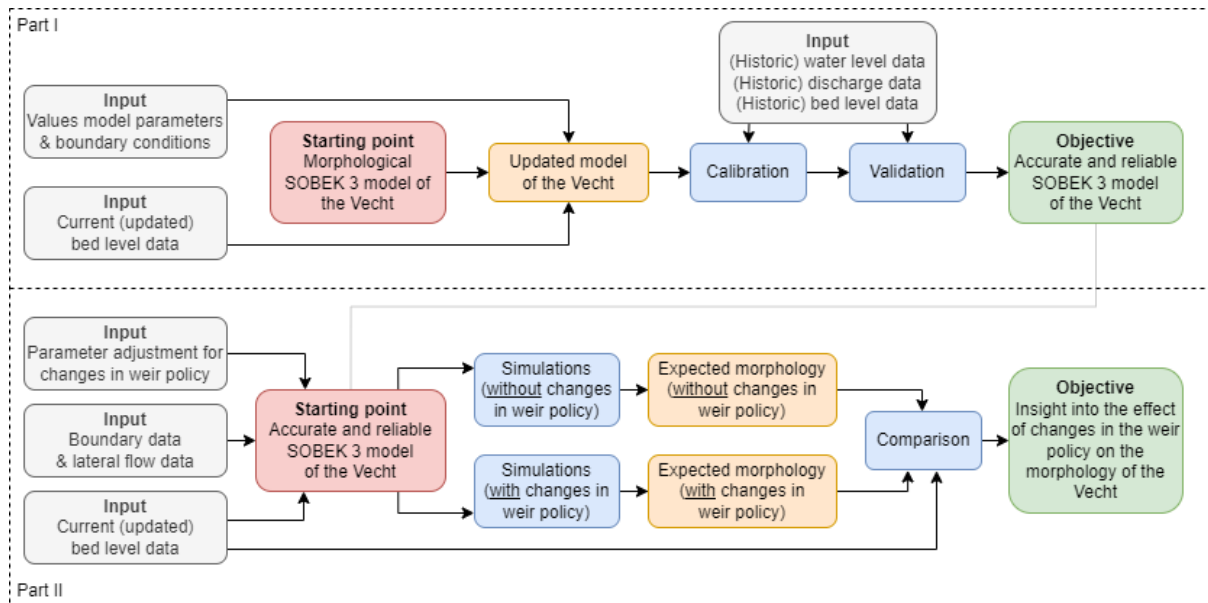

Figure 3.1. *Schematisation of research framework (grey boxes indicating input, red boxes indicating starting point, orange boxes indicating intermediate results/products, blue boxes indicating processes, green boxes indicating objectives)*

3.1.   Model choice and description

As a starting point for part one of the research, the morphological SOBEK 3 model that was set up by Lamers (2017) was used. The choice for this model was made since it can simulate morphology and has sufficient detail in the model schematisation to achieve the research objective. For a better understanding of the model set-up and to ease the interpretation of the simulation results in Chapter 4 and 5, this section further elaborates on the model schematisation, the flow module, the morphological component that is used, the set-up of the RTC module that is used, and how the different modules interact in the integrated model. As Section 3.2. explains, several adjustments were made to the model that was set up by Lamers (2017). In this section (Section 3.1.) the model set-up is described that was used for the rest of this study, which was the result of the adaptation of the model that was set up by Lamers (2017).

3.1.1.   Model schematisation

The trajectory of the river that is schematised in SOBEK 3 is shown in Figure 3.2. In this figure, the locations of the 336 ZW-cross sections (which define a depth-width relation at a point in the river, as explained in Section 3.2.1.) are visible that were used to define the geometry of the river on 91 different branches. The computational grid nodes (572 in total) are not visible in the figure, but they are located at every cross section, at the beginning and end of every branch, and two metres upstream and downstream of every structure (such as weirs and bridges). This placement results in a varying distance between the computational grid nodes. The location of twelve different weirs is also shown in Figure 3.2, the weirs being both movable weirs (at De Haandrik, Hardenberg, Mariënberg, and Junne,
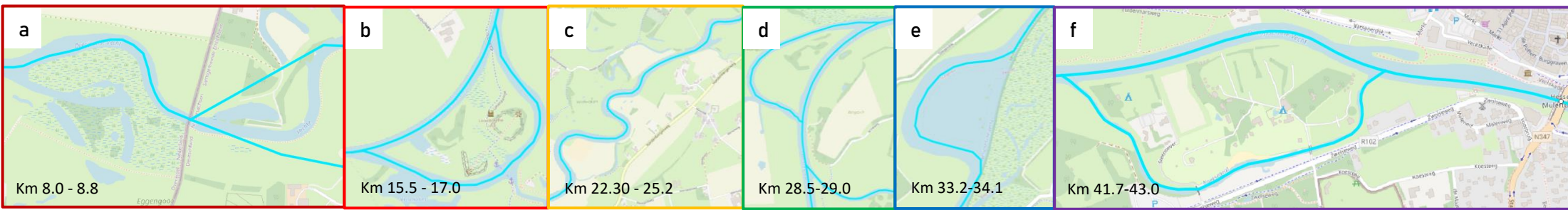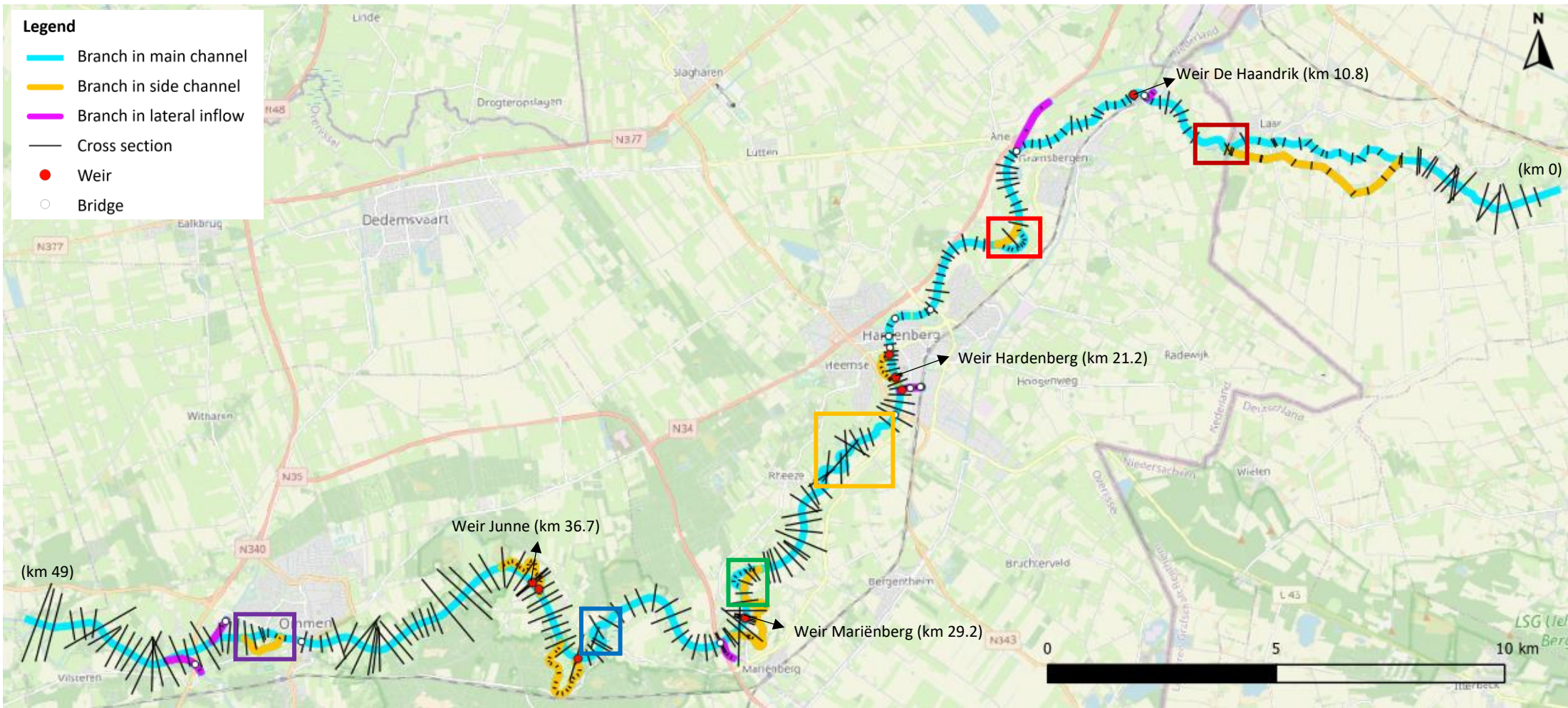
Figure 3.2. *Model schematisation including branches, all cross sections, weirs, and bridges. Coloured boxes highlighting location of interventions that have been newly implemented in the model and points of interest along the river: (a) Grensmeander and river bend near Laar (intervention/point of interest), (b) Loozensche Linie (point of interest), (c) Rhezermaten (intervention), (d) meander near Rheeze and entrance to side channel Mariënberg (point of interest), (e) meander near Karshoek-Stegeren (intervention), (f) side channel near Koeksebelt and widening of river near Ommen (interventions)*

the weirs this study focusses on) and fixed weirs. Most of the fixed weirs are located at the entrance of side channels and at the confluence of lateral inflows with the main channel. The four movable weirs are all located in the main channel, and they are schematised as compounds. This means that two weirs are located at the same location to form a larger structure (Deltares, 2019b). In this compound the gate position of the movable weir is controlled based on the weir policy, while the other is a fictitious fixed weir with a crest level equal to the average height of the floodplain. This approach allows flow through the floodplain once the water level reaches this crest level, thereby mimicking the flow of water through a floodplain past the movable weir. This set-up has been used before by Van der Mheen et al. (2015) and by Lamers (2017) as a workaround to simulate flow through the floodplain around the movable weir when the water reaches the bed level of the floodplain, which would not be possible in a 1D model if the crest level of the movable weir is higher than the bed of the floodplain.

3.1.2. Flow module

The model contains eight side channels and five lateral inflows, indicated in Figure 3.2. At the upstream boundary and at the lateral inflows, discharge time series can be used as hydraulic input, whereas the downstream boundary prescribes an *h(Q)* relation which is based on water level and discharge measurements at the upstream side of weir Vilsteren, which itself is not included in the model. The set-up of the discharge time series is explained in Appendix D, whereas the discharge time series that were used for the actual simulations are shown in Appendix E.

In SOBEK 3 the bed roughness can be prescribed per branch, and a distinction can be made between the bed roughness in the main channel and the bed roughness in the floodplains. The roughness in the main channel is defined by the Chézy friction coefficient (*C*), whereas the roughness in the floodplains is defined by the Strickler roughness coefficient (k_n), and the roughness in the side channels was defined by the De Bos and Bijkerk roughness coefficient (*γ*). This use of different bed roughness types was the same in the model that was set up by Lamers (2017) and remained unchanged (although the values for the Chézy bed roughness in the main channel were adjusted) since water level simulations performed reasonably well in that model (see Section 2.3.). The final bed roughness values that were used are shown in Section 4.1. (Table 4.1).

For the initial conditions of the flow module a restart file can be used that specifies the water levels and flow velocities at the start of the simulation for every grid node. With the use of a restart file no warm-up period is required, which reduces the computational time of the model. For the different simulation runs that were done for this study, different restart files were used. These were made by running the model for some time before the desired start time of the model. At the moment that the desired start time was reached, the model saved the water levels and flow velocities in a restart file.

3.1.3. Morphological component

The morphological component can be activated within the flow module of the model. Once activated, morphological boundary conditions should be specified, as well as the median grain diameter (D_{50}) and the sediment transport formula that is used. Depending on the desired settings, several other specifications should be given as well. In this model, the boundary conditions are formed by an upstream fixed bed level (at Emlichheim) and a free bed level downstream (at weir Vilsteren). Based on literature, the D_{50} was initially set at 0.325 mm before it was calibrated (Wolfert et al., 1996). The calibrated D_{50} value that was used for the evaluation of the different weir policies is given in Section 4.2. Since Lamers (2017) proved that the Vecht met the applicability criteria of the Engelund and Hansen sediment transport formula (specified in Section 2.1.), this sediment transport formula has also been used for this study in the updated model. The use of this formula requires the definition of the calibration parameter *α*, as can be seen in Equation C.4 in Appendix C, which was initially set at 1 before calibration. The calibrated *α* value is given in Section 4.2. Lastly, it was specified that updating

of the bed levels is activated after the first week, so that the sediment that is in the system would match the local flow conditions before morphological processes are activated. It was assumed that one week is sufficient for this, since it only takes ten hours for a discharge wave to propagate through the entire study area (Spruyt, 2021).

3.1.4. RTC module

The RTC module stands apart from the flow module and contains several control groups to adjust the position of structures in the model. For this model, a total of four control groups were set up that control the gate position of the movable weirs using PID controllers. These PID controllers calculate an error value between the set target water level and the simulated water level. To get this error as small as possible, the crest level of the weir gates is increased or decreased with a maximum speed of 0.001 m/s, with a lower height limit and an upper height limit specific for each weir, to accommodate for higher or lower discharges. The exact set-up of the different PID controllers is shown in Appendix F.

Similar to the flow module, a restart file can be used for the RTC module as well. Instead of information about the water levels and flow velocities, information in the restart file for the RTC module consists of the weir gate positions of the movable weirs. The restart files that were used for the initial conditions of the RTC module were set up similarly to the restart files of the flow module.

3.1.5. Integrated model set-up

For the different modules to successfully interact, a time step of the flow module is defined after which a coupling is made with the RTC module and the weir gate positions are adjusted. For all simulations that were done during this study this time step was set at 15 minutes. During this time step a water particle travels a maximum distance of approximately 900 metres (assuming a maximum flow velocity of 1 m/s). Since the distance between the different computational grid nodes is a few hundred metres on average, this time step is judged to be sufficiently small to keep the model stable. Morphological updating is also done every 15 minutes, since the morphological component was part of the flow module. No morphological scaling factor is used to speed up the morphological processes. Besides the time step for the interaction of the modules, a start and end time must be defined that is the same for both modules (start and end times used for all simulations are shown in Table 3.1).

Table 3.1. *Start and end time used for all simulations*

Simulation	Start time	End time	Total duration
Calibration (high flow)	20 February 2022	28 February 2022	8 days
Calibration (medium flow)	1 December 2021	7 December 2021	6 days
Calibration (low flow)	16 December 2021	23 December 2021	7 days
Calibration (morphology)	1 June 2013	1 March 2022	8.75 years
Validation (high flow)	25 February 2020	3 March 2020	7 days
Validation (medium flow)	10 January 2020	17 January 2020	7 days
Validation (low flow)	7 November 2019	14 November 2019	7 days
Validation (morphology)	1 June 2013	1 March 2022	8.75 years
Long-term morphology	1 October 2021	1 October 2071	50 years

3.2. Updating, calibrating, and validating the model

In order to obtain the model that is described in Section 3.1., several steps had to be taken to transform the available SOBEK 3 morphological model. In order to update the model, such as refining parts of the model that were schematised roughly in the original model, adjusting the trajectory of the river to include interventions that have been taken in the river after 2012, and updating of the bed levels to match the current bathymetry. After the model was updated, it could be calibrated and validated.

3.2.1. Updating the model

For the updated model, the trajectory of the river was first refined in parts where the network was schematised with so little detail that the curvature of the river was not followed by the branches in the model anymore. This was done to ensure that inaccuracies in the model would not lead to unreliable simulation results. The refinement was done by relocating several grid points and nodes.

Secondly, recent interventions had to be added to the model in order to make the model representative of reality at those locations, so that the measurement data for calibration and validation could be used. For this, it had to be determined which alterations had been made to the river since the SOBEK 3 model was set up. For each alteration, expert judgement was used to assess whether the alteration had significant effects. This was done so that the computational time would not increase unnecessarily, which would likely be the case if all interventions were implemented. For this step, WDOD and WVS provided a list of interventions they have done along the river from 1999 to 2022 (Appendix B, Tromp & van der Scheer, personal communication, 2023). Relevant interventions were judged to be the Grensmeander, Rhezermaten, the meander near Karshoek-Stegeren, and the side channel near Koeksebelt. The locations of these interventions can be seen in Figure 3.2. They were implemented in the model by altering the river schematisation, with an approach similar to the refinement of the trajectory described above, by adding a branch to the network reconnecting at (newly added) nodes on the main channel, and by adjustments of the river profiles defined by Lamers (2017). The difference before and after implementation can be seen in Figure 3.3-3.6.

Figure 3.3. *Grensmeander (a) before implementation (satellite), (b) after implementation (satellite), (c) before implementation (branches in model), and (d) after implementation (branches in model)*
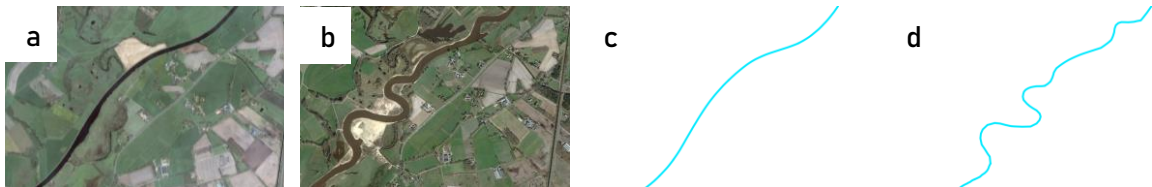
Figure 3.4. *Rhezermaten (a) before implementation (satellite), (b) after implementation (satellite), (c) before implementation (branches in model), and (d) after implementation (branches in model)*

Figure 3.5. *Meander near Karshoek-Stegeren (a) before implementation (satellite), (b) after implementation (satellite), (c) before implementation (branches in model), and (d) after implementation (branches in model)*

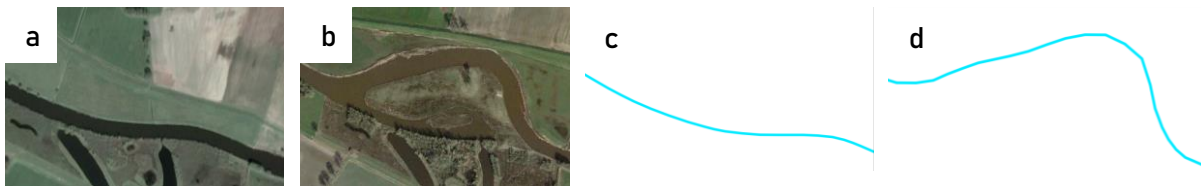**Figure 3.6.** *Side channel near Koeksebelt (a) before implementation (satellite), (b) after implementation (satellite), (c) before implementation (branches in model), and (d) after implementation (branches in model)*

As a last step towards the updated model, the profiles that were schematised by Lamers (2017) had to be updated. For this, multi-beam bed level measurements of the main channel were available from March 2022 on a 1x1 metre grid. For each location on the river network where a profile was defined in the model, the bed levels were taken from the bed level measurements. Since the profiles in the model are defined as symmetrical ZW-profiles (which is required for morphological calculations in SOBEK 3), while the profiles obtained from the bed level measurements were YZ-profiles (which define a depth-location relation), the profiles that were obtained directly from the bed level measurements had to be interpolated to form ZW-profiles (Figure 3.7). After the new ZW-profiles of the main channel were constructed, they were merged with the part of the existing profiles that defined the floodplains at each location, thereby forming an updated complete profile. The main channel profile was not updated near the weirs and in several side channels, since no bed level measurements were available at these locations. In order to still update the bed levels near the weirs, the profiles at these locations were replaced by the profiles defined in the 1D model that was set up by Van der Mheen (2015).
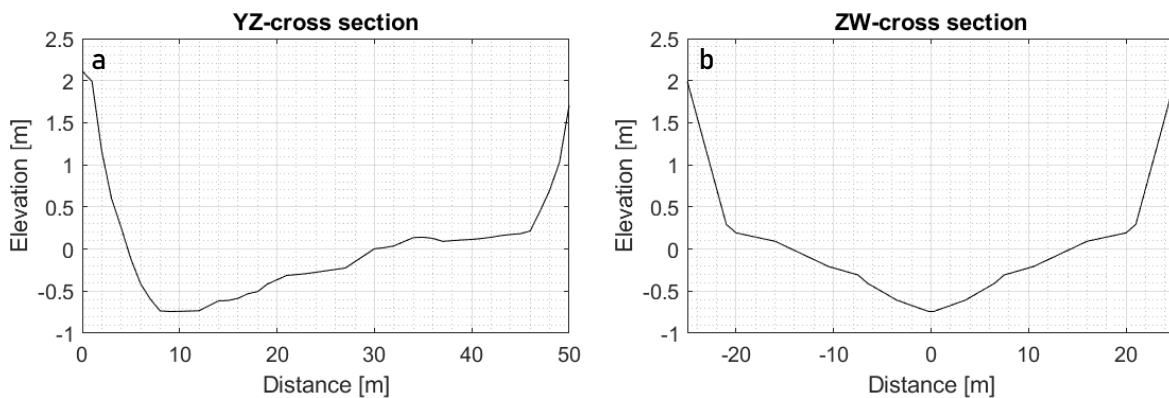

Figure 3.7. *Example of (a) a YZ cross section and (b) a ZW cross section, where (b) is interpolated from (a)*

The choice was made to use the floodplain bed levels that were schematised by Lamers (2017) and not update the floodplains in the profiles, since there was a broad interval for the time of measurement (somewhere between 2014 and 2019) of the available floodplain bed level data (publicly available satellite measurements from Algemeen Hoogtebestand Nederland (AHN)). Another reason to not update the bed levels in the floodplains was that it was judged that changes in the bed level of the floodplains occur so gradually that it is likely that there are no big differences between the current (real) bed levels and the bed levels in the floodplain in the model. Lastly, the main point of interest for this research is to find what the effect of changes in the weir policy are, where the changes in the weir policy are most noticeable for lower flow conditions (as explained in Section 3.4.). Since floodplains only flood during high flow conditions, it was expected that not adjusting the bed levels of the floodplain does not significantly alter the results of the research.

During the process of determining the new profiles, it was found that there were some profile definitions that seemed to contain an error, either in the floodplain or in the main channel (width). These profiles were first replaced by the profiles defined in the SOBEK 3 model that was set up by Van der Mheen et al. (2015) or adjusted manually, before the new main channel profile was added.

Lastly, the computational time of the model was reduced in several steps. It was found that the presence of structures in side channels (such as bridges, fixed weirs, and culverts) and branches including fish ladders increased the computational time significantly. However it was judged that they did not impact the morphology of the dominant flow path that much, since there is only a small part of the flow that is directed through these fish ladders and side channels. Therefore, most of the structures were removed from the side channels, and the branches containing fish ladders that were

included by Lamers (2017) were removed, thereby removing the lateral extraction and inflow from the fish ladders. At some locations, multiple cross sections were placed very close to each other in the original model schematisation by Lamers (2017) (<50 metre distance in between) without the cross sections having large variations. At these locations only one of the cross sections was kept in the model, which reduced the computational time. Finally, some simplifications were made in the network of the model when several branches were used to schematise flow into different parallel structures such as weir gates or culverts. In such cases only one branch was kept to convey all discharge and parallel branches were deleted, and the dimensions of the structure on the remaining branch were adjusted so that they matched the summed dimensions of all structures that were previously present (Figure 3.8 and Table 3.2). It was assumed that this adjustment had minimal impact on the longitudinal morphology, although local morphology (such as scour holes) could be affected slightly.
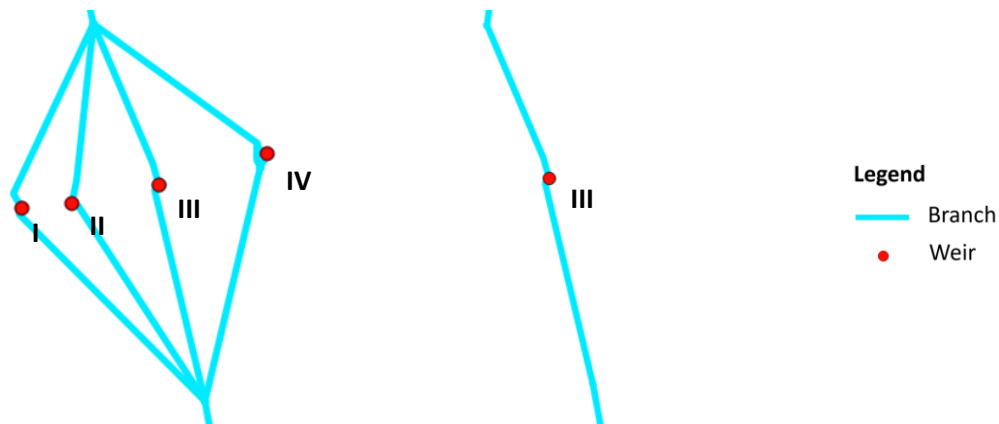

Figure 3.8. *Example of branch restructuring at the entrance of the side channel near Junne, with branch structure before adjustments (left) and after adjustments (right), weir dimensions given in Table 3.2*

Table 3.2. *Weir dimensions at the entrance of the side channel near Junne (Figure 3.8) before and after branch restructuring*

Weir	Before branch restructuring		After branch restructuring	
	Crest level [m+NAP]	Crest width [m]	Crest level [m+NAP]	Crest width [m]
I	4.6	2.6	-	-
II	4.6	6.5	-	-
III	4.6	6.5	4.6	30.5
IV	4.6	14.9	-	-

3.2.2. Hydrodynamic calibration

To calibrate the hydrodynamics in the model, simulations were done in which the Chézy value for the bed roughness of the main channel was uniformly varied from 28 to 48 m$^{1/2}$/s. These values were selected based on expert judgement of the realistic roughness values in the river system. The model set-up for the simulations was similar to the set-up described in Section 3.1., with bed levels from 2022. As input for the upstream and lateral boundaries discharge series were used, which were either based on measurements or generated using the lateral inflow generator (Randvoorwaarden Generator Water Modellen) provided by Deltares and Van der Scheer (personal communication, March 2023). The lateral inflow generator is a Python tool that generates discharge time series for a river system. Appendix D contains a detailed description of the set-up of all discharge series that were used as input. For the hydrodynamic calibration process the morphological component was deactivated to reduce computational time.

Simulations were done for three different historical periods with a duration of six to eight days (sufficiently long for a discharge wave to travel through the study area) in the winter of 2021-2022,

one of low flow (average discharge of < 15 m³/s), one of medium flow (average discharge of 20 m³/s), and one of high flow (average discharge of 85 m³/s, see Appendix E for hydrographs). For each simulation, the simulated water levels were compared to the water levels that were observed during the corresponding periods at the location of five measurement stations (at all weirs and at the Hessel Muelert bridge south of Ommen, visible in Figure 3.2) using the Root Mean Square Error (RMSE) value. The RMSE was used as an indicator since it does not decrease the total error by adding the positive errors to the negative errors.

The RMSE value for a specific location can be calculated using Equation 1:

$$RMSE = \sqrt{\frac{1}{n}\sum\nolimits_{i=1}^{n}\left(y_{s,i} - y_{o,i}\right)^2} \qquad \text{Eq. 1}$$

Where n is the number of simulated or observed values, $y_{s,i}$ is the simulated value of variable y (here water level [m]) at time step i and $y_{o,i}$ is the observed value of variable y. The closer the RMSE value is to zero, the closer the simulated water level is to the observed water level, thus the better the model performs in the simulation of water levels. The measured water levels were provided by WVS. The RMSE was calculated for the water levels simulated at each time step at a location, and an average RMSE of all locations together was calculated as well. This was done to see whether the model performed good or bad overall with the given parameters, or that there were specific locations where the performance of the model stood out either positively or negatively.

After the different RMSE values were calculated for the simulations with uniform Chézy coefficients along the main channel, another simulation was done for which Chézy coefficients were used that varied on branch-scale. The varying values were determined by looking at the location of each measurement station and choosing the Chézy coefficient that resulted in the best model performance at that location during simulations with uniform values, and interpolating the value between two measurement stations. The different flow scenarios resulted in different optimal Chézy coefficients, so the choice was made to base the varying values on the medium flow scenario. This was done since the medium flow scenario is the intermediate scenario, and since this flow regime eventually is the most important during the simulations of different weir policies (as explained in Section 3.4.). The Chézy coefficient values that were used for this final run are shown in Section 4.1. (Table 4.1).

After the RMSE values were calculated for the final calibration simulation, some simulations were done for high flow in which the bed roughness of the floodplains was adjusted to an extreme low and an extreme high value (Table 3.3), as was done for the bed roughness of the side channels. This was done to check the sensitivity of the flow through these parts of the system to the bed roughness. Although an effect was expected, the different simulation results showed little difference for varying bed roughness values in the floodplains and side channels, due to which the choice was made to keep the default values in the model. The same response to adjustments of the floodplain and side channel bed roughness was observed by Lamers (2017). A possible explanation for this could be that the discharge that was used for the high flow scenario only barely leads to flooding of the floodplains (Tromp, personal communication, 2023), due to which the effect of adjusted bed roughness values for the floodplains is not very noticeable.

Table 3.3. *Roughness values used for sensitivity check floodplains and side channels*

	Minimum value	Default value	Maximum value
Strickler k_n [m] (floodplain)	0.05	0.20	3.00
De Bos & Bijkerk coefficient [-] (side channel)	25	33.8	40

3.2.3. Morphodynamic calibration

To calibrate the morphodynamics in the model, simulations were done in which the calibration parameter α and the median grain diameter D_{50} were varied, according to the values shown in Table 3.4. These variables were initially chosen for calibration since they are both used in the sediment transport formula of Engelund and Hansen (Equation C.4, Appendix C, repeated below), they are meant specifically for calibration (α), and they provide insight into the physical working of the model (D_{50}). While a calibration based on adjustment of the upstream sediment inflow was also tried at first, similar to the approach used by Lamers (2017), it was found that the effect of variations in the upstream sediment inflow did not propagate downstream far enough to calibrate based on this variable.

Table 3.4. *Variations of calibration parameter α and median grain diameter D₅₀ used for runs of morphological calibration*

		D_{50}			
		50%	100%	125%	150%
	0.50		Run 1	Run 2	Run 3
	0.75		Run 4	Run 5	Run 6
α	1.00	Run 7	Run 8	Run 9	Run 10
	1.25		Run 11		

Equation C.4 (Deltares, 2019c) shows that there is a linear relationship between α and the calculated sediment transport rate (S), and an inverse linear relationship between D_{50} and S. Since there is no other inclusion of either α or D_{50} in the calculation of sediment transport this means that adjustment of one of these two variables with a certain factor can also be interpreted as an adjustment of the other variable with the inverted factor. If this logic was correct, the results for runs 1 and 6 should be equal, as well as runs 4 and 9, which was confirmed during the calibration process. Even though the adjustment of both variables is equal to the adjustment of just one of the variables with a different factor, the choice was made to continue with adjustment of both variables. This is since α covers variations in multiple variables (not just D_{50}), and since α does not have a physical meaning (it is just a calibration parameter), while D_{50} does have a physical meaning. By adjusting both, the understanding of the physical impact of the calibration was increased. Secondly, while the initial value of D_{50} (0.325 mm) was based on literature, this literature is a little outdated (Wolfert et al., 1998). Although no large changes in the D_{50} were expected over time, this uncertainty and the fact that there is a slight variation of the D_{50} in the longitudinal direction were also reasons for calibration of this variable.

$$S = \frac{0.05\alpha q^5}{\sqrt{g}C^3\Delta^2 D_{50}}$$

Eq. C.4

Where S is the sediment transport rate ($[m^2/s]$), α is a sediment transport calibration parameter ([-]), q is the flow velocity ($[m/s]$), g is the gravitational acceleration ($[m/s^2]$), C is the Chézy friction coefficient ($[m^{1/2}/s]$), Δ is the relative density ([-]), and D_{50} is the median sediment diameter ([m]) (Deltares, 2019c).

The period used for the calibration simulations ran from June 1st of 2013 until March 1st of 2022, covering a total time span of approximately nine years. This calibration period was used since the available bed level measurements consisted of data starting from 2013 until 2022, and since morphological processes such as bed level change take a long time to develop significantly compared to the original situation. Therefore, the simulation is preferably as long as possible when comparing simulated bed level to observed bed levels to increase the accuracy of the calibration. Taking the measurements of 2013 as a starting point and running the simulation until 2022 is judged to cover a period that is long enough to accurately calibrate the model.

For the model set-up used for the calibration simulations, the set-up as described in Section 3.1. was used, but with bed levels from 2013. The approach to set up these bed levels was the same as the approach described in Section 3.2.1., however the channel widths were not adjusted this time since overall there seemed to be little difference in the channel width between 2013 and 2022. As input for the upstream and lateral boundaries again several discharge time series were used, of which hydrographs can be found in Appendix E.

Since the morphological component of the model also had to be validated and only one data set was available, the decision was made to calibrate on a small part of the river (see Figure 3.9) and do a spatial validation with the rest of the river instead of a temporal validation. In this way the same bed level data set could be used for the calibration as for the validation, making the timespan for the simulation longer. The section of the river that was chosen for the calibration stretches from weir De Haandrik (km 10.8) to weir Hardenberg (km 21.2) and was selected based on the absence of large scale interventions in the calibration period that could affect the morphology in this section during the simulated time period. Also the choice was made to have weirs both at the upstream and downstream ends of the section to have clear boundaries.

For the calibration the RMSE was used to compare the simulated bed levels at the end of this period to the bed levels measured in March 2022, according to Equation 1 with variable y being the bed level (measured at the thalweg) and i being the location of the simulated/observed bed level (measured at the thalweg) instead of a point in time. The locations that were included for the calculation of the RMSE were all grid points located at a cross section (in the main channel) at which no interventions had taken place during the simulated period (Figure 3.9).
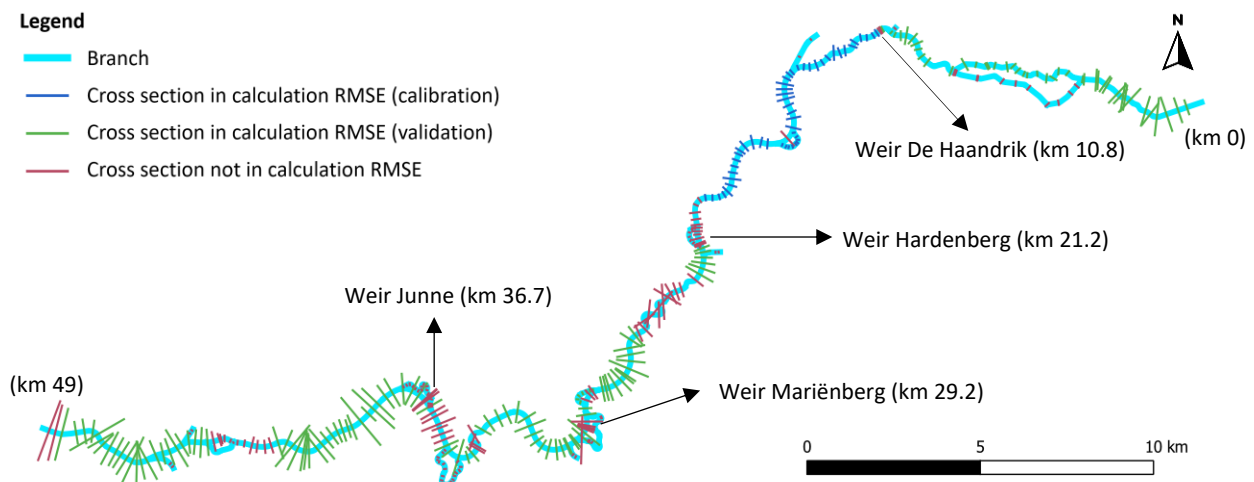

Figure 3.9. *Cross sections used in calculation of RMSE during morphodynamic calibration and validation, weir locations indicated by arrows*

After the RMSE values were calculated, the calibration coefficient α and the D_{50} were set to the values that gave the best morphodynamic performance.

3.2.4. Hydrodynamic validation

For the hydrodynamic validation the model was run for three different historical periods in the winter of 2019-2020, with the updated bed roughness in the model. The three periods were seven day periods of low flow (average discharge of 10 m³/s), medium flow (average discharge of 25 m³/s), and high flow (average discharge of 65 m³/s), similar to the calibration periods. For each simulation the RMSE values were calculated again with the same method as described in Section 3.2.2. using Equation 1.

For the set-up of the model the bed levels were adjusted to the bed levels measured in February 2019, since these bed levels were expected to match the actual bed levels in the simulated time period better than the bed levels used in the model that was used for the hydrodynamic calibration (containing 2022 bed levels). The discharge series that were used are shown in Appendix E. Again, the morphological component was deactivated to reduce computational time.

3.2.5. Morphodynamic validation

Although the morphodynamic calibration was done for just a small part of the river, the entire model was run for the calibration simulations. This meant that there were also simulation results for the rest of the river (excluding the calibration area), which could be used for the morphodynamic validation. Therefore the RMSE values were calculated for the best-performing morphological model set-up (during calibration), according to the method described in Section 3.2.3., for the part of the model that was not used for calibration (Figure 3.9). Again, the locations that were included for the calculation of the RMSE were all grid points located at a cross section (in the main channel) at which no interventions had taken place during the calibration/validation period.

3.3. Determining morphology due to recent interventions (reference scenario)

In order to determine the morphological effects of changes in the weir policy, first a reference scenario had to be determined in which no changes to the weir policy were implemented. Based on this reference scenario, the effects of changes in the weir policy could be (partially) isolated from the morphological effects of other (previous) interventions in the river system.

For the simulations of the reference scenario the model set-up was used as explained in Section 3.1. In the schematisation the bed levels of 2022 were used (the same bed levels that were used for the calibration of the water levels), and the calibrated bed roughness, calibration coefficient α, and median grain size D_{50} were implemented. The simulated time covered a period of 50 years. This time span was chosen since it was judged that 50 years is sufficiently long to differentiate between initial changes in the system and slower long-term changes towards an equilibrium situation.

Since there were no historical time series of 50 years long, the discharge series that were used as input for the simulation of the reference scenario were set up by duplicating the discharge series that were used for the morphodynamic calibration and validation several times, similar to the approach described by Gradussen and Blom (2020). The connection between the end of one repetition and the beginning of a new repetition was put at a time with low discharge, so that there would not be any discontinuities in the constructed time series. The duplicated time series started at 1 October 2013 and ran until 30 September 2021. This gave a total time span of eight years, so the series was repeated a little over six times. A hydrograph of the resulting discharge series can be found in Appendix E.

3.4. Determining morphology due to changes in weir policy

In order to determine what the effects of changes in the weir policy are on the morphology of the Vecht, it first had to be determined which changes in the weir policy would be made. To ease the decision-making process for the set-up of the different weir policy scenarios, first exploratory meetings were held with employees of WVS and WDOD to determine the general idea of new weir policies. These weir policies were used as a starting point and were finetuned with the help of literature and feedback of the same experts.

The current water level controlled weir policy often leads to the opening of the weir gates at a discharge of roughly 70 m³/s (measured at Ommen), so the idea was to increase the flow by opening the gates at lower discharges. In order to determine how often the weirs are opened if the current

weir policy is maintained, an empirical cumulative distribution function (ECDF) of the discharge at Ommen was set up for the period between 31 January 2002 and 1 January 2014 (Figure 3.10). This period was chosen since the start of this period is the earliest point in time from which hourly discharge data is available, and it is expected that after 2014 a systematic measurement error occurred in the discharge data (Bijlsma, 2022; Tromp, personal communication 2023). From Figure 3.10 it was deducted that a discharge of 70 m^3/s at Ommen has a non-exceedance probability of 0.95, meaning that 5% of the time this discharge is reached which is equal to eighteen days per year. This was taken as the reference scenario (current weir policy).
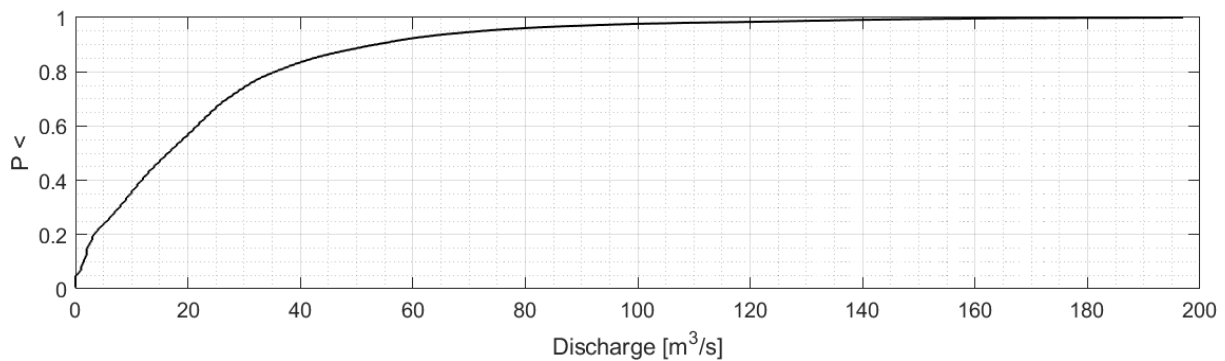

Figure 3.10. *ECDF of discharge measured at Ommen between 31 January 2002 and 1 January 2014*

A first alternative weir policy was set at the most extreme case that was deemed feasible; namely the full opening of all weir gates at all times, independent of the water levels and discharge. This alternative does not include the removal of the weirs, which means that the unmovable part of the structure (not the gates) is still present in the system. In other words, there is a permanent decrease of the crest level, since the lowest gate position is not at the river bed but above (1.83 m above the bed at De Haandrik, 1.76 m above the bed at Hardenberg, 3.96 m above the bed at Mariënberg, and 1.44 m above the bed at Junne).

Two other alternatives were set up based on a study by Tuijnder (2017a), who showed that over time most sediment in the Vecht would theoretically be transported at a discharge of 30 m^3/s (measured at Ommen) if the movement of sediment would not be blocked by the weirs. At a discharge of 30 m^3/s 25% of the total sediment transport is expected, compared to 13% at a discharge of 70 m^3/s (Figure 3.11). On top of this, the study by Duró et al. (2022) qualitatively assessed the impact of a discharge controlled weir policy where the discharge threshold is set at 30 m^3/s, before advising to do a quantitative analysis of this weir policy. The second alternative was thus to adapt a discharge controlled weir policy, for which the weirs open at a discharge of 30 m^3/s, measured at Ommen. According to Figure 3.10 a discharge of 30 m^3/s at Ommen has a non-exceedance probability of 0.74, meaning that 26% of the time this discharge is reached (and the weirs are thus opened), which is equal to 95 days per year. Tuijnder (2017a) also found that theoretically a discharge of 50 m^3/s (measured at Ommen) contributes to 20% of the total sediment transport through the Vecht (Figure 3.11), which was the basis for the set-up of the third alternative: a discharge controlled weir policy where the weirs open at a discharge of 50 m^3/s measured at Ommen. According to Figure 3.10 a discharge of 50 m^3/s at Ommen has a non-exceedance probability of 0.89, meaning that 11% of the time this discharge is reached, which is equal to 40 days per year.

Since these alternative weir policies have discharge thresholds of 30-50 m^3/s (at Ommen) it was judged that for the calibration of the bed roughness especially the medium flow scenario was of importance. The medium flow scenario has an average discharge of 20 m^3/s, and lateral inflows slightly add to this discharge before Ommen is reached, so this flow scenario is closest to the discharge thresholds.
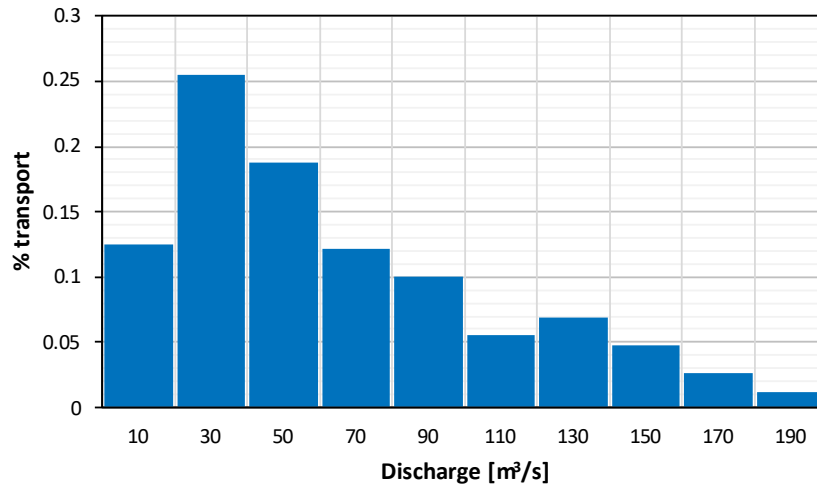
Figure 3.11. *Relative distribution of sediment transport in the Vecht, adapted from Tuijnder (2017a)*

It was decided to maintain the water level controlled weir policy if the discharge threshold was not met, so that an appropriate water level would be kept if there was insufficient discharge to reach the discharge threshold. Taking all this into account, eventually the scenarios for the evaluation of the final weir policies were formulated as follows:

- (Reference scenario: weir gates open if target water levels in Table 1.1 are reached);
- Q_{50} scenario: weir gates open at a discharge of 50 m^3/s, measured at Ommen, or if target water levels in Table 1.1 are reached;
- Q_{30} scenario: weir gates open at a discharge of 30 m^3/s, measured at Ommen, or if target water levels in Table 1.1 are reached;
- Q_0 scenario: weir gates are always in fully open position

Together these scenarios provide a range for the morphology that can be expected if a discharge controlled weir policy is to be implemented.

In order to evaluate the impact of these scenarios three model runs were done (one for each alternative weir policy) of which the results could be compared to the reference scenario. For these runs the same model set-up and input as for the reference scenario were used, although several changes were made in the RTC module to implement the different weir policies. The exact adjustments can be found in Appendix F. The comparison of the scenarios was done by looking at the simulated bed levels along the river, specifically near the weirs, and by calculating the bed level changes over time for each scenario.

4.   Results – Accuracy and reliability of the updated model

In this chapter the results of the calibration and validation of the updated model are described. The updated model has been calibrated and validated according to the methodology described in Section 3.2. The assessment of the accuracy (are simulated values correct for this system) and the reliability (does the model simulate correct values if the system is adjusted/different) is based on the interpretation of the results of the calibration and validation. For the interpretation of the results it must be taken into account that there are several locations in the river where interventions have been implemented during the simulated periods, or just before the simulated periods. This affects the simulated flow and bed levels in the river not only at the locations of these interventions, but also upstream and downstream of these locations. As explained in Section 3.2.3. and Section 3.2.5., not all locations along the river were included in the calibration and validation process, but still part of the differences between simulated water and bed levels and observed water and bed levels can be explained by these interventions.

4.1.   Accuracy and reliability of the hydrodynamics

Figure 4.1 shows the simulated water levels over time for the different calibration runs downstream of weir Hardenberg and upstream of weir Mariënberg. These two locations form the boundaries of one weir section, with the water levels at the most upstream location (downstream of weir Hardenberg) depending on the weir crest level at the downstream side (location upstream of weir Mariënberg), and it is judged that they represent the behaviour of the system at the other measurement stations well. The bed roughness values that were used for the final calibration run are shown in Table 4.1, where the roughness decreases in downstream direction as is also found in literature (Lamers, 2017; Van der Mheen et al., 2015; Spruyt, 2021). Overall, the simulation results at locations downstream of weirs show that water levels decrease as the value of the Chézy coefficient increases, meaning a decrease of the bed roughness (Figure 4.1-a,-c,-e), which is as expected. However, for locations just upstream of a weir the bed roughness does not affect the water level for low and medium flow (Figure 4.1-d,-f), which can be explained by the fact that the weir maintains a target water level which is not impacted by the bed roughness. For high flow, however, the weir gate is fully opened and the water flows (almost) freely past the weir, due to which variations in the simulated water levels are visible at the upstream side of the weir (Figure 4.1-b).

Table 4.2 shows the RMSE values that resulted from the calibration and validation of the bed roughness in the main channel. In the table only the RMSE values of the final calibration run with varying Chézy values for the main channel are shown (Table 4.1). The RMSE scores of the other calibration runs can be found in Appendix G. As could be expected, the model performs better overall for the calibration period than for the validation period. Also, it can be seen in Table 4.2 that the model performs best (lowest RMSE scores) for medium and low flow, both during the calibration and validation. This likely results from the fact that the final bed roughness values in the model were based on the medium flow scenario, to which the low flow scenario is relatively close. For the high flow scenarios it stands out that especially downstream of weir Junne and at the Hessel Muelert bridge there is a large underestimation of the water levels, which was also the case for Van der Mheen et al. (2015). However, a physical explanation for this could not be found. On the other hand, there is a systematic overestimation of the water levels during several of the medium and low flow scenarios at these locations in the validation. It is possible that this overestimation is the result of inclusion of the Rhezermaten (artificial meanders at km 22.5-25, Figure 3.2-c) in the model. While this intervention was implemented only in 2022, the validation is done with measurements from 2019 and 2020.

It can be seen in Figure 4.1-a and -b that a hysteresis effect occurs during high flow at both locations, which is not captured well by the model (possibly by the lack of a 2D schematisation). The hysteresis effect means that the front of a discharge wave has a steeper slope than the back of the wave, which results in a steeper slope in water levels at the start of a discharge wave as well, compared to the back of the wave (Kumar, 2011).
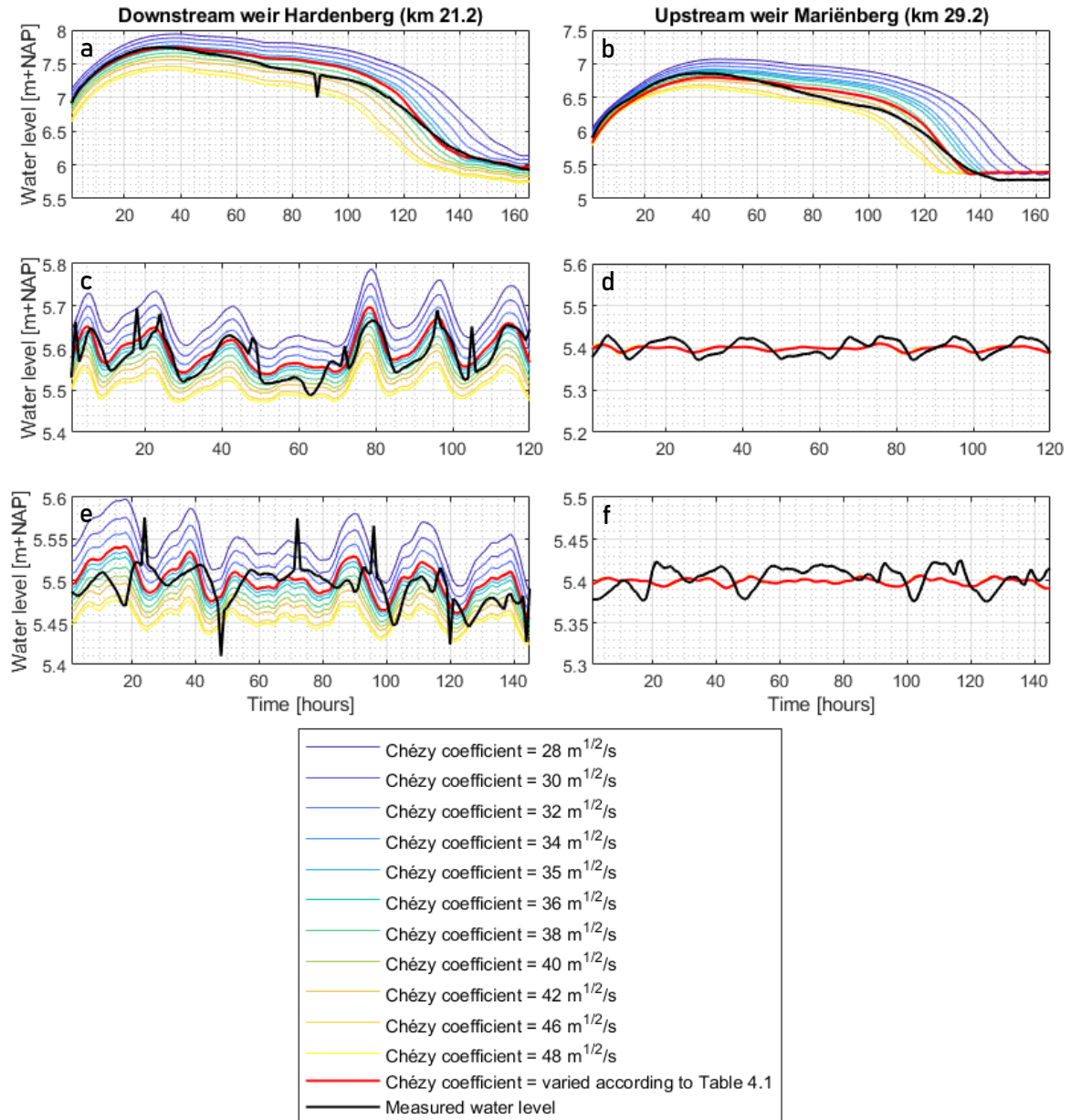
Figure 4.1. *Observed and simulated water levels during the calibration period for (a,b) high flow, (c,d) medium flow, and (e,f) low flow at measurement locations (a,c,e) downstream of weir Hardenberg and (b,d,f) upstream of weir Mariënberg*

Table 4.1. *Chézy coefficients used for final calibration run, locations form the boundaries of different reaches*

Location	Chézy coefficient [$m^{1/2}/s$]
Emlichheim	36
Weir De Haandrik	36
Weir Hardenberg	36
Weir Mariënberg	32
Weir Junne	44
Hessel Muelert bridge	48
Weir Vilsteren	48

Table 4.2. *RMSE values of the water levels for hydrodynamic calibration and validation, dashes indicate missing data, averages are calculated excluding these scenarios. Red/green colours indicate systematic under-/overestimation of water levels.*

Measurement station	RMSE values calibration [m]			RMSE values validation [m]		
flow scenario	High	Medium	Low	High	Medium	Low
Downstream weir De Haandrik	0.13	0.03	0.05	0.17	0.14	0.14
Downstream weir Hardenberg	0.10	0.03	0.03	0.16	0.13	0.11
Downstream weir Mariënberg	0.11	0.07	0.07	-	-	0.02
Downstream weir Junne	0.29	0.06	0.06	0.26	0.11	0.18
Hessel Muelert bridge	0.26	0.05	0.06	0.28	0.12	0.04
Upstream weir De Haandrik	0.08	0.01	0.01	0.19	0.01	0.02
Upstream weir Mariënberg	0.09	0.02	0.02	0.10	0.02	0.01
Upstream weir Junne	0.17	0.02	0.01	0.18	0.02	0.02
Average (excl. upstream weirs)	0.18	0.05	0.05	0.22	0.12	0.10

In Figure 4.2 a correlation plot of the simulated and the observed water levels can be seen for different flow scenarios at two locations, which are again downstream of weir Hardenberg (Figure 4.2-a,-c) and upstream of weir Mariënberg (Figure 4.2-b,-d). Correlation plots for the other measurement locations can be found in Appendix G. The hysteresis effect is clearly visible in Figure 4.2-a,-b, where the water levels are initially simulated correctly, but when decreasing they are overestimated. For the validation the effect is a bit more difficult to see in Figure 4.2-a,-b, because of the curve in the plotted results. This curve is caused by the fact that the discharge input consists of two consecutive waves. Although only the results at the measurement stations downstream of weir Hardenberg and upstream of weir Mariënberg are shown in Figure 4.1 and Figure 4.2, the water levels at the other measurement stations also show the hysteresis effect, which explains part of the high RMSE values for the high flow scenarios.

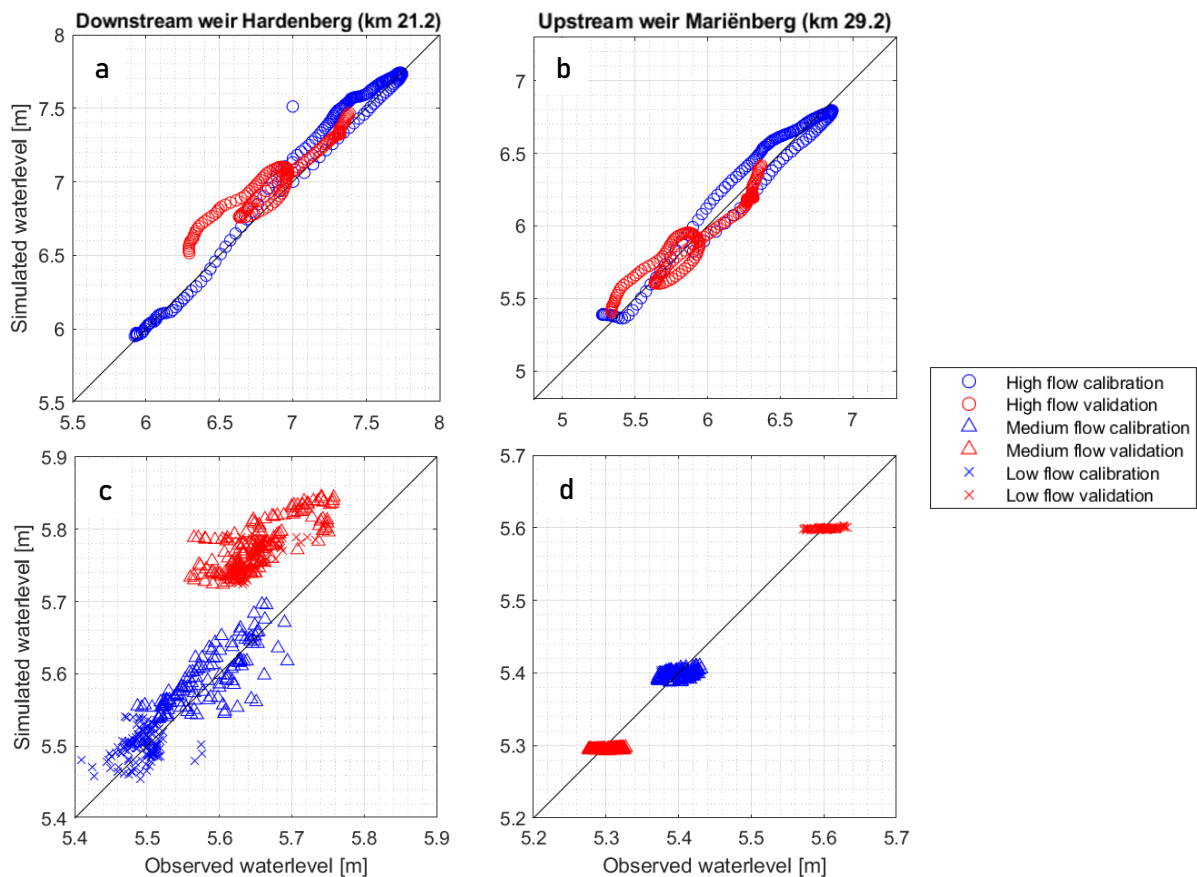**Figure 4.2.** *Observed vs. simulated water levels for calibration and validation of all flow scenarios: (a,b) high flow, (c,d) medium/low flow, (a,c) downstream weir Hardenberg, (b,d) upstream weir Mariënberg, black line representing perfect fit*

Besides the hysteresis at high flow, the overestimation of the water levels downstream of weir Hardenberg in the validation periods can be clearly seen. Lastly, Figure 4.2-d shows that the model performs very well in maintaining the water levels upstream of the weirs that are set as target levels during medium and low flow, even better than the weirs do in reality. This is visible in the small horizontal lines formed by the symbols during these flow scenarios, which means that there is variation in the observed water levels (horizontal variation in the figure), while there is no variation in the simulated water levels (no vertical variation in the figure).

4.2. Accuracy and reliability of the morphodynamics

The RMSE scores that have resulted from the calibration of the calibration coefficient α and the median grain diameter D_{50} are shown in Table 4.3. As explained in Section 3.2.3. and Section 3.2.5., the locations on which interventions have been implemented during the simulated period are not taken into account for the calculation of the RMSE scores. The calculated scores show that overall a higher D_{50} leads to a better morphodynamic performance of the model, whereas a higher α leads to a worse morphodynamic performance. This can be explained by the fact that the model tends to simulate too much sediment transport for almost all morphological settings that were tried (see peaks in Figure 4.3), and a higher D_{50} results in less sediment transport and a higher α results in more sediment transport. This is conform the Engelund and Hansen sediment transport formula (Equation C.4, Appendix C). The fact that a larger grain size (higher D_{50}) gives less sediment transport, can also be explained physically by the fact that large grains are heavier to pick up and they deposit at higher flow velocities compared to smaller grains. Since α is only a calibration parameter, no physical explanation can be provided for its effect on the morphodynamics.

Table 4.3. *RMSE values of bed levels for morphodynamic calibration for different morphological settings, value between brackets is the RMSE value of the validation*

		D_{50}			
		50%	100%	125%	150%
	0.50		0.57 m	0.55 (0.43) m	0.55 m
	0.75		0.63 m	0.61 m	0.57 m
α	1.00	0.73 m	0.64 m	0.63 m	0.62 m
	1.25		0.64 m		

Figure 4.3 shows the bed level change that has been simulated along the river over nine years (2013-2022) for the different calibration runs, where the best performing model set-up was found and kept at α = 0.50 and D_{50} times 1.25 (final D_{50} = 0.406 mm). On most locations the sign of the bed level change is similar for the measured and simulated bed level change, which means that erosion is simulated at locations where erosion has occurred and deposition is simulated at locations where deposition has occurred. In the calibration section one of the largest exceptions of this can be seen, from km 11 to km 14, where a small increase in bed level has been observed whereas a decrease in bed level has been simulated. It is expected that a decrease in the bed level has been simulated as a consequence of a local initial response upstream of this location (at km 10.8) to the presence of weir De Haandrik in the system, since local bed features such as an erosion pit downstream of the weir were not in the schematization at the start of the simulation. However, Figure 4.4 shows that at the end of the simulated period the bed level is still decreasing. Apart from this section (km 11-14) the erosion and deposition patterns are simulated well in the calibration section.
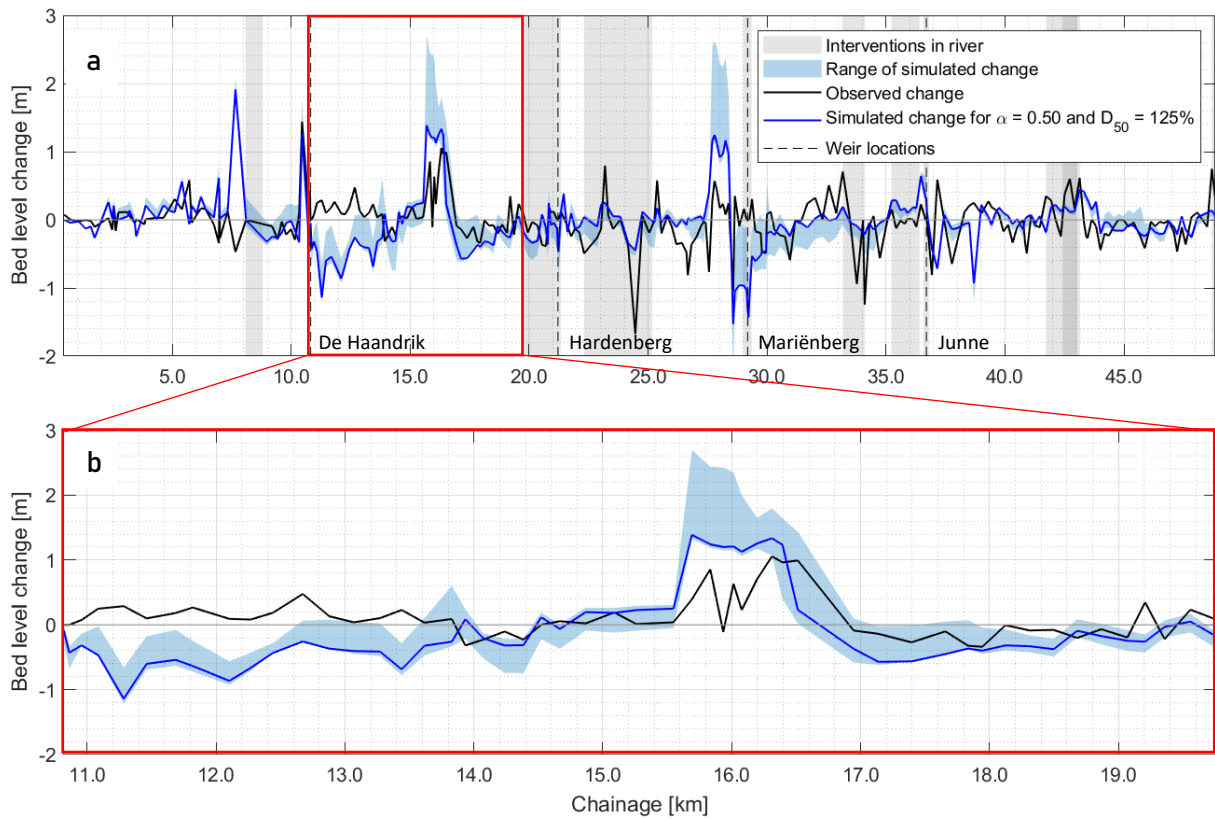
Figure 4.3. *Observed and simulated bed level change for the morphodynamic calibration and validation period (2013-2022) along (a) the entire river, and (b) the calibration section. The blue area covers the area between the maximum and minimum bed levels that were simulated for all combinations of α and D_{50} values*
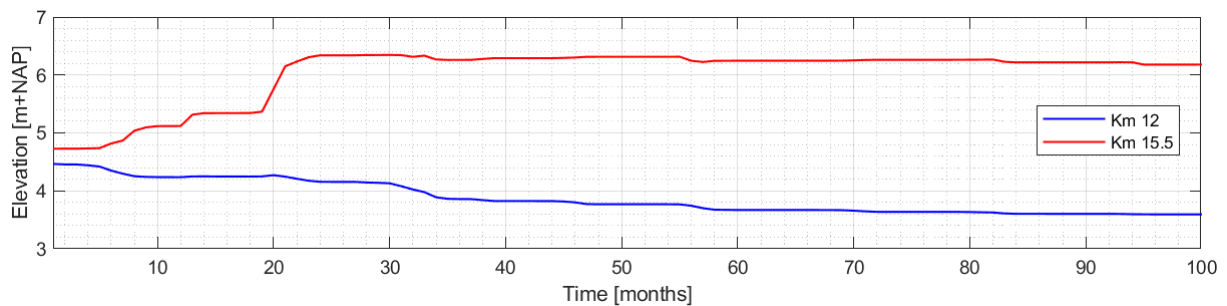

Figure 4.4. *Simulated bed level over time (monthly averaged) for the calibration of the morphology at km 12 and km 15.5*

Another section in the calibrated area that stands out is at km 15.5 to km 16.5, where many of the calibration runs simulated a much larger bed level increase than the increase that has been observed. This can be explained by the presence of the Loozensche Linie (Figure 4.5-b), an artificial meander of which the construction took place in 2009. Similar behaviour can be observed in the validation section, at the meander near Rheeze (km 28.5 to km 29.5, Figure 4.6-c) just north of weir Mariënberg, where the simulated bed level increase is also an overestimation of the observed bed level increase. This seems to be the case only at meanders where the old channel is kept intact as some form of side channel, since no such behaviour is observed at the newly constructed Grensmeander (km 8.5), Rhezermaten (km 22.5 to km 25), and the meander near Karshoek-Stegeren (km 33), which are shown in Figure 4.6-a,-b,-d. These three locations all have in common that they do not have an old part of the river as a side channel, while the Loozensche Linie and the meander near Rheeze do have such a side channel. The reason for the overestimation at these two location is expected to depend on the fact that the model does not schematize a clear barrier for the water to enter the old channel at these two locations, while there is a sudden bed level increase in both the old and the new channel compared to

the bed level in the main channel upstream of the bends. Since more water flows through the old channel in the model than in reality, less water flows through the new channel in the model than in reality and an overestimation of deposition in the new channel can be expected as an initial response of the system, which is visible in Figure 4.4. Since an increased bed level is simulated in the entire meander, while the increase suddenly stops when the old and new channel merge downstream of the meander, this reasoning seems plausible.

Figure 4.5. *Vecht in 2005 (a) and 2012 (b) at the location of the Loozensche Linie (km 15.5-16.5). The meandering river stretch forms the main channel of the river, the old river stretch serves as a side channel with a barrier at the entrance to the side channel to guide the main flow into the meander. Red arrows indicate flow direction. Figures are adapted from Google Earth (2005 and 2012)*
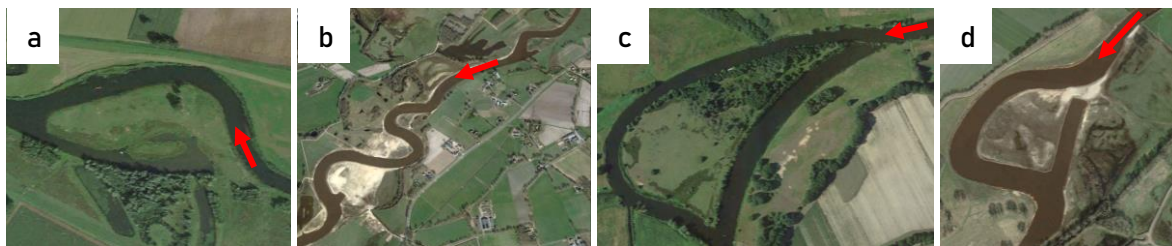

Figure 4.6. *Meanders along the river: (a) Grensmeander (km 8.5), (b) Rhezermaten (km 22.5-25), (c) near Rheeze (km 28.5-29.5), (d) near Karshoek-Stegeren (km 33). Red arrows indicate flow direction. Figures are adapted from Google Earth (2022)*

In the validation section several sections stand out that have not been discussed yet, such as at km 7.5 where a large bed level increase is simulated (almost two m increase, compared to an observed bed level decrease of 0.5 m), and at km 28.5 to km 30 where a bed level decrease of 1-1.5 m has been simulated, while in reality the bed level has not changed that much (0-0.4 m increase). It is expected that the reason for the large difference at the first section (at km 7.5, a river bend near Laar) is that based on the measurements there initially is a relatively deep erosion pit at this grid point compared to the two neighbouring grid points, since it is located in a sharp river bend. This sharp river bend is schematised with little detail in the model, which could lead to the model working towards an equilibrium at this location (no erosion pit) while in reality more erosion has occurred in the outer side of the bend due to movement of the thalweg towards the outer bend. The second location (at km 28.5 to km 30) is located between the meander near Rheeze and the entrance of the side channel at weir Mariënberg. It is likely that the erosion stretch is a result of the simulated increased bed level at the meander, similar behaviour is observed just downstream of the Loozensche Linie. A reason for this erosion downstream of the deposition peak can be that there is a higher sediment transport capacity available after sediment has deposited upstream, which leads to more erosion and more transport of the eroded sediment downstream.

5.   Results – Long term morphology

In this chapter the results of the long term simulations are discussed. The simulations were done for a reference scenario (with the current weir policy) and for three alternative scenarios (with adjusted weir policies), according to the methodology described in Chapter 3.

5.1.   Long term morphology for the reference scenario

The model was run for 50 years to find a reference situation for the morphology of the Vecht in case no further adjustments to the river are made, with the model set-up and input as described in Section 3.3. The results of this simulation are shown in Figure 5.1 and Figure 5.2-a, where Figure 5.1 shows the bed level change at the end of the simulated period, whereas Figure 5.2 shows the bed level change during the entire simulation. Figure 5.1-b highlights one weir section, as well as just up- and downstream of the boundaries of this section to look closer at the local morphology around weirs.
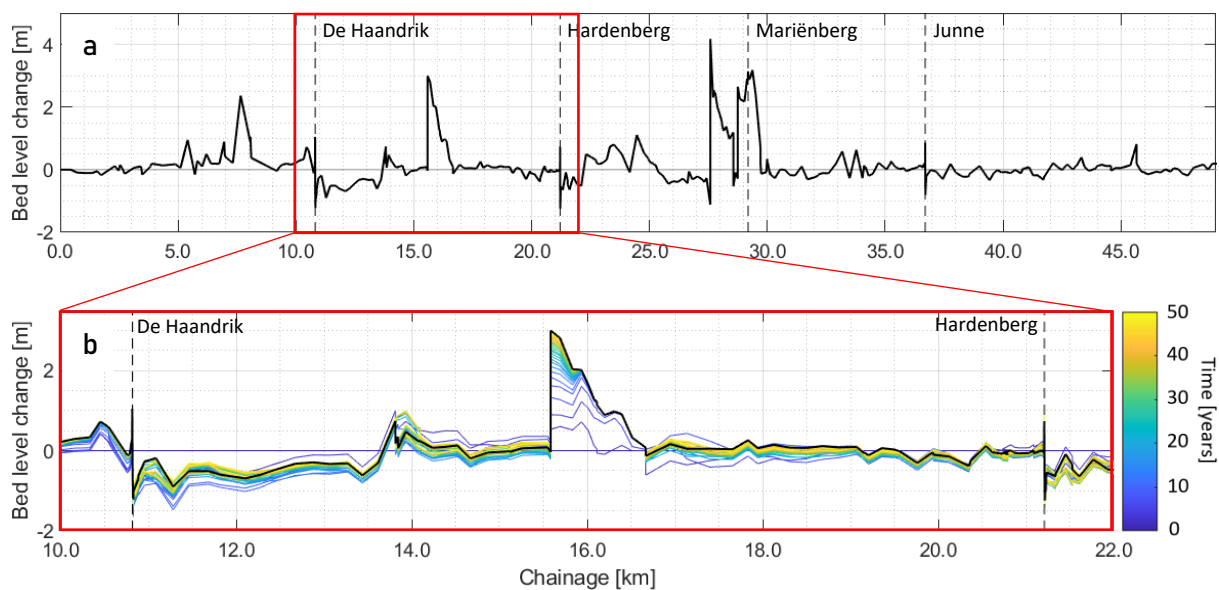

Figure 5.1. *Bed level change over 50 years, simulated with the current weir policy. Colours in (b) indicate the time step*

5.1.1.   Morphology around weirs

Around all weirs except weir Mariënberg a pattern is observed (the exception around Mariënberg is explained below) that consists of a small bed level increase just upstream of the weir and erosion downstream of the weirs (Figure 5.1-b at km 11.8 and km 21.4). An erosion pit forms directly downstream of the weirs, and a little further downstream the erosion is still visible (Figure 5.1-b from km 11.4 until km 13.7). These bed features are observed often in literature (e.g. by Ohmoto & Une, (2018), or by Nguyen et al. (2015)) and in reality the features are expected to be present before the start of the simulated period. However, no cross sections are specified sufficiently close to the weir to represent these bed features, due to which they form during the simulated period. It can be seen in Figure 5.1-b and Figure 5.3 that the initial erosion downstream of the weir (km 10.8-13) is larger than the erosion that has been simulated after 50 years. Furthermore it can be seen that a small bed level increase forms downstream of this eroded area (Figure 5.1 at km 13.7). Initially this bed level increase is larger than the increase that has been simulated after 50 years, similar to the erosion pattern. This similar behaviour through time can be explained by the fact that sediment erodes due to increased flow velocities downstream of the weirs, after which it deposits again when flow velocities decrease further downstream. If more sediment erodes at a point in time, the local deposition can also be expected to increase at that time. The fact that initially the erosion and deposition are higher than at

37

the end of the simulated period can likely be explained by the fact that the initial response of the system to the activation of morphological processes and to the presence of the weir is very strong. The effect of this initial response diffuses over time, to work towards a dynamic equilibrium (Figure 5.3).
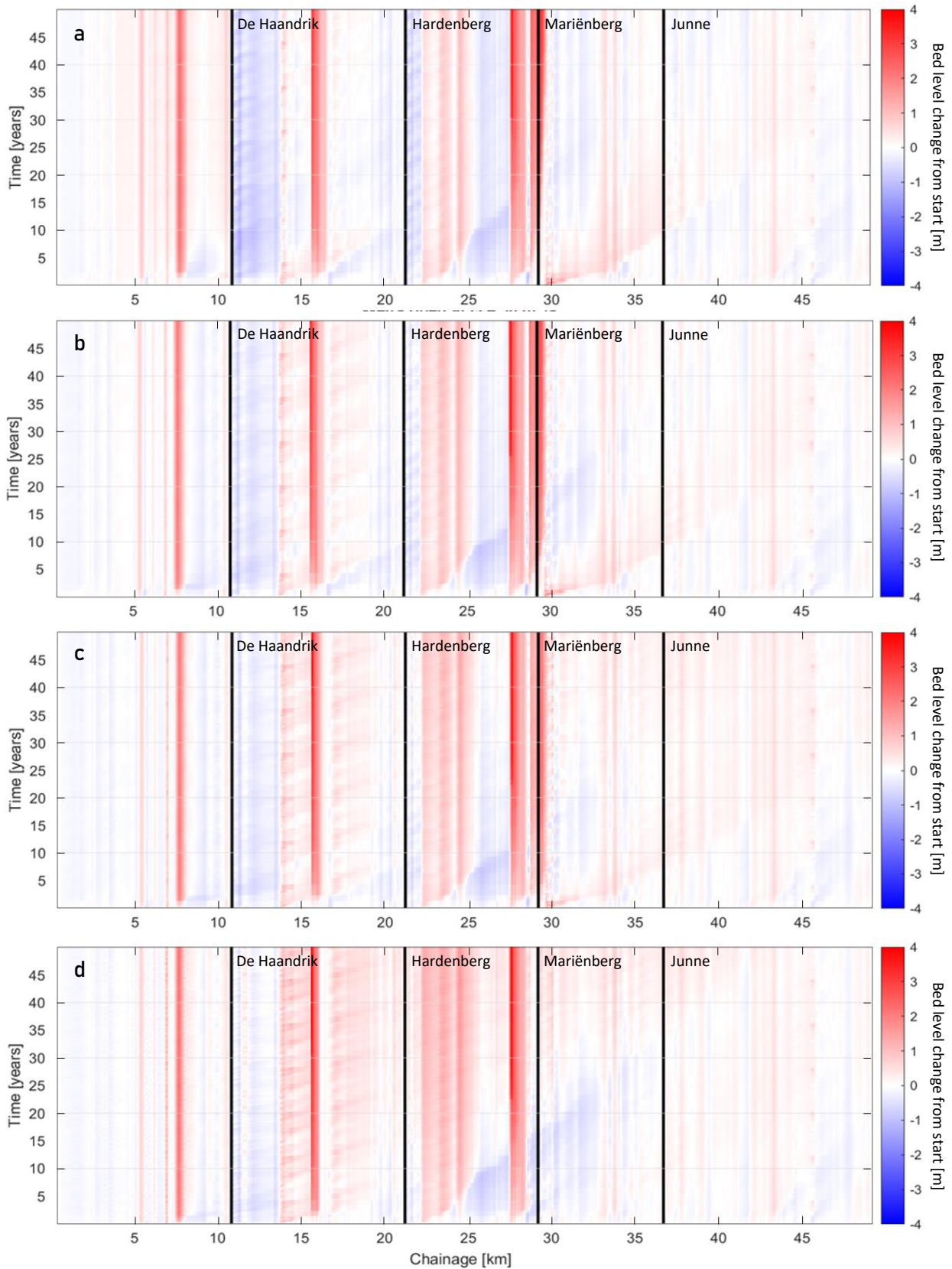

Figure 5.2. *Bed level change from start for: (a) reference scenario, (b) Q_{50}-scenario, (c) Q_{30}-scenario, and (d) Q_0-scenario. Black lines represent the location of the weirs. Positive values represent deposition, negative values represent erosion*
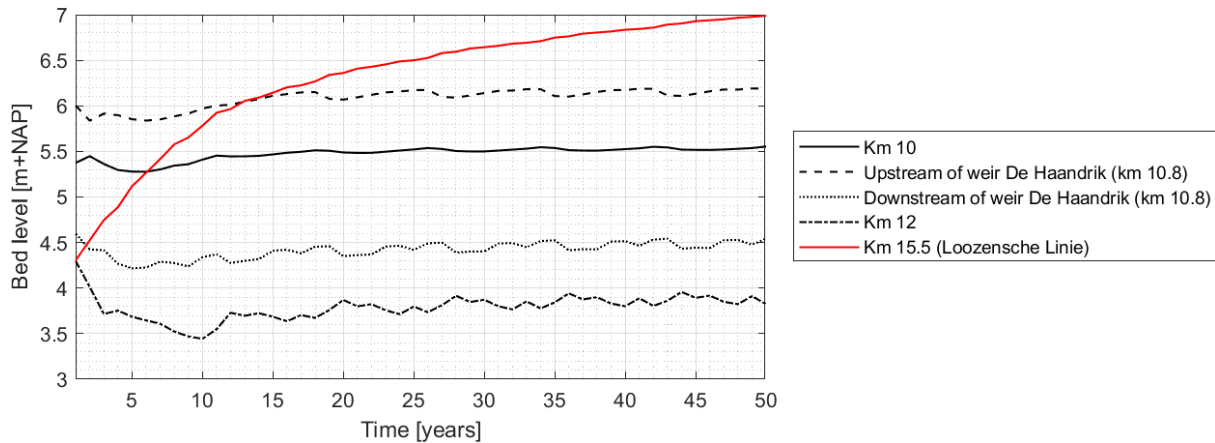
Figure 5.3. *Bed level change over time (yearly averaged) for reference scenario at km 10, upstream and downstream of weir De Haandrik, at km 12, and at km 15.5*

5.1.2. Deposition peaks

It can be seen in Figure 5.1-a that there are several locations along the river where peaks of deposition occur. These locations are mostly similar to the locations that were found to have a lot of deposition during calibration: at km 7.5 (bend near Laar, Figure 3.2-a), around km 15.5 (the Loozensche Linie, Figure 3.2-b), between km 27.5 and km 28.5 (at the meander near Rheeze, Figure 3.2-d). It is therefore expected that the reason for these peaks to occur again is similar to the reason that was explained in Section 4.2. It can be seen in Figure 5.2-a that the bed level increase at km 7.5 is an initial change, which occurs within the first five years. The reason for this is expected to be the same as during the validation process, an issue in the schematization as described in Section 4.2. At the peaks around km 15.5 and km 28 the increase in bed level is also largest at the beginning of the simulated period (in the first ten years) after which the velocity of the bed level increase reduces. However, a (dynamic) equilibrium bed level is not reached during the simulated period (Figure 5.2-a, Figure 5.3).

5.1.3. Propagation of erosion and deposition waves

Several patterns in the bed are visible in Figure 5.2-a that develop more slowly than the deposition peaks, such as erosion and deposition waves at the downstream sides of each weir section, which propagate with a velocity with an order of magnitude of a few hundred metres per year. These waves have a larger magnitude (higher erosion/deposition) during the first few years of the simulated period than at the end of the simulated period (Figure 5.2). It can be seen that the downstream propagation of the waves is blocked partially by the weirs at De Haandrik and at Hardenberg, or at locations where the bed elevation is much higher (e.g. at km 15.5). However, the deposition wave downstream of weir Mariënberg does propagate past weir Junne. While weirs do limit the propagation of erosion or deposition waves to some extent, sometimes the weirs are opened (during high flow), which allows for propagation of the waves to the downstream side of the weirs. Also propagation of the waves through the side channel can possibly occur.

5.1.4. Deposition around weir Mariënberg

Besides the deposition peaks at km 7.5, 15.5, and 28, a large bed level increase (of approximately three metres) is also found around weir Mariënberg (km 29). The results also show a decrease in water levels from this location until weir Hardenberg (km 21-29), with the decreased water levels eventually being closer to the target level set at weir Junne (Figure 5.4). Furthermore the results show that the side channel around weir Mariënberg has eroded in the first three years with two to three metres while the water depth increases in the side channel (Figure 5.4), due to which it is expected that after ten years the side channel starts to function as the main channel, with most of the water flowing through the side channel instead of through the main channel past the weir. While in reality there is a structure

in the side channel that prevents this from happening, such a structure is not schematised in the model. Since less water flows past the weir, more sediment is deposited upstream of the weir. Because of this behaviour, the area around weir Mariënberg (km 21-30) is not included in the rest of the analysis.
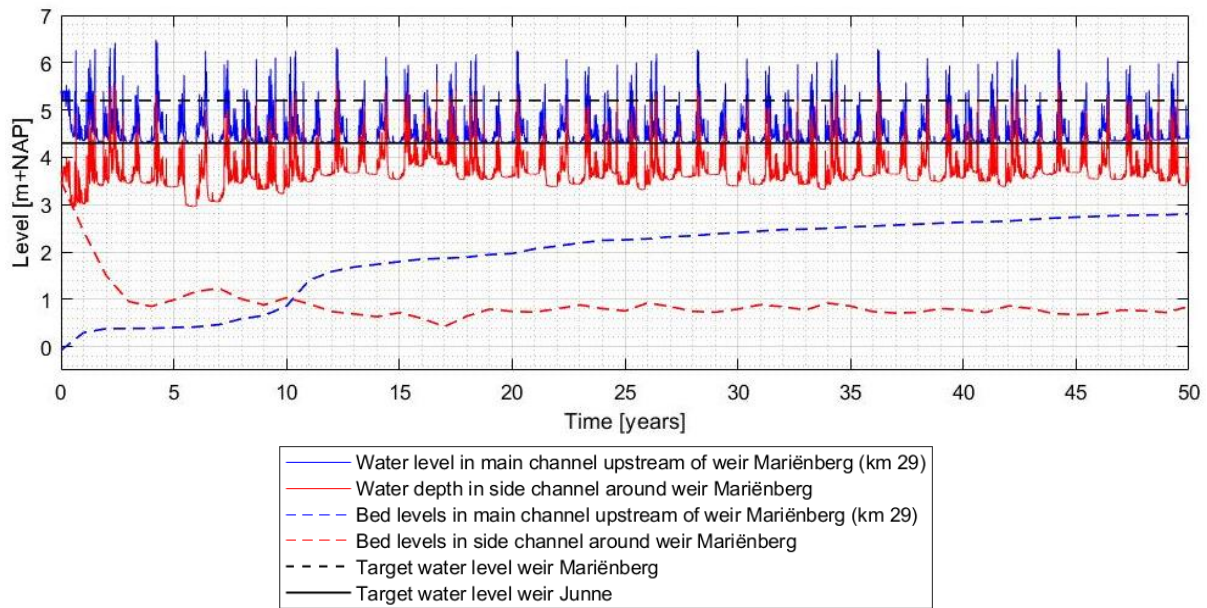

Figure 5.4. *Water levels and bed levels in main channel upstream of weir Mariënberg, and bed levels in side channel Junne*

Since water levels upstream of weir Hardenberg still depend on the target level set for Hardenberg, the area upstream of weir Hardenberg is assumed to be unaffected by the fact that the side channel at Mariënberg starts to function as the new main channel over time. Downstream of weir Mariënberg, after the side channel confluences with the main channel (km 30), a deposition wave is observed that propagates in downstream direction, even past weir Junne. However, the water levels between km 30 and weir Junne still comply with the target water level at Junne, and no strange peaks in the bed level are observed (Figure 5.1 km 30-49). Therefore it is judged that the area downstream of km 30 can be used for the analysis of the morphology.

5.1.5. Sediment transport and discharge

Changes in the bed level seem to vary strongly through time, even if an equilibrium is reached. This can be explained by the effect that the discharge has on the sediment transport in the river. Figure 5.5 shows the sediment transport and discharge in the main channel at km 10 for the first 200 days of the simulation. It can clearly be seen that more sediment is transported during peak discharges, which affects the erosion and deposition in the river.
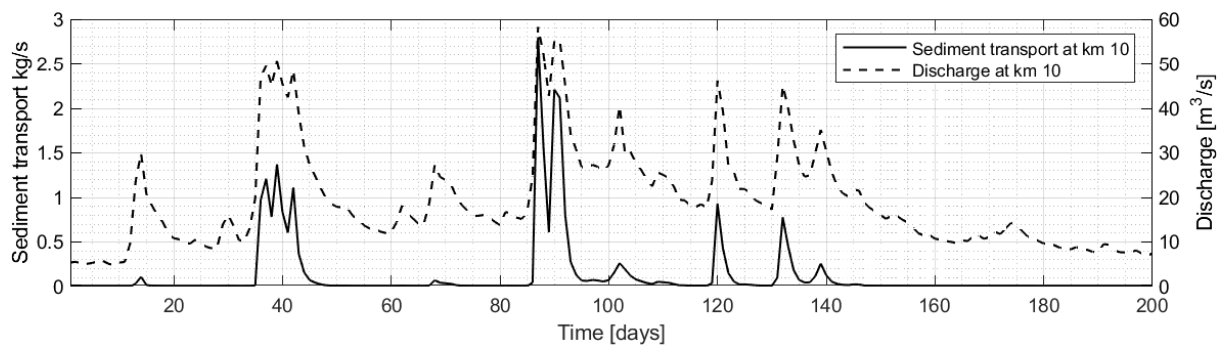

Figure 5.5. *Sediment transport and discharge at km 10 for the first 200 days of simulation*

5.2. Long term morphology for the alternative weir policies

The analysis of the bed level change that has been simulated with the alternative weir policies can be divided into several sections. Firstly a quick comparison of peaks in the bed level change is done, after which an analysis follows of the local patterns around the weirs and how these local patterns compare for the different scenarios. Furthermore, the occurrence of erosion and deposition waves is highlighted, and the approach of a dynamic equilibrium is discussed.

5.2.1. Comparison of peaks

Figure 5.6 shows the total bed level change that has been simulated over 50 years for the different weir policy scenarios. Overall it can be seen that the patterns of deposition peaks are very similar to the reference scenario for all alternative weir policies, with peaks around km 7.5, km 15.5, and km 27.5 (see Figure 5.6-a). Since these peaks also occur in the other scenarios and simulations, the results are further used in the comparison of the different weir policies. It can also be seen that for the Q_0-scenario the bed level increase around weir Mariënberg (km 29) is not as large as for the other scenarios. The closer a scenario is to the reference scenario, the higher the bed level increase around weir Mariënberg is. This can likely be explained by differences in the morphology upstream of the weirs.

5.2.2. Morphology around weirs

It can be seen in Figure 5.6-b that local deposition peaks and erosion pits still occur upstream and downstream of the weirs for the alternative weir policies. However, Figure 5.7-b shows that there is less deposition and less erosion for the new weir policies compared to the reference scenario. For the Q_0-scenario the differences are largest, while they are smallest for the scenario in which the weirs open at a discharge of 50 m^3/s (Q_{50}-scenario). Since the weirs are not fully removed from the system and the weir gates do not lay flat on the bottom, it makes sense that these typical bed features around weirs are still present. Note that, while Figure 5.7 shows the difference between the simulated bed level changes for the alternative weir policies compared to the bed level change simulated with the reference scenario, a positive difference in this figure does not necessarily mean that deposition occurs for the alternative weir policies, it can also be that there is less erosion for the alternative weir policies than for the reference scenario. The same holds for a negative difference with regards to erosion.

Looking on a larger scale around the weirs in Figure 5.7, upstream of the weirs a pattern of decreased deposition is visible, while downstream decreased erosion is visible. This is especially noticeable upstream of weir De Haandrik (km 0-10.8) and downstream of weir De Haandrik (km 10.8-15), weir Hardenberg (km 21.2-27), and weir Junne (km 36.7-49). Upstream of other weirs than De Haandrik (e.g. at km 21 and at km 36), a decrease in deposition is not observed. In fact, Figure 5.6-a and Figure 5.7 show that between weir De Haandrik and weir Junne (from km 10.8 to 36.7) an overall increase in bed levels is simulated with the new weir policies compared to the reference scenario, which is largest for the Q_0-scenario and smallest for the Q_{50}-scenario. It is expected that the reason for the increased bed levels is that the decrease in erosion downstream of the weirs is dominant, and the distance between the weirs is not large enough for both patterns (large-scale decreased deposition and large-scale decreased erosion/increased deposition) to fully develop. At weir Mariënberg the patterns are difficult to recognise due to the deposition peak in all scenarios except the Q_0-scenario. The reason that there is no deposition peak in the Q_0-scenario is expected to be related to the pattern of reduced deposition upstream of the weirs. Since there is reduced deposition at km 29, water keeps flowing through the main channel instead of the side channel, which prevents further deposition in the main channel.
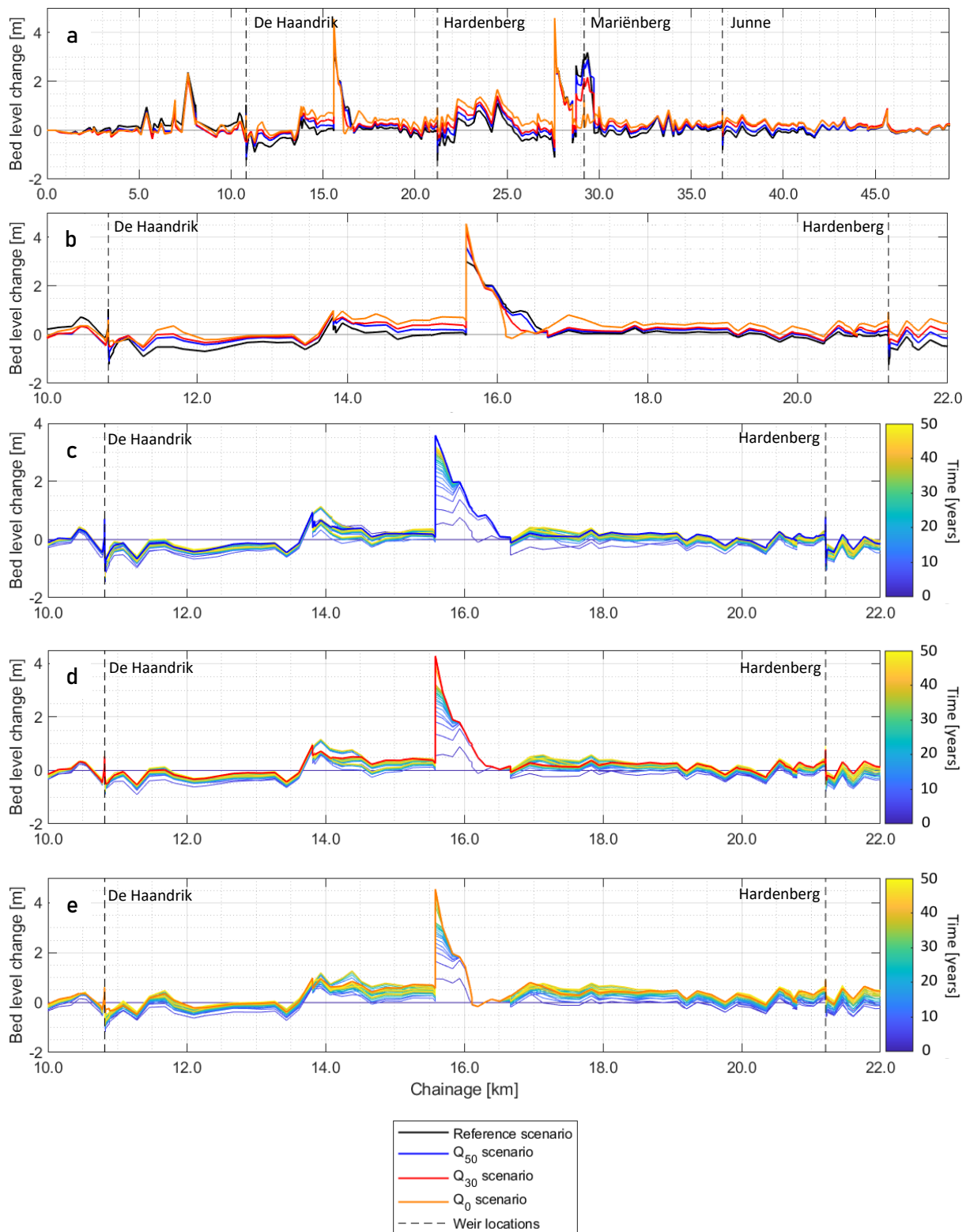
Figure 5.6. *Bed level change over 50 years, simulated with the new weir policies, (b), (c), (d), and (e) are zoomed in from (a) on one weir section, with (c) the Q_{50}-scenario, (d) the Q_{30}-scenario, and (e) the Q_0-scenario. Colours in (c), (d), and (e) indicate the time step*
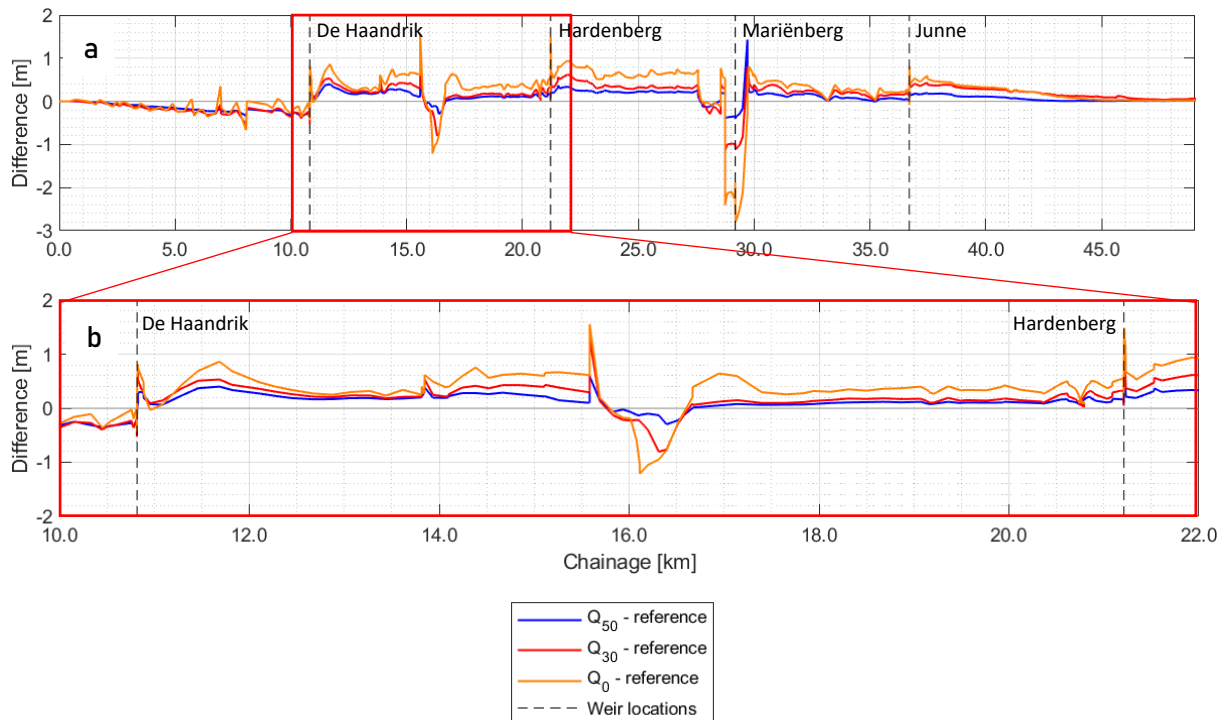
Figure 5.7. *Difference between the bed level change simulated for the Q_{50}-/Q_{30}-/Q_0-scenarios and the bed level change simulated for the reference scenario, (a) for the whole river, (b) for one weir section*

5.2.3. Propagation of erosion and deposition waves

A last comparison with the patterns that were observed for the reference scenario shows that the erosion and deposition waves that were observed at the downstream side of weir sections in the reference scenario are still present, but they decrease in number (Figure 5.2-b,-c,-d). Especially for the Q_0-scenario one large erosion wave is now observed that starts downstream of weir Hardenberg (at km 23, which diffuses in time and turns into a deposition wave), instead of several smaller waves. While this one wave was already present in the reference scenario, it propagates further downstream in the Q_0-scenario than in the reference scenario. Also in the Q_{50}-scenario and in the Q_{30}-scenario this wave was observed, although it did not propagate as far in these scenarios as in the Q_0 scenario and it was not followed by a deposition wave.

5.2.4. Equilibrium

The diffusion of the bed forms and initial changes in the bed is also visible in Figure 5.6-c,-d,-e (for one weir section) and in Figure 5.8 (locally around weir De Haandrik). Upstream of weir De Haandrik (at km 10 and 10.8) all new weir policies show similar behaviour through time (Figure 5.8), but contrary to the reference scenario the initial response of the system is erosion instead of deposition. Downstream of the weir (at km 10.8 and 12) all scenarios including the reference scenario initially lead to erosion, although the initial response is largest for the reference scenario (Figure 5.8). Locally, a dynamic equilibrium seems to be reached already after ten to fifteen years for the new scenarios, while this takes a little longer for the reference scenario for which the equilibrium was described in Section 5.1.1. and Section 5.1.2. A possible reason for the different time periods to reach equilibrium is that the reference scenario has a much stronger initial response than the other scenarios. Also for the alternative scenarios fluctuations in the bed remain visible after an equilibrium is reached, which can again be related to fluctuations in the discharge as is described in Section 5.1.5.
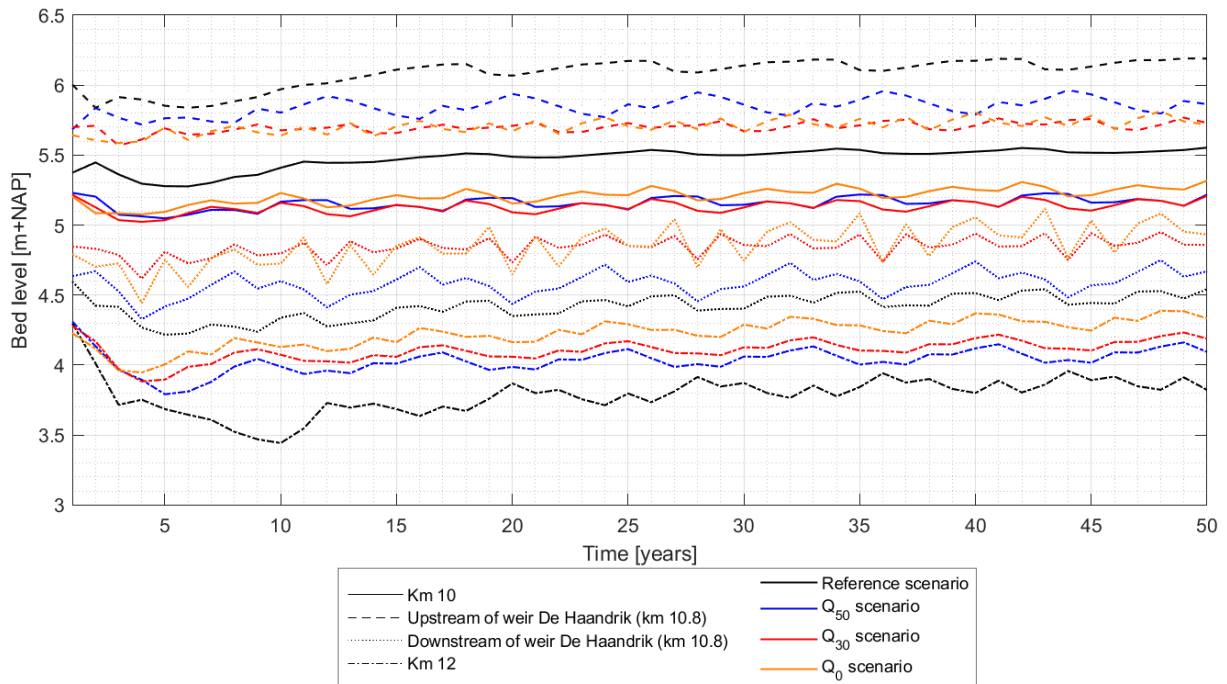
Figure 5.8. *Bed level change over time (yearly averaged) for all scenarios at km 10, upstream and downstream of weir De Haandrik, and at km 12*

As for the deposition peaks, an equilibrium is not reached after ten to fifteen years (Figure 5.6-c,-d,-e and Figure 5.9). It can be seen in Figure 5.9 that the bed level at the Loozensche Linie (km 15.5.) keeps increasing for all scenarios. What stands out is that the increase for the Q_0-, Q_{30}-, and Q_{50}-scenario continues gradually until a bed level of 7.2 m+NAP is reached, after which the velocity with which the bed level increases suddenly is much higher. For the Q_0- and the Q_{30}- scenario it seems that after seven years of this extra bed level increase the bed level converges to an equilibrium, while for the Q_{50}- and the reference scenario no equilibrium is reached in 50 years. It is expected that the sudden extra bed level increase is the result of the bed level reaching a threshold above which the dominant flow goes through the old channel, instead of through the new channel. This decrease in flow results in more deposition, similarly to what was observed around weir Mariënberg for most scenarios. It can clearly be seen that the Q_0-scenario reaches the equilibrium earliest of all scenarios (Figure 5.9), which can be explained by the fact that this is the scenario in which most sediment transport occurs. The reason for the fact that the deposition peaks in this scenario are highest of all scenarios could not be found.
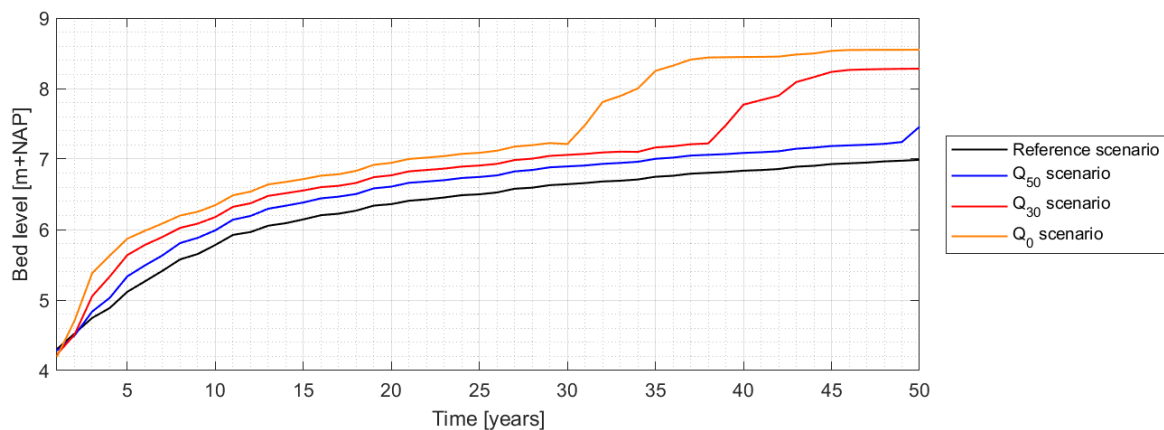

Figure 5.9. *Bed level change over time for all scenarios at km 15.5 (Loozensche Linie)*

6. Discussion

The findings of this research provide insight into the potential morphology of the Vecht over the coming 50 years if different weir policies were to be implemented. However, some assumptions were made during the study that could have affected the results that have been presented in Chapter 4. This chapter focusses on the most important assumptions and limitations that were part of this study, and how they shape the interpretation of the results.

6.1. Limitations and their implications in the model set-up

Several assumptions and choices were made during the set-up of the model that have affected the simulated hydrodynamics and morphodynamics. These assumptions and choices include the choice for a 1D model, and the generation and set-up of discharge time series for the boundary conditions. For all the assumptions and choices that were made, a substantiation has been provided, but this section explains how the simulation results could have been affected by the final model set-up on each of these aspects.

6.1.1. 1D model choice

Firstly the choice for a 1D model has limited the analysis of the bed level change in the river to a thalweg elevation change, even though literature has shown that also horizontal changes in the river occur, for example at river bends (Duró et al., 2022). It could not be found in literature how SOBEK 3 simulates flow through river bends in a 1D model. However, if a 2D model would have been used it is expected that some locations would have shown a different bed level change than the one which was currently simulated. Especially in river bends this could have made a difference, due to the variation in hydrodynamics in width-direction that is taken into account in a 2D model, due to possible bank erosion, or due to the possible shift of the thalweg (such as at km 7.5, in the river bend near Laar). Also at the entrance of side channels a 2D model might serve better than the 1D model that was used, since there were limitations in smoothing of the bed at locations where the channel split into multiple branches. At these locations the bed level could only be averaged for two of the connected branches, but not for all of the branches. The entrance of the side channels is therefore quite abrupt in terms of bed level change, which can be prevented with the use of a 2D model.

6.1.2. Generation and set-up of discharge time series

A second discussion point in the set-up of the model is the generation of the discharge time series that were used as input for the model. Even though the lateral inflow generator tries to mimic the discharge patterns that were originally observed at each inflow location, the simulated discharge series resemble the input discharge series very closely in shape. This means that flow patterns such as discharge waves or low flow periods are magnified in the model, due to which it could be that the model calculates the hydrodynamics and morphodynamics with higher (or lower) discharge input than what has actually occurred. Therefore the simulated sediment transport is expected to be larger during the high flow moments than in reality.

For the set-up of the 50-year discharge series also several simplifications were done compared to discharges that occur in reality. This is especially the case for the repetition of peak discharges, which have a certain frequency of occurrence in reality that is not always captured well if shorter discharge series are used for duplication. However, the impact on the research findings is expected to be limited, since the main findings were based on a comparison of different scenarios, which were all simulated with the same discharge series.

6.2.   Limitations and implications in the interpretation of the results

The results that were presented in Chapter 4 show some discrepancies with the observed water and bed levels. Part of these can be explained by the choice to include or exclude certain interventions in the model schematisation, whereas in other cases they can be explained by choices in the model set-up. For several interventions their impact on the hydrodynamics and morphodynamics was studied before and during implementation, such as for the Rhezermaten (Tuijnder, 2017b).

6.2.1.   Impact of interventions on the model results

In Section 3.2.1. it was explained that the interventions that were added in the model consisted of several meanders (the Grensmeander, the Rhezermaten, the meander near Karshoek-Stegeren), and the side channel near Koeksebelt. However, not all of these interventions were present in reality when the water levels for the hydrodynamic validation were measured, and none of them were present when the bed levels were measured that were used as a starting point for the morphodynamic calibration and validation. During the morphodynamic calibration and validation no large effect of the newly implemented interventions was visible in the bed levels, the reason for which is expected to be that they are simulated in the 1D model only as an elongation of the channel (except for the side channel near Koeksebelt). The impact of the interventions on the water levels was visible in the fact that the water levels were systematically overestimated at several measurement stations during the hydrodynamic validation. It was expected that water levels would increase between Hardenberg and Junne if the Rhezermaten were implemented in the model without adjusting the river profile (Tuijnder, 2017b), which shows in the overestimation of the water levels.

6.2.2.   Erosion/deposition near Mariënberg

Another point of attention is the behaviour of the system around weir Mariënberg. During the validation it was observed that this section eroded quite a lot in the simulations, while during the 50-year runs a lot of sedimentation was observed. This can be explained by the fact that different bed levels were used as input for the simulations. While the observed bed level just upstream of the entrance to the side channel showed an increase between 2013 and 2022 (from 0.96 to 1.36 m+NAP), the observed bed level in the main channel just downstream of the entrance to the side channel showed a decrease in this period (from 2.24 to 1.95 m+NAP). This means that at the start of the validation simulation, the bed was steeper than at the start of the 50-year simulation. It is expected that this steep slope led to erosion in the main channel in the validation simulation, while the more gradual bed slope led to deposition in the 50-year simulation. The bed level increase at Mariënberg is not seen in the Q_0-scenario. It is expected that the cause of this is that in that case less deposition occurs just upstream of all weirs, so also just upstream of weir Mariënberg.

6.2.3.   Comparison to literature

Comparing the local morphological patterns that were observed near the weirs to the research of Ni et al. (2021) and Nguyen et al. (2015) it is found that the bed level decrease upstream of weirs is observed in all studies, similarly to the existence of an erosion pit downstream of the weirs that does not disappear for different weir policies. Also the finding that the initial strong response of the system to the weirs initially gives a larger bed level change than the bed level change that has occurred when an equilibrium is reached is supported by literature (Duró et al., 2022).

On the contrary, on the large scale the findings of the study differ from the analysis results of Duró et al. (2022), where it was expected that on average the bed level would decrease if a discharge controlled weir policy were to be implemented, while an average increase of the bed level was simulated in this study. The difference between these studies can likely be explained by the fact that while the analysis of Duró et al. (2022) focussed on a simplified river, this study used a model that is much more detailed

than the river to which the theory was applied by Duró et al. (2022). It is expected that the increased detail (e.g. in terms of side channels, the presence of local bed features, and a limited distance between the weirs) has led to a different simulation outcome than what would be expected based on theory.

Another aspect on which the findings of this study differ from the findings Duró et al. (2022) is the time required to get to a dynamic equilibrium. While for most scenarios in this study an equilibrium is reached after approximately 20 years (with an exception for deposition peaks), it was expected by Duró et al. (2022) that an equilibrium would form only after 100-200 years. It is possible that the model that was used simulates too much sediment transport, which would seem a valid explanation taking into account that higher sediment transport decreases the time that is required to get an equilibrium (see e.g. Figure 5.8 and Figure 5.9). The hypothesis of sediment transport overestimation is also supported by the fact that erosion and deposition waves propagate with a velocity of several hundred metres per year in the model, while it was predicted by Duró et al. (2022) that propagation of bed forms through the river would occur with a velocity of less than hundred metres per year.

6.3. Expectations for climate other rivers and climate change

Based on the findings of this study, estimates for the effect of alternative weir policies can be made for other rivers, and for the effect of climate change on the morphology of the Vecht.

6.3.1. Applicability of results to other rivers

Firstly, it is expected that similar behaviour of bed level changes around weirs occurs in other river systems with weirs, since it was also found in literature that deposition occurs upstream of a flow obstruction, while erosion occurs downstream of the obstruction (Zhang et al., 2008; Ohmoto & Une, 2018). Local erosion in the form of an erosion pit is observed directly downstream of the weir, and on the large scale also erosion is found downstream of the weir. The latter can be explained by the fact that much of the sediment that was carried by the flow has deposited upstream of the obstruction, so much of the sediment transport capacity of the flow can be occupied by newly eroded sediment downstream of the obstruction. The pattern of reduced deposition upstream of the weir, as well as decreased erosion downstream of the weir, can be expected based on this theory if the obstruction decreases. In this case, the decrease of an obstruction means that the weir is opened more frequently, for lower flows, which means that overall the flow past the weir increases.

Besides the patterns of bed level changes around weirs, also the propagation of deposition or erosion waves is expected to show similar behaviour in other river systems. In theory the weir forms less of an obstruction for the flow and for sediment if it is opened at a lower discharge threshold. Therefore, sediment can pass the weir and the erosion or deposition wave can propagate downstream. However, this is only the case for suspended sediment. In case bed load is the dominant sediment load type, the sediment will still be blocked by the weir at the bottom of the channel (depending on the minimum crest level of the weir) and erosion or deposition waves will not propagate downstream of the weir.

6.3.2. Expectations for climate change

For climate change it is expected that discharge peaks will increase in magnitude and frequency, while periods of drought will increase in length and frequency (KNMI, 2021). If this happens, the consequence for sediment transport will be that the (total) amount of sediment that is transported during high flows will increase. Overall this can lead to sudden large changes in the bed, such as cut-offs at meanders where only a small obstruction separates the flow from the old main channel (for example at the Grensmeander or the meander near Karshoek-Stegeren), or increased deposition in the main channel after which more water flows through the side channels (as observed at Mariënberg).

Smaller changes that can be expected are magnified patterns of deposition or erosion during peak discharges, which can be explained by the fact that sediment transport is higher during high discharges.

If climate change brings the expected changes in the discharge regime, it is expected that adjustment to one of the weir policies that have been evaluated in this study has a smaller effect on the morphology than what was found in this study. The reason for this is that sediment that is transported during high discharges will contribute more to the total sediment transport load in the river, instead of sediment that is transported during low/medium discharges (which is the case in the current discharge regime). For high discharges the weir gates are fully opened (for all weir policies), meaning that the new weir policy will contribute less to the total sediment transport than it does for the current discharge regime.

7.   Conclusion and recommendations

The aim of this study was to set up and use a reliable and accurate model of the Vecht, in order to formulate an answer to the question: *What is the expected effect of changes in the weir policy on the longitudinal morphology of the Vecht, based on morphological model simulations?* The answer to this question is provided in this chapter, structured in four sections that each answer one of the research (sub-)questions that were formulated at the beginning of the research. Besides the answer to the research questions, also several recommendations are done for further research into the topic.

7.1.   Performance of the updated model

RQ 1: How well does the morphological model of the Vecht perform after it has been adjusted and recalibrated to take into account recent interventions in the Vecht?

During the calibration and validation of the updated model it was found that the model performs well in the simulation of water levels. With a varying bed roughness in the model the simulations show to match observed water levels especially well during medium and low flow, with RMSE scores of less than 10 cm (calibration) and 15 cm (validation) at all measurement locations. However, there are some errors in the simulation of the water levels during high flow. Part of these errors can be explained by the hysteresis effect, although there is also a systematic underestimation of water levels in the downstream river area (+/- 25-30 cm). During the validation of the medium and low flow there was a slight overestimation of the water levels along the entire river, although part of this can be explained by the presence of several meanders in the model schematisation that were not present in reality during the validation period.

The model performs reasonably well in the simulation of bed level changes, with erosion and deposition patterns generally matching the observed bed level changes. However, the RMSE scores of the calibration and validation results are 0.55 m and 0.43 m, which means that the average error in simulated bed levels is quite large. This can be explained by a few specific locations where the measured bed level changes differ largely from the simulated bed level changes. However, for most of these locations many the cause of these differences can be explained by the model schematisation and bed level input, such as the implementation of interventions at a point in time that was different in reality than in the model.

For the reliability of the model it is most of all important that erosion and deposition patterns match, which after visual inspection of the simulation results showed to be the case along the largest part of the river. Based on the above, it was therefore concluded that the model performs well enough to have reliable morphological simulation results for the analysis done for research questions two and three, with the knowledge that for some locations the simulated bed levels might be a little off.

7.2.   Expected morphology with the current weir policy

RQ2: What is the expected short- and long-term morphology of the Vecht, taking recent interventions in the Vecht into account?

Several patterns along the river are observed in the bed level change that occurs over a period of 50 years. Initial changes that were found in the model appeared mostly at locations where there were anomalies in the model, such as at erosion pits or sudden bed level increases that were already in the model at the start of the simulation. Surrounding the weirs also strong initial changes were observed, but they diffused over time to a smaller magnitude. These changes around the weirs consist of the formation of upstream local deposition peaks and downstream local erosion pits, and on the large scale also erosion was observed downstream of the weirs.

Apart from the patterns around the weirs several long term changes were observed in the form of erosion and deposition waves that slowly propagate downstream. However, when they reached a weir this propagation was limited and the magnitude of the waves was smaller downstream of the weirs. Over time, the waves diffused and a dynamic equilibrium was reached after approximately 20 years (excluding locations with a deposition peak, where bed levels kept increasing). This is much quicker than what was expected in literature, and could be the effect of an overestimation of sediment transport in the model. While the bed level at deposition peaks did not reach an equilibrium during the simulated period, the velocity with which the peaks increased reduced over time.

7.3. Expected morphology with alternative weir policies

RQ3: What is the expected short- and long-term morphology of the Vecht, taking both recent interventions and various scenarios for changes in the weir policy into account?

The alternative weir policies that were evaluated consisted of three alternatives, being (1) opening all weir gates at a discharge of 50 m^3/s (measured at Ommen), (2) opening all weir gates at a discharge of 30 m^3/s (measured at Ommen), and (3) always having all weir gates fully open.

With the implementation of the alternative weir policies, simulated bed level changes showed similar patterns of erosion and deposition around the weirs, compared to bed level changes simulated with the current weir policy (i.e. the reference scenario). However, the magnitude of local deposition upstream and local erosion downstream of the weirs decreased. The large scale erosion that was initially observed downstream of the weirs in the reference scenario decreased. Also similar to what was observed with the current weir policy, are erosion and deposition waves that occurred, which propagated downstream through the river. Contrary to the reference scenario, where the propagation of these waves was mostly blocked by the weirs, the bed levels simulated with the alternative weir policies showed a propagation of the waves past the weirs. The propagation velocity of the waves was few hundred metres per year, which is faster than what has been predicted by literature. Eventually through time the waves diffused and eroded areas eventually got an increased bed level compared to the start of the simulation.

Based on the model results, the large-scale difference between bed levels simulated with the current weir policy and bed levels simulated with the alternative weir policies can be categorised into a decrease in deposition upstream of weir De Haandrik, and an increase in deposition between weir De Haandrik and downstream of weir Junne. The differences are largest for the weir policy that has all weirs fully opened at all times, while the differences are smallest for the weir policy that opens the weir gates at a discharge of 50 m^3/s at Ommen. The latter is the weir policy that is closest to the current weir policy that is maintained in the Vecht. However, the findings contradict the study of Duró et al. (2022), where large-scale erosion was expected throughout the entire channel. Although part of the differences between the findings of both studies can likely be explained by a different complexity of the analysed river system, further research is required to make sure what causes the opposite response of the system to the increased opening frequency of the weirs, and which response can actually be expected in the Vecht.

7.4. Effect of changes in the weir policy on the morphology of the Vecht

In conclusion, the findings of this study lead to the following description of the morphological effect of changes in the weir policy. Opening the weirs for a lower discharge increases the flow through the river, thereby decreasing both local and large-scale deposition upstream of weirs, decreasing local erosion downstream of weirs, and increasing large-scale deposition downstream of weirs. Based on the simulation results of this study it appears that the weir sections in the Vecht are too short for the

large-scale patterns to fully develop both up- and downstream of the weirs, with increased deposition downstream of the weirs being the dominant pattern throughout the entire weir section. However, there is some uncertainty in the reliability of the large-scale findings. Another effect of the opening of the weirs at lower discharges, is that erosion or deposition waves that can be caused by the implementation of interventions in the river propagate downstream more easily.

Increased morphological activity in the form of visible processes of erosion and sedimentation is desired in the Vecht. This study has shown that flow velocities throughout the river can be increased by opening the weir gates more frequently, especially locally upstream of the weirs, which increases the sediment transport (capacity) in the river. This is for example visible in the propagation of erosion and deposition waves. In that sense the morphological activity in the river will increase by implementation of a discharge controlled weir policy, although the large-scale effect on the bed cannot be predicted with full certainty based on this study. The reason for this is that differences between the findings of this study and findings of other studies partially contradict each other, and a clear explanation about the reason for this difference could not be provided.

7.5. Recommendations

Based on this study, two recommendations are done for further research. Firstly, it is suggested to look into the contradiction between the findings of the study of Duró et al. (2022) and the findings of this study. Although it is expected that the reason for the differences is related to the complexity of the system and a potential overestimation of sediment transport in the model that was used for this study, it would be good to substantiate these expectations before making a recommendation with regards to the implementation of a discharge controlled weir policy in the Vecht.

Secondly it is advised to study the effect of climate change on the Vecht. The reason for this is that a change in the discharge regime is expected to impact the effect of the weirs on the morphology of the Vecht. Several changes in the bed that were found in this study as an effect of the implementation of a discharge controlled weir policy could also occur as a result of climate change, while the effects that can be expected by implementing a discharge controlled weir policy might actually reduce due to climate change.

References

Bijlsma, A. (2022). *Debietmetingen Overijselse vecht.* Aquavision.

Bijzitter, W. (2019, October 29). De stuw en brug over de Vecht bij Junne in vogelvlucht. De Stentor, https://www.destentor.nl/ommen/omwonenden-stuw-junne-verbaasd-door-aangekondigde-snoeiwerkzaamheden~ae6a8e7d/.

Candel, J., Berg, M., Schollema, P., Toorn, L. V., & Ruijtenberg, R. (2020). Kort door de bocht - Geulpatronen van beken en de implicaties voor beekherstel. *Stromingen*, 5-18.

Deltares. (2019a). *D-Real Time Control User Manual.* Delft: Deltares.

Deltares. (2019b). *SOBEK 3, D-Flow 1D User Manual.* Delft: Deltares.

Deltares. (2019c). *D-Morphology, 1D/2D/3D User Manual.* Delft: Deltares.

Duró, G., Gradussen, S., & Schippers, M. (2022). *Morfodynamiek Overijsselse Vecht, eindrapportage.* Deventer: Witteveen+Bos.

Fonstad, M. (2006). Cellular automata as analysis and synthesis engines at the geomorphology-ecology interface. *Geomorphology*, 217-234, doi:10.1016/j.geomorph.2006.01.006.

Gradussen, S., & Blom, A. (2020). Synthetic discharge time series for river models. NCR.

Kitsikoudis, V., & Huthoff, F. (2021). *River Flow Processes, Lecture Notes.* University of Twente.

KNMI (Koninklijk Nederlandsch Meteorologisch Instituut), Ministerie van Infrastructuur en Waterstaat. (2021, October 25). *KNMI Klimaatsignaal '21*. Opgehaald van knmi.nl: https://www.knmi.nl/kennis-en-datacentrum/achtergrond/knmi-klimaatsignaal-21

Kumar, V. (2011). Hysteresis. *In: Singh, V.P., Singh, P., Haritashya, U.K. (eds) Encyclopedia of Snow, Ice and Glaciers. Encyclopedia of Earth Sciences Series*. Springer, Dordrecht. doi:https://doi.org/10.1007/978-90-481-2642-2_252

Lamers, M. (2017). *Analysing the morphological consequences of the preferred design of the Overijsselse Vecht with SOBEK 3.* Enschede: University of Twente.

Mheen, M. v., Keizer, A., & Jong, J. d. (2015). *SOBEK 3-model van de Overijsselse Vecht, Modelbouw, kalibratie en verificatie.* Deltares.

Nguyen, V., Moreno, C., & Lyu, S. (2015). Numerical Simulation of Sediment Transport and Bedmorphology around Gangjeong Weir on Nakdong River. *KSCE Journal of Civil Engineering*, 2291-2297, doi:10.1007/s12205-014-1255-y.

Ni, Y., Cao, Z., Qi, W., Chai, X., & Zhao, A. (2021). Morphodynamic processes in rivers with cascade movable weirs - A case study of the middle Fen River. *Journal of Hydrology*, https://doi.org/10.1016/j.jhydrol.2021.127133.

Ohmoto, T., & Une, H. (2018). Effects of weir with an opening on bed morphology and flow patterns. *International Symposium on Hydraulic Structures* (pp. doi: 10.15142/T3ND24 (978-0-692-13277-7)). Aachen, Germany: Utah State University.

Schmidt, G., & Lips, C. (2017). *Analyse hoogteligging rivierbodem Overijsselse Vecht 2008, 2013 en 2016, mede in het licht van de optie van verruiming van de vaardiepte bovenstrooms Ommen.* Waterschap Vechtstromen.

Spruyt, A. (2021). *Ontwikkeling zesde-generatie model Overijsselse Vechtdelta.* Deltares. Opgeroepen op December 2, 2022

Sumida, H., Muto, Y., & Tamura, T. (2014). IMPAct on bed morphology due to partially removed weir. *19th IAHR-APD Congress* (pp. ISBN 978604821338-1). Hanoi: University of Tokushima.

Tuijnder, A. (2017a). *Memo Morfologische activiteit Vecht Hardenberg-Junne.* Arcadis.

Tuijnder, A. (2017b). *Memo Potentieel voor oeverafzetting Hermeandering Vecht Hardenberg Junne.* Arcadis.

Wang, S., & Wu, W. (2004). River sedimentation and morphology modeling - the state of the art and future development. *Ninth International Symposium on River Sedimentation* (pp. 71-94). Yichang, China: The University of Mississippi.

Waterschap Drents Overijsselse Delta. (n.d.). *Stuw Vechterweer en Vilsteren*. Opgehaald van wdodelta.nl: https://www.wdodelta.nl/stuw-vechterweerd-en-vilsteren

Waterschap Vechtstromen. (2021, November 24). *De sluizen in de Vecht*. Opgehaald van vechtstromen.nl: https://www.vechtstromen.nl/beleven/genieten-water/sluizen-vecht/

Waterschap Vechtstromen. (n.d.). *Vecht*. Opgeroepen op November 28, 2022, van vechtstromen.nl: https://www.vechtstromen.nl/beleven/vecht/

Wikiwand. (n.d.). *Vaarweg.* Opgehaald van wikiwand.com: https://www.wikiwand.com/nl/Vaarweg

Williams, R., Brasington, J., & Hicks, D. (2016). Numerical Modelling of Braided River Morphodynamics: Review and Future Challenges. *Geography Compass*, https://doi.org/10.1111/gec3.12260.

Wolfert, H., & Maas, G. (2007, August). Downstream changes of meandering styles in the lower reaches of the River Vecht, the Netherlands. *Netherlands Journal of Geosciences - Geologie en Mijnbouw*, pp. 257-271. Opgeroepen op December 2, 2022

Wolfert, H., Corporaal, A., Maas, G., Maas, K., Makaske, B., & Termes, P. (2009). *Herstelonderzoek Vecht werkdocument.* Wageningen: Alterra.

Wolfert, H., Corporaal, A., Maas, G., Maas, K., Makaske, B., & Termes, P. (2009). *Toekomst van de Vecht als een halfnatuurlijke laaglandrivier.* Alterra Wageningen.

Wolfert, H., Maas, G., & Dirkx, G. (1996). *Het meandergedrag van de Overijsselse Vecht; historische morfodynamiek en kansrijkdom voor natuurontwikkeling.* Wageningen: DLO-Staring Centrum.

Yang, C., & Huang, C. (2001). Applicability of sediment transport formulas. *International Journal of Sediment Research*, 335-353.

Zhang, H., Kanda, K., Muto, Y., & Nakagawa, H. (2008). Morphological response of river channel due to weir reconstruction. *Fourth International Conference on Scour and Erosion*, (pp. 574-579).

Zhang, H., Muto, Y., Nakagawa, H., & Nakanishi, S. (2012). Weir removal and its influence on hydro-morphological features of upstream channel. *応用力学論文集*, 591-599.

Appendix A. List of abbreviations

This appendix provides an overview of the definition of abbreviations that are used in the report.

ECDF   Empirical Cumulative Distribution Function

NAP   Normaal Amsterdams Peil, reference level for elevation measurements

PID   Proportional-Integrate-Derivative

RMSE   Root Mean Square Error

RTC   Real Time Coupling, module used by SOBEK 3 to update structure positions

WDOD   Waterschap Drents Overijsselse Delta (Waterboard Drents Overijsselse Delta)

WVS   Waterschap Vechtstromen (Waterboard Vechtstromen)

Appendix B. Interventions in the Vecht

Table B.1 and Table B.2 show an overview of the projects that have been done in and along the Vecht since 1998 in the area of respectively WVS and WDOD. The highlighted rows show the projects that have been newly implemented in the model. Figure B.1 shows a map of several of the projects in Table B.1 and Table B.2 (mostly in the area of WVS).

Table B.1. *Projects along the Vecht executed since 1998 in the area of WVS, based on personal communication (Tromp & van der Scheer, personal communication, 2023). Highlighted rows show recent interventions in the model that have been newly implemented in the model*

Finished	Project (translated)	Description of project
1999/2000	Construction Noord- & Zuid-Meene	Emergency retention area (included in SOBEK 3)
2004	Uilenkamp	Digging side channel
2008	Molnmarsch	Digging weir passing side channel next to weir Mariënberg
2008	Brucht	Widened shallow meandering river, 2 bumps
2009	Loozensche Linie	Digging side channel
2010/2017	Vecht parks Hardenberg	Lowering ground level, destoning, canoe ditch, construction fish ladder
2012	Side channel Junne phase 1	Digging weir passing side channel next to weir Junne
2012	Barrier Vecht	Barriers near Ommen South, Stekkenkamp and the Laar brought to higher level
2013	Sluice Hardenberg	Construction sluice around weir
2014/2016	Grensmeander	Side channel, destoning, shallowing, dike replacement
2016	Vecht bank North	Widening northern banks (urban side) and widening beneath the bridge Ommen
2017	Barrier Vecht	Regional barrier brought to higher level
2018	Vecht bank South	Side channel has been realised near camping Koeksebelt
2019	Sluice Junne	Construction sluice around weir
2019	Sluice Mariënberg	Construction sluice around weir
2022	Baalder floodplain	Digging graben, removing sand resisting bank
2022	Elongating side channel Junne	Side channel- has been elongated on upstream side
2022	Karshoek-Stegeren	Elongating side channel, meander, nature friendly banks, destoning
2022	Rhezermaten	Meanders, nature friendly banks, design dimensions Vecht, destoning
2023*	Gramsbergen	Digging side channel De Haandrik, removing sand resisting bank, nature friendly banks, destoning
Unknown	De Haandrik - Vecht	Widening cross section of the crossing with channel Almelo de Haandrik until inlet Zuid-Meene

* Is currently being prepared

Table B.2. *Projects along the Vecht executed since 1998 in the area of WDOD, based on personal communication (Tromp & van der Scheer, personal communication, 2023)*

| Finished	Project (translated)	Description of project
2000	Water supply plan Dalfsen (Emmertochtsloot)	Construction of pools in floodplain from which water can be abstracted in dry periods
2002	Construction settling pool Vilsteren	Construction settling pool at the south side of the Vecht
2006	Destoning river bank Vechterweerd	Destoning southern river bank of summer bed
2007	Construction floodplain Berkum	Construction graben in floodplain and small design measures
2010	Construction natural buffer Agnietenberg	-
2010	Construction side channel Den Doorn	Construction of shallow side channel at Huis Den Doorn
2012	Destoning Varse	Destoning side channel Varse (northern side)
2012	Destoning river banks Vecht	Destoning (complete and partial) of a part of the river banks on this trajectory
2014	Nature friendly river bank Vilsteren-Dalfsen	Destoning of river bank, breaching summer banks, construction of bumps in summer bed
2014	Construction Vecht park Dalfsen	Construction Vecht park with heightening/deepening in floodplain Vecht
2014	Construction waterfront Dalfsen	Dike strengthening at the urban area Dalfsen (northern side Vecht)
2014	Construction Vechtcorridor	-
2015	Construction side channel Vilsteren	Construction blue side channel with inlet
2015	Dike strengthening Hessum	A very small part of the barrier was heightened (until T1250)
2015	Construction green ditch Vechterweerd	Construction of green ditch in southern floodplain weir Vechterweerd
2015	Construction access bridge weir Vechterweerd	The accessway with culvert to the weir complex was replaced by a bridge (flow width ±90 m)
2016	Area development Varse	Digging northern floodplain of the Vecht
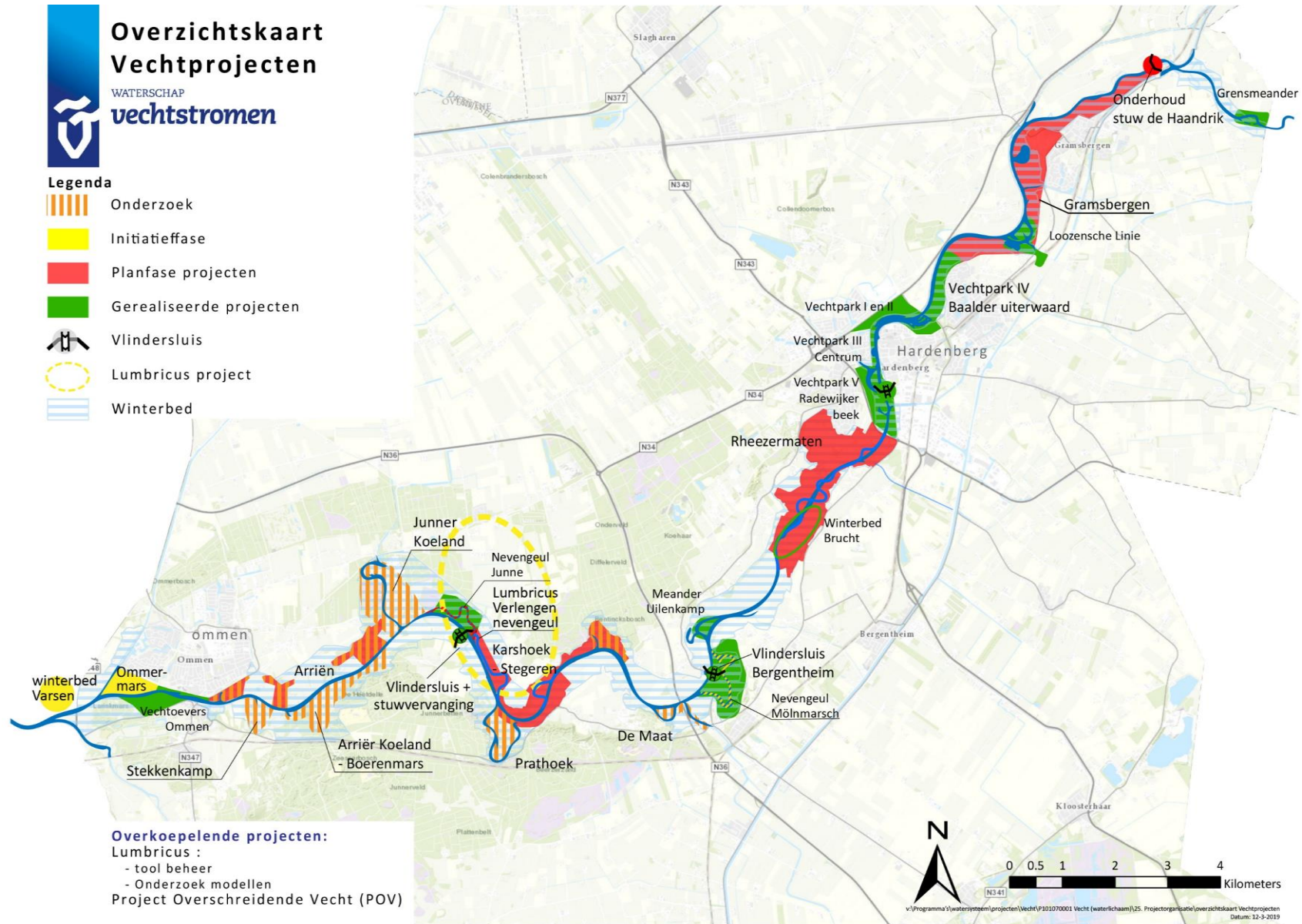
Figure B.1. *Map showing some of the projects along the Vecht in the area of waterboard Vechtstromen (Tromp, personal communication, 2023)*

Appendix C. Formulas for morphological processes

For 1D hydraulic equations, the continuity equation (Equation C.1) and the Saint-Venant equation (Equation C.2) can be used. For morphological calculations such as bed updating and sediment transport, the Exner equation (bed updating, Equation C.3) and the formula of Engelund and Hansen (sediment transport, Equation C.4) can be used.

Continuity equation

$$\frac{\partial A}{\partial t} + \frac{\partial (Av)}{\partial x} = 0$$

Eq. C.1

Where:

A	[m^2]	= wet cross-sectional area
t	[s]	= time
v	[m/s]	= flow velocity
x	[m]	= distance along river axis

Saint-Venant equation

$$\frac{\partial v}{\partial t} + v\frac{\partial v}{\partial x} + g\frac{\partial y}{\partial x} = -\frac{P}{A}\frac{\tau}{\rho}$$

Eq. C.2

Where:

v	[m/s]	= flow velocity
t	[s]	= time
x	[m]	= distance along river axis
g	[m/s^2]	= (9.81) gravitational acceleration
y	[m]	= free surface elevation
P	[m]	= wetted perimeter
A	[m^2]	= wet cross-sectional area
τ	[N/m^2]	= shear stress
ρ	[kg/m^3]	= density of water

Exner

$$(1 - \varepsilon_0)\frac{\partial z_b}{\partial t} + \frac{\partial q_{bk}}{\partial u} \cdot \frac{\partial u}{\partial x} = 0$$

Eq. C.3

Where:

ε_0	[-]	= (0.4) sediment porosity
z_b	[m]	= width-averaged bed level
t	[s]	= time
q_{bk}	[m^2/s]	= width-averaged sediment transport
u	[m/s]	= width-averaged flow velocity
x	[m]	= distance along river axis

Engelund-Hansen (Deltares, 2020)

$$S = \frac{0.05\alpha q^5}{\sqrt{g}\, C^3 \Delta^2 D_{50}}$$

Eq. C.4

Where:

S [-]   = sediment transport rate ($_b$ bedload/$_{s,eq}$ equilibrium suspended sediment)

α [-]   = sediment transport calibration parameter

q [m/s]   = magnitude of flow velocity

g [m/s^2]   = (9.81) gravitational acceleration

C [m$^{1/2}$/s] = Chézy friction coefficient

Δ [-]   = relative density $(\rho_s - \rho_w)/\rho_w$

D_{50} [m]   = median sediment diameter

Appendix D. Set-up of discharge series

D.1.   General approach for generation of discharge series

Not for all lateral inflows of the Vecht reliable and complete discharge measurements are available. Therefore the lateral inflow generator can be used to generate lateral inflow time series for locations for which this is the case. It requires input in the form of an upstream discharge series (at Emlichheim), at least one lateral inflow discharge series (either Ane Gramsbergen or Drentsche Stuw), and the relations between the discharge series used as input and the lateral inflows to be generated. The first two were measurements provided by WVS and the German partners of WVS, the latter was part of the lateral inflow generator provided by Deltares and Van der Scheer (personal communication, March 2023). With the lateral inflow generator timeseries were generated for all lateral inflows described in Section 3.2.1. Only for Ommerkanaal mostly a measured discharge series was used, since there were little gaps in these series that could not be filled with alternative measurements, as described in Section D.2. The gaps that remained in the discharge series were filled by the lateral inflow generator.

D.2.   Filling gaps in the available data

For several periods there are gaps in the measurements of Ane Gramsbergen and Ommerkanaal, which have either been filled by WVS by linear interpolation over the missing period, or they have remained in the data as gaps (see Figure D.2-a and Figure D.3-a). All gaps that were spotted (also the ones filled by interpolation) were filled with measurements from nearby measuring stations, since the discharge at those locations is comparable (see Figure D.1 for the locations of these stations). This was done with measurements from Drentsche Stuw and weir Bisschopshaar, if data from these measurement location was available for such a period.
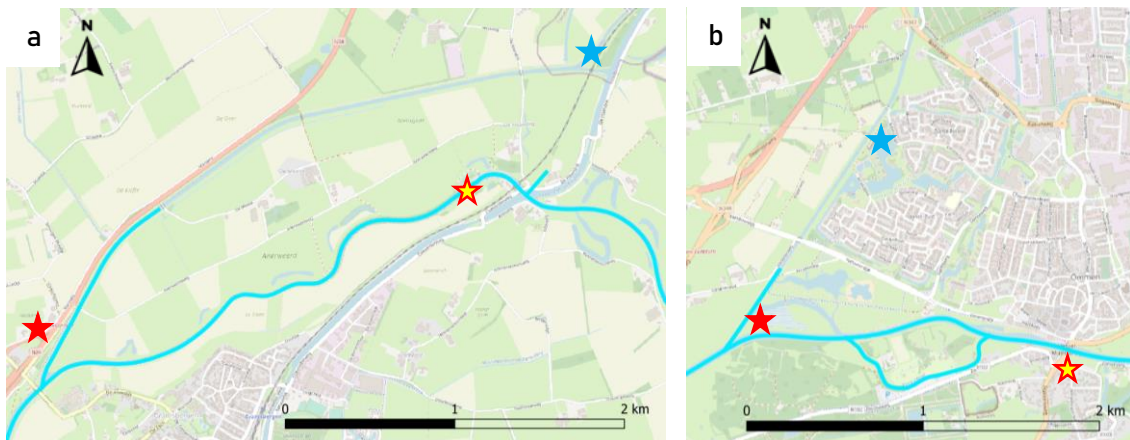

Figure D.1. *Locations of measurement stations (a) near De Haandrik and (b) near Ommen. Red stars are stations (a) Ane Gramsbergen and (b) Ommerkanaal, blue stars are stations (a) Drentsche Stuw and (b) weir Bisschopshaar, yellow centred stars at (a) weir De Haandrik and (b) measurement station Hessel Muelert bridge*

For two periods (January 2016 and July 2016 - September 2017), there were no measurements available for both Ane Gramsbergen and Drentsche Stuw. To fill these gaps the inflow in this period was checked for the upstream boundary (Emlichheim) and a lateral inflow (Ommerkanaal), to see find other measured periods during which the discharge pattern showed behaviour similar to the missing period (see Figure D.4). The discharge measured at Ane Gramsbergen during these other periods was then copied into the gap and connected to the rest of the measurement series (and to each other). When there was a difference of more than 1 m^3/s between the discharge measured at the previous hour and the first hour of the newly copied discharge series linear interpolation over a few hours was used to make this difference more gradual. The resulting time series are shown in Figure D.5.
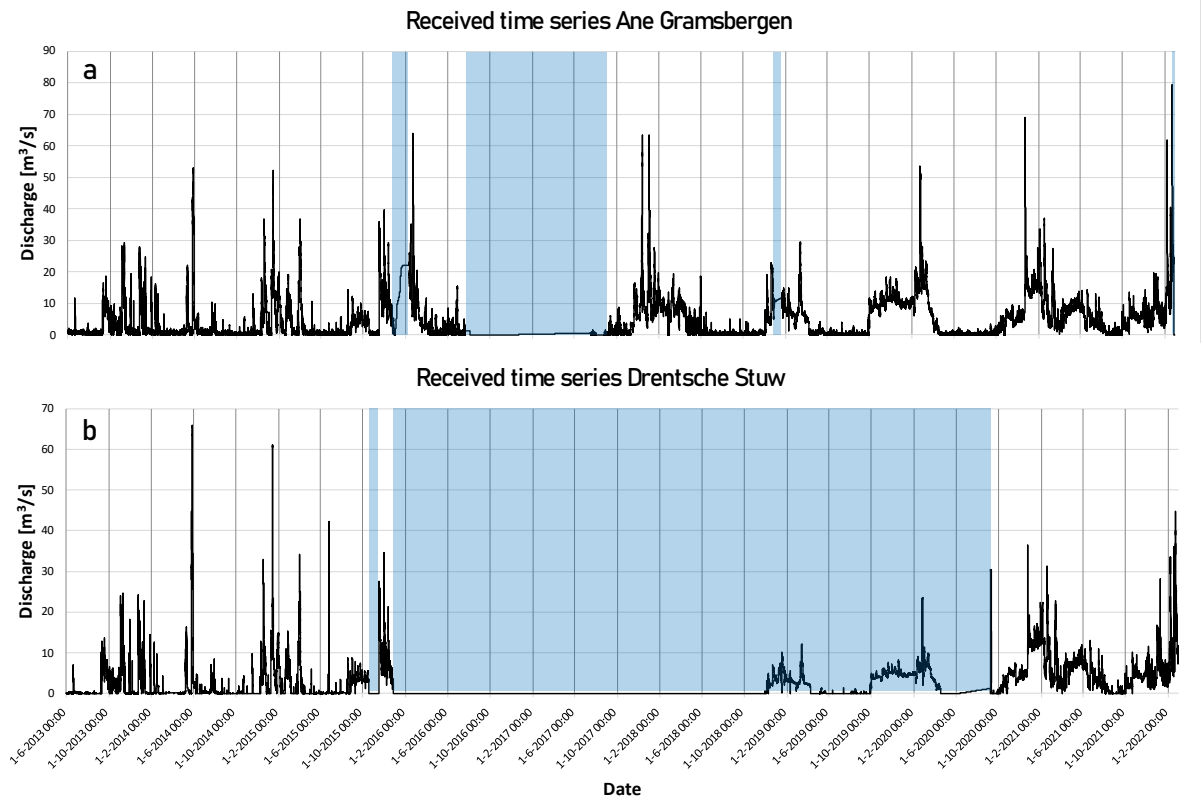
Figure D.2. *Unprocessed discharge series of (a) Ane Gramsbergen and (b) Drentsche Stuw, blue area indicating time periods with wrong measurements or missing data*
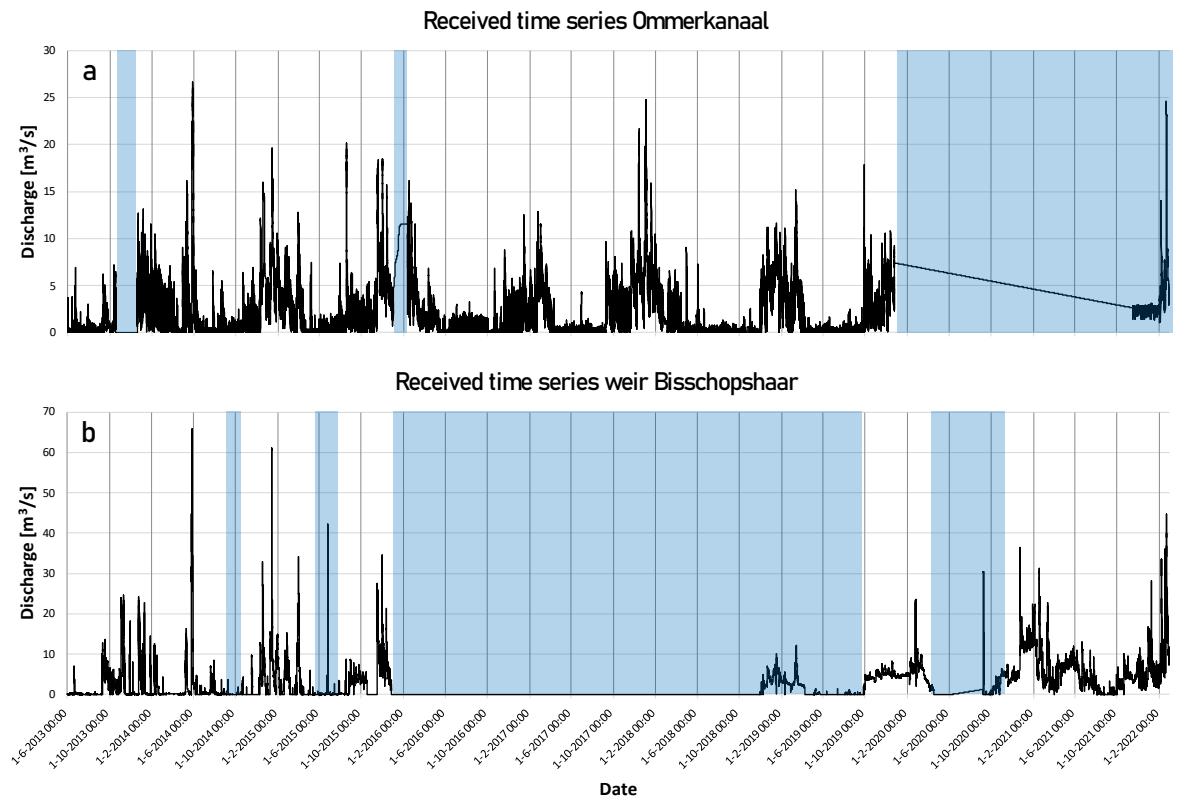

Figure D.3. *Unprocessed discharge series of (a) Ommerkanaal and (b) weir Bisschopshaar, blue area indicating time periods with wrong measurements or missing data*
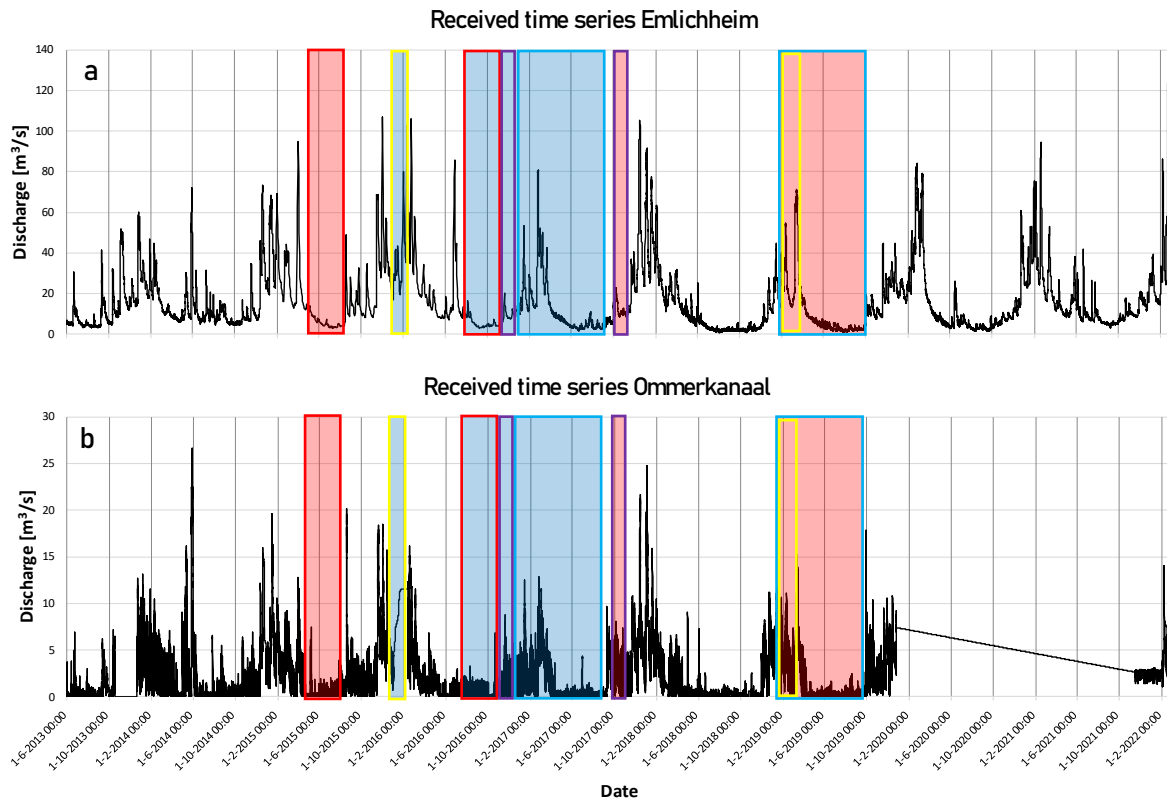
Figure D.4. *Unprocessed discharge time series of (a) Emlichheim and (b) Ommerkanaal, blue areas indicating periods with missing/wrong measurements that could not be replaced with measurements from Drentsche Stuw, red areas indicating periods that show discharge patterns similar to blue areas (outline colour of boxes matching for missing/available periods)*
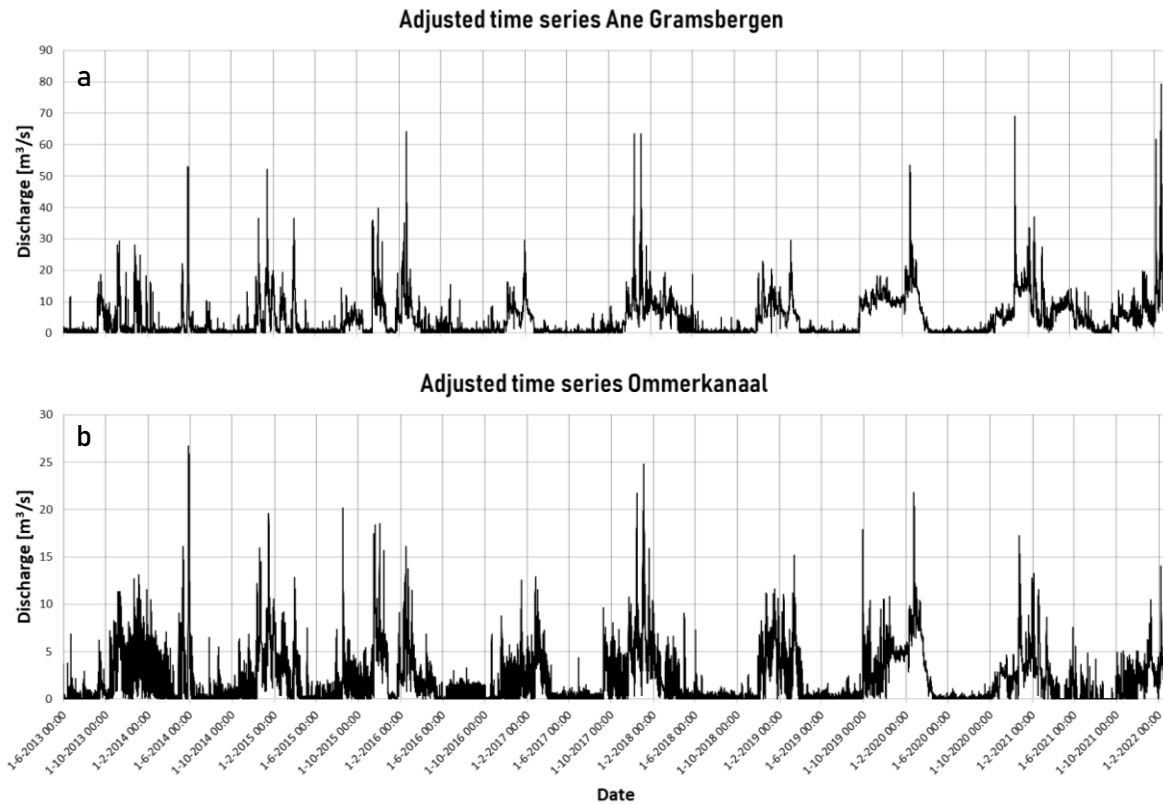

Figure D.5. *Adjusted time series of (a) Ane Gramsbergen and (b) Ommerkanaal*

Appendix E. Discharge series used as input for simulations

Many simulations were done with the model, which were for the hydrodynamic calibration and validation, morphodynamic calibration and validation, and the longer runs. Hydrographs of the discharge series that were used as input for these runs are shown in the sections below.

E.1.   Discharge series used for hydrodynamic calibration and validation
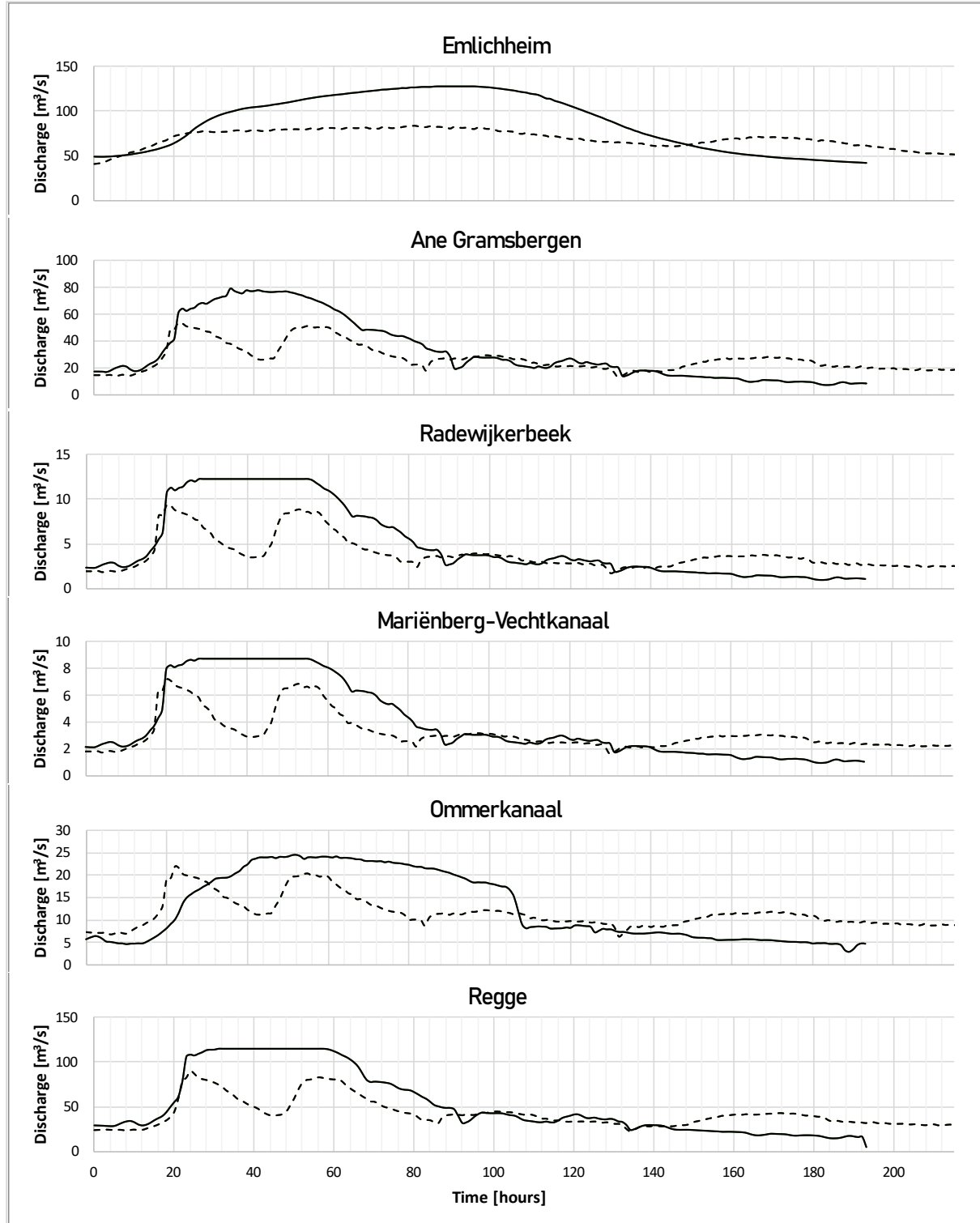

Figure E.1. *Discharge series used for hydrodynamic calibration (solid line) and validation (dashed line) of high flow. Periods of high flow range from 20 Feb. 2022 to 28 Feb. 2022 (calibration) and from 25 Feb. 2020 to 3 Mar. 2020 (validation)*
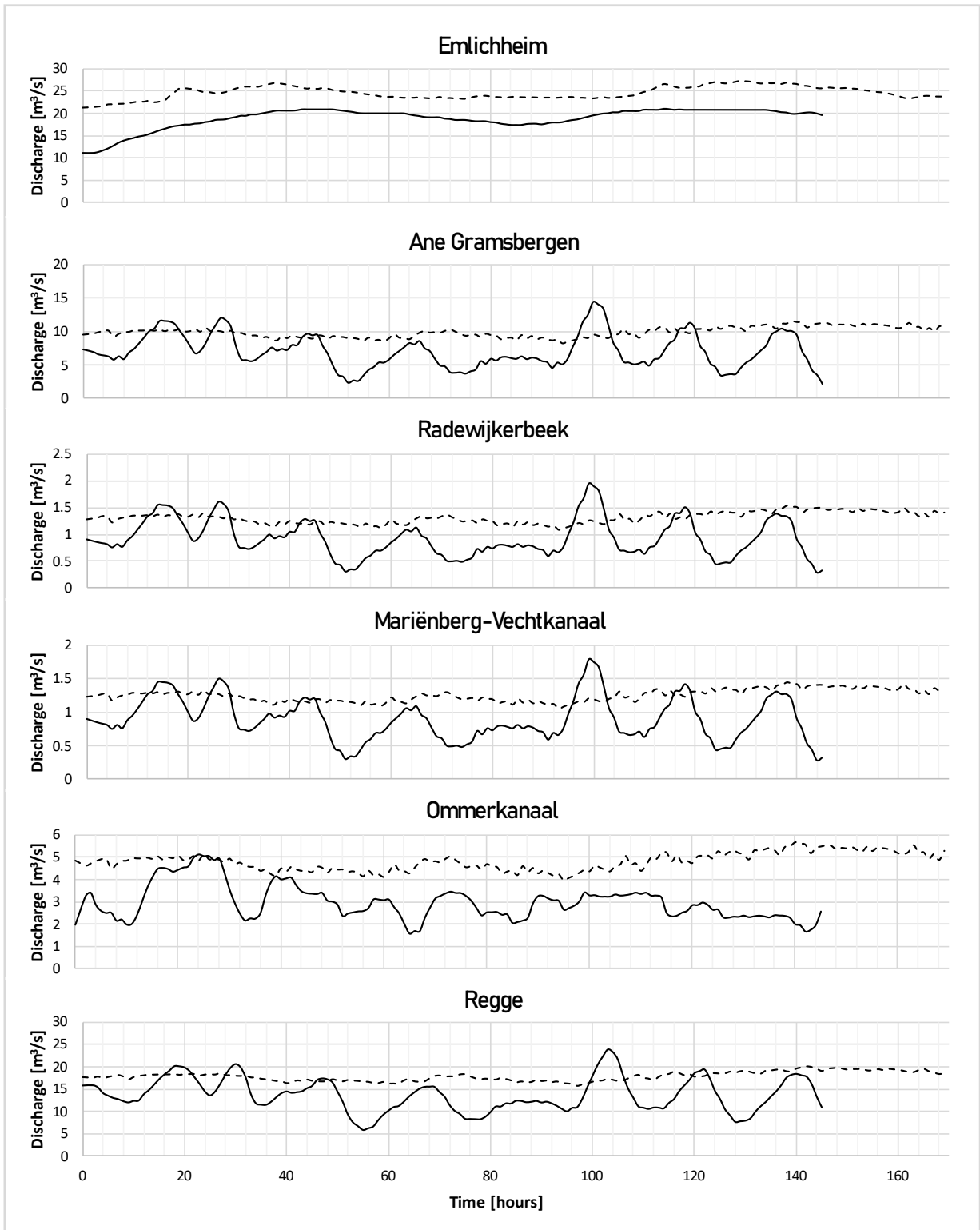
Figure E.2. *Discharge series used for hydrodynamic calibration (solid line) and validation (dashed line) of medium flow. Periods of medium flow range from 1 Dec. 2021 to 7 Dec. 2021 (calibration) and from 10 Jan. 2020 to 17 Jan. 2020 (validation)*
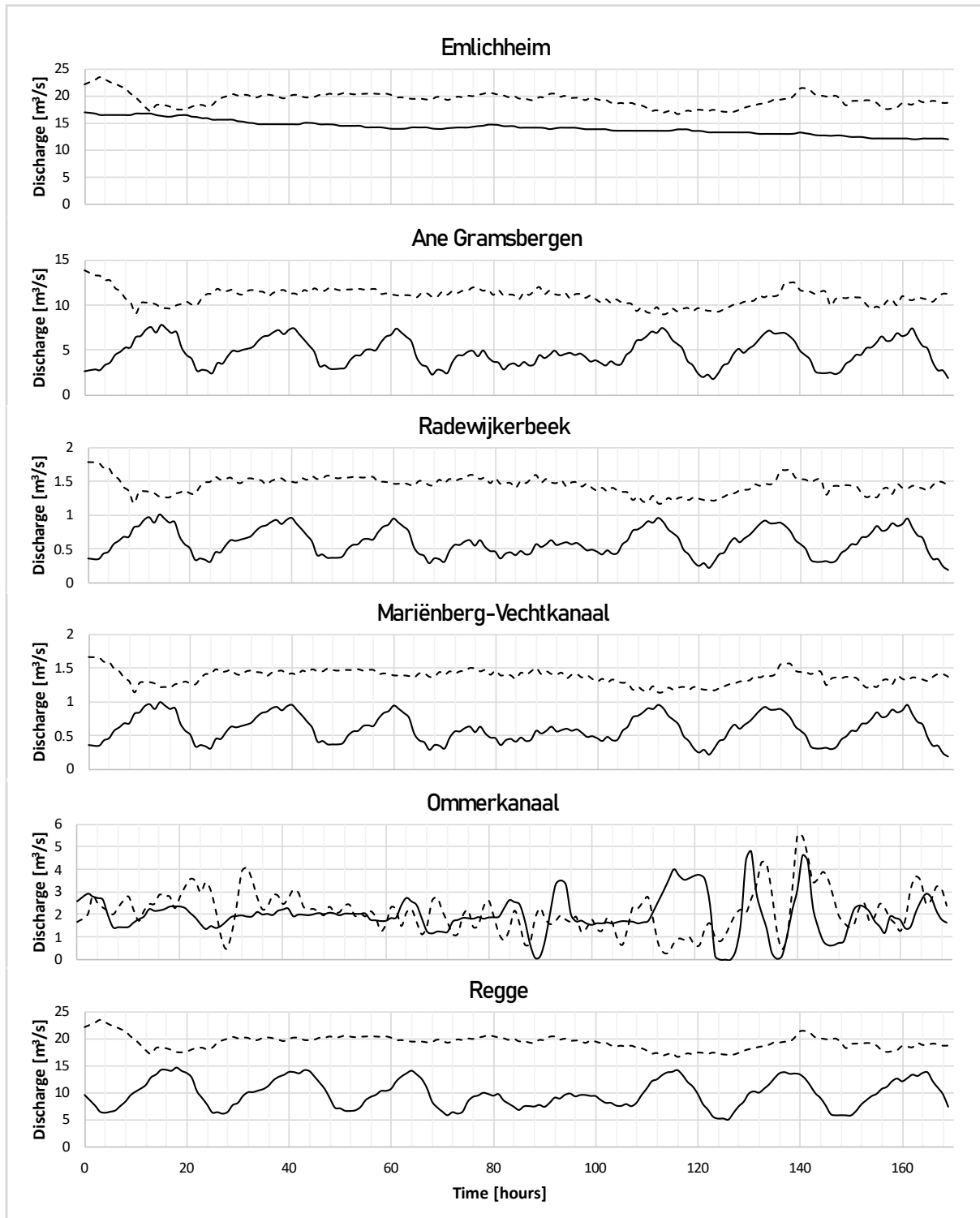
Figure E.3. *Discharge series used for hydrodynamic calibration (solid line) and validation (dashed line) of low flow. Periods of low flow range from 16 Dec. 2021 to 23 Dec. 2021 (calibration) and from 7 Nov. 2019 to 14 Nov. 2019 (validation)*

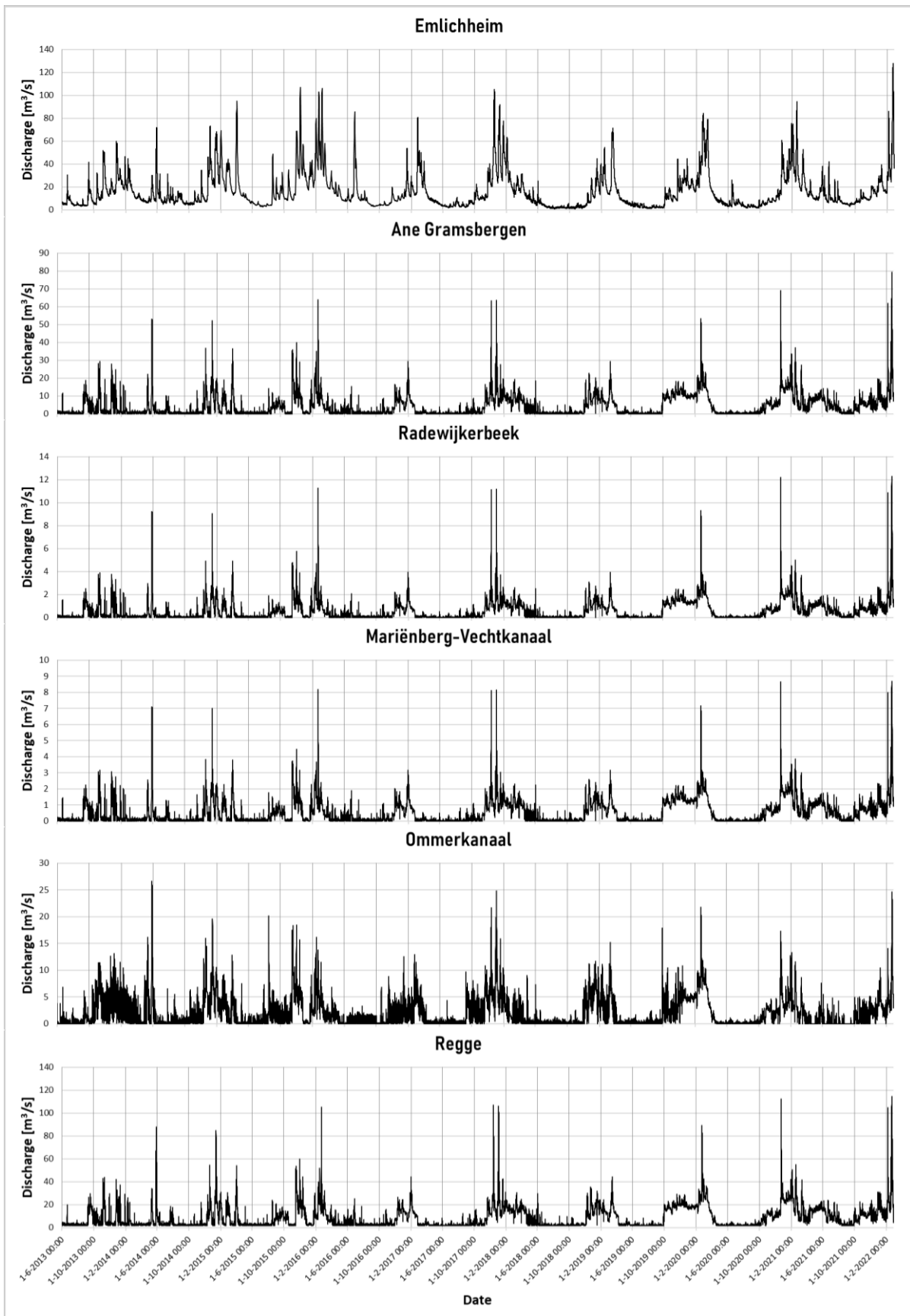## E.2.   Discharge series used for morphodynamic calibration and validation

Figure E.4. *Discharge series used for morphodynamic calibration and validation*

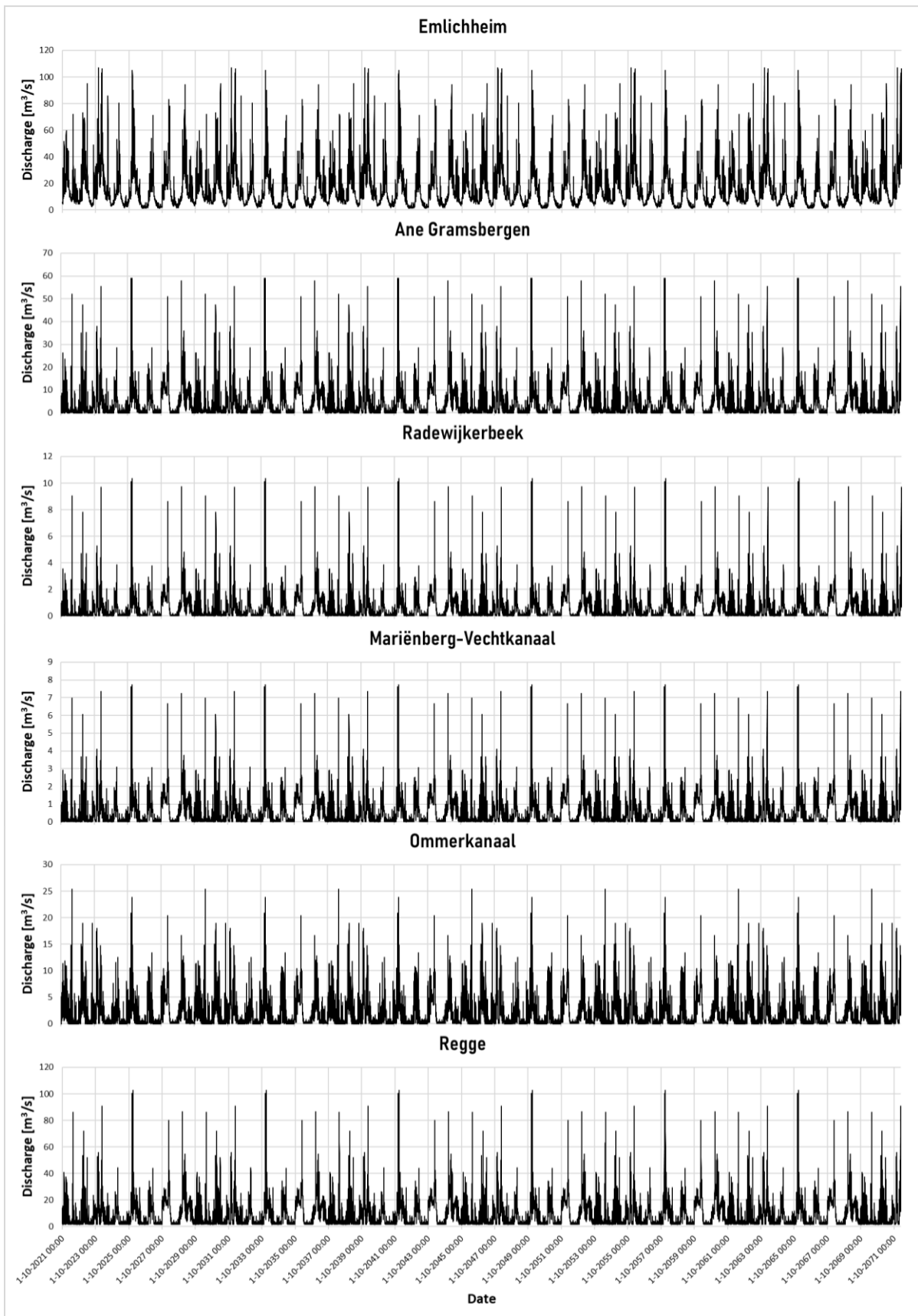## E.3. Discharge series used for 50 year runs

Figure E.5. *Discharge series used for 50-year runs*

Appendix F. Set–up of PID controllers

To maintain a target water level in SOBEK 3, the RTC module can be used to control the crest level of the movable weirs. The RTC module contains several control groups, one per controlled structure, which in general contain a control parameter (e.g. the water level at a certain location), a controlled parameter (e.g. the crest level of a weir), and a specification of a rule (Deltares, 2019a). The morphological model of the Vecht that is used in this study has control groups in which the rule type is a PID rule. A PID rule contains a control loop feedback mechanism to determine the ideal value for the controlled parameter. For this Equation F.1 and F.2 are used, where the different gain factors $(K_{p/i/d})$ can be seen as a sort of tuning parameters.

$$e(t) = x_{sp}(t) - x(t) \qquad \text{Eq. F.1}$$

$$y(t) = K_p e(t) + K_i \int_0^t e(\tau)d\tau + K_d \frac{d}{dt} e(t) \qquad \text{Eq. F.2}$$

Where:

$e(t)$	=	Difference between $x(t)$ and $x_{sp}(t)$
$x(t)$	=	Process variable at time t
$x_{sp}(t)$	=	Setpoint at time t
$y(t)$	=	Controller output at time t
$K_{p/i/d}$	=	Proportional/Integral/Derivate gain factors

Equation F.1 calculates the difference ($e(t)$) between the target value and the observed (simulated) value of a parameter, which is used in Equation F.2 to calculate a value ($y(t)$) for the controlled parameter so that $e(t+1)$ will be smaller than $e(t)$.

The control groups that are used in the model that is used in this study are shown below in Figure F.1 and Figure F.2. Each control group consists of at least one control parameter (green ovals, referred to as *input locations*), at least one controlled parameter (blue ovals, referred to as *output locations*), and at least one rule (orange boxes). The set-up of the water level rule can be seen in Table F.1.

For the implementation of the new weir policies (Q_{30}- and Q_{50}-scenario), several control parameters and a rule were added to the control group. The set-up of the discharge rule can be found in Table F.2. A condition was added to the control groups as well (grey diamonds), of which the set-up is shown in Table F.3. The condition determines whether the discharge rule is followed (if the condition is true) or if the water level rule is followed (if the condition is false). For the implementation of the Q_0-scenario the RTC module was removed from the integrated model, and a fixed crest level was put at the minimum crest level from the reference scenario.
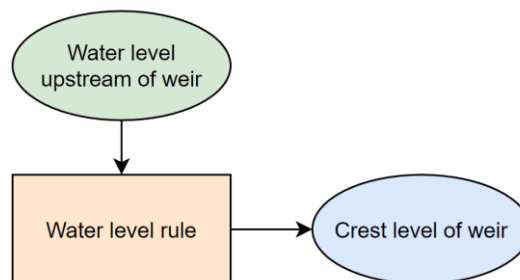

Figure F.1. *Control group set-up for reference scenario and calibration/validation runs*
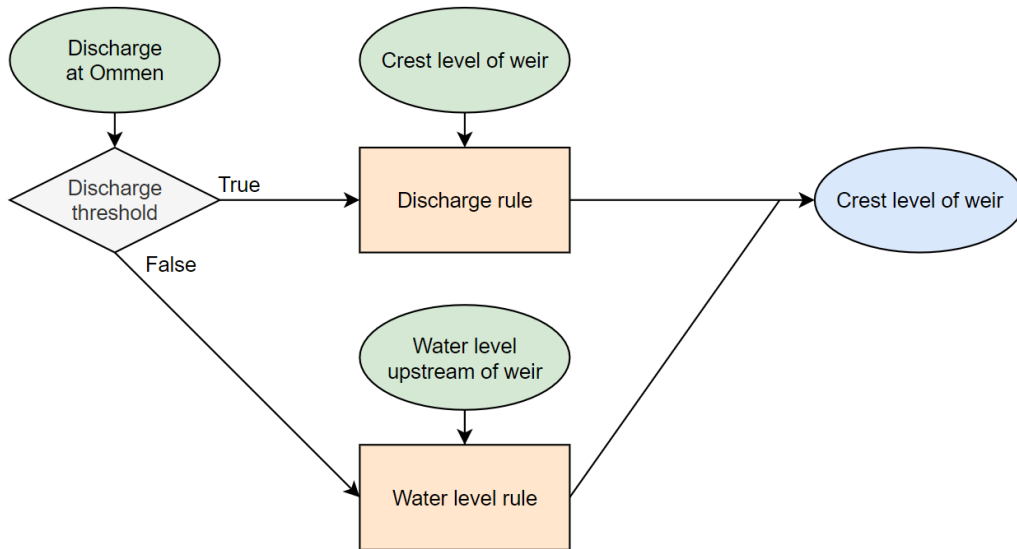
Figure F.2. *Control group set-up for Q_{30} and Q_{50} scenario*

Table F.1. *Set-up water level rule*

Data	
Constant set point	<Target water level [m]>
Setpoint mode	Constant
Gain factor	
K_p	2
K_i	0.001
K_d	-1000
Limits	
Minimum	<Minimum crest level [m]>
Maximum	<Maximum crest level [m]>
Maximum speed	0.005 [m/s]

Table F.2. *Set-up discharge rule*

Data	
Constant set point	<Minimum crest level [m]>
Setpoint mode	Constant
Gain factor	
K_p	2
K_i	0.001
K_d	-1000
Limits	
Minimum	<Minimum crest level [m]>
Maximum	<Maximum crest level [m]>
Maximum speed	0.005 [m/s]

Table F.3. *Set-up discharge threshold*

Input	
Operation	>=
Value	<30 or 50 [m³/s]>

Appendix G. Results of hydrodynamic calibration and validation

Table G.1, G.2, and G.3 show the RMSE values that were calculated for all hydrodynamic calibration runs for all measurement stations with valid measurements. Figure G.1 and G.2 show correlation plots of the final hydrodynamic calibration run (with varying Chézy coefficient) and the hydrodynamic validation run for all flow scenarios, for the measurement stations with valid measurements.

Table G.1. *RMSE scores for different calibration runs for the high flow period, green shades representing low values and red shades representing high values per location*

Measurement station	RMSE for different Chézy friction coefficients [m]												
	28	30	32	34	35	36	38	40	42	44	46	48	Varying
Downstr. De Haandrik	0.48	0.38	0.28	0.20	0.16	0.12	0.07	0.07	0.12	0.18	0.24	0.30	0.13
Downstr. Hardenberg	0.40	0.31	0.22	0.15	0.12	0.10	0.09	0.13	0.19	0.24	0.30	0.35	0.10
Downstr. Mariënberg	0.50	0.40	0.30	0.21	0.17	0.14	0.10	0.12	0.18	0.24	0.30	0.36	0.11
Downstr. Junne	0.58	0.45	0.33	0.22	0.17	0.13	0.06	0.10	0.17	0.24	0.32	0.38	0.29
Hessel Muelert bridge	0.40	0.30	0.21	0.13	0.10	0.07	0.06	0.11	0.16	0.21	0.26	0.31	0.26
Upstr. De Haandrik	0.30	0.24	0.18	0.13	0.10	0.08	0.05	0.05	0.07	0.11	0.14	0.17	0.08
Upstr. Mariënberg	0.46	0.37	0.30	0.23	0.19	0.16	0.11	0.09	0.09	0.12	0.16	0.19	0.09
Upstr. Junne	0.51	0.41	0.31	0.23	0.19	0.15	0.09	0.06	0.10	0.14	0.19	0.23	0.17
Average (excl. upstream weirs)	0.47	0.37	0.27	0.18	0.14	0.11	0.08	0.11	0.16	0.21	0.26	0.34	0.18

Table G.2. *RMSE scores for different calibration runs for the medium flow period, green shades representing low values and red shades representing high values per location*

Measurement station	RMSE for different Chézy friction coefficients [m]												
	28	30	32	34	35	36	38	40	42	44	46	48	Varying
Downstr. De Haandrik	0.19	0.13	0.08	0.04	0.03	0.03	0.05	0.08	0.11	0.14	0.17	0.19	0.03
Downstr. Hardenberg	0.09	0.06	0.04	0.03	0.03	0.03	0.04	0.05	0.06	0.07	0.08	0.09	0.03
Downstr. Mariënberg	0.05	0.03	0.02	0.04	0.05	0.06	0.07	0.09	0.10	0.11	0.12	0.13	0.07
Downstr. Junne	0.36	0.30	0.24	0.19	0.17	0.15	0.11	0.08	0.06	0.06	0.07	0.08	0.06
Hessel Muelert bridge	0.26	0.22	0.19	0.16	0.15	0.14	0.12	0.10	0.09	0.07	0.06	0.05	0.05
Upstr. De Haandrik	0.01	0.01	0.01	0.01	0.01	0.01	0.01	0.01	0.01	0.01	0.01	0.01	0.01
Upstr. Mariënberg	0.02	0.02	0.02	0.02	0.02	0.02	0.02	0.02	0.02	0.02	0.02	0.02	0.02
Upstr. Junne	0.02	0.02	0.02	0.02	0.02	0.02	0.02	0.02	0.02	0.02	0.02	0.02	0.02
Average (excl. upstream weirs)	0.19	0.15	0.12	0.09	0.08	0.08	0.08	0.08	0.08	0.09	0.10	0.11	0.05

Table G.3. *RMSE scores for different calibration runs for the low flow period, green shades representing low values and red shades representing high values per location*

| Measurement station	RMSE for different Chézy friction coefficients [m]												
	28	30	32	34	35	36	38	40	42	44	46	48	Varying
Downstr. De Haandrik	0.11	0.07	0.04	0.04	0.04	0.05	0.07	0.09	0.11	0.13	0.15	0.16	0.05
Downstr. Hardenberg	0.06	0.04	0.03	0.03	0.03	0.03	0.03	0.03	0.04	0.04	0.04	0.05	0.03
Downstr. Mariënberg	0.03	0.03	0.04	0.05	0.06	0.06	0.07	0.08	0.09	0.09	0.10	0.10	0.07
Downstr. Junne	0.30	0.25	0.21	0.17	0.16	0.14	0.12	0.10	0.08	0.07	0.06	0.06	0.06
Hessel Muelert bridge	0.18	0.16	0.14	0.12	0.11	0.11	0.10	0.09	0.08	0.07	0.06	0.06	0.06
Upstr. De Haandrik	0.01	0.01	0.01	0.01	0.01	0.01	0.01	0.01	0.01	0.01	0.01	0.01	0.01
Upstr. Mariënberg	0.02	0.02	0.02	0.02	0.02	0.02	0.02	0.02	0.02	0.02	0.02	0.02	0.02
Upstr. Junne	0.01	0.01	0.01	0.01	0.01	0.01	0.01	0.01	0.01	0.01	0.01	0.01	0.01
Average (excl. upstream weirs)	0.13	0.11	0.09	0.08	0.08	0.08	0.08	0.08	0.08	0.08	0.08	0.08	0.05
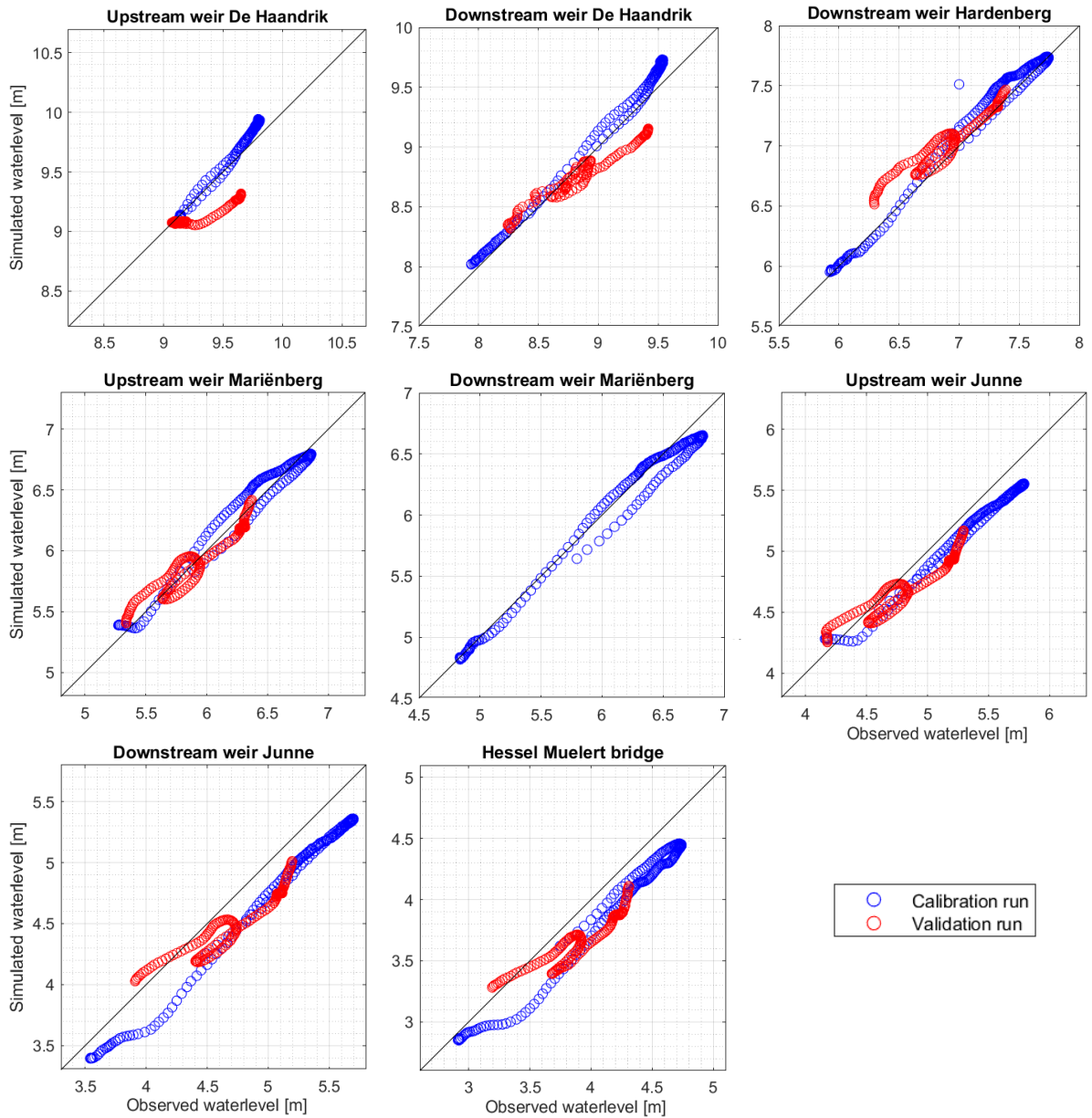
Figure G.1. *Observed vs. simulated water levels for calibration and validation of high flow, diagonal black line representing perfect fit*
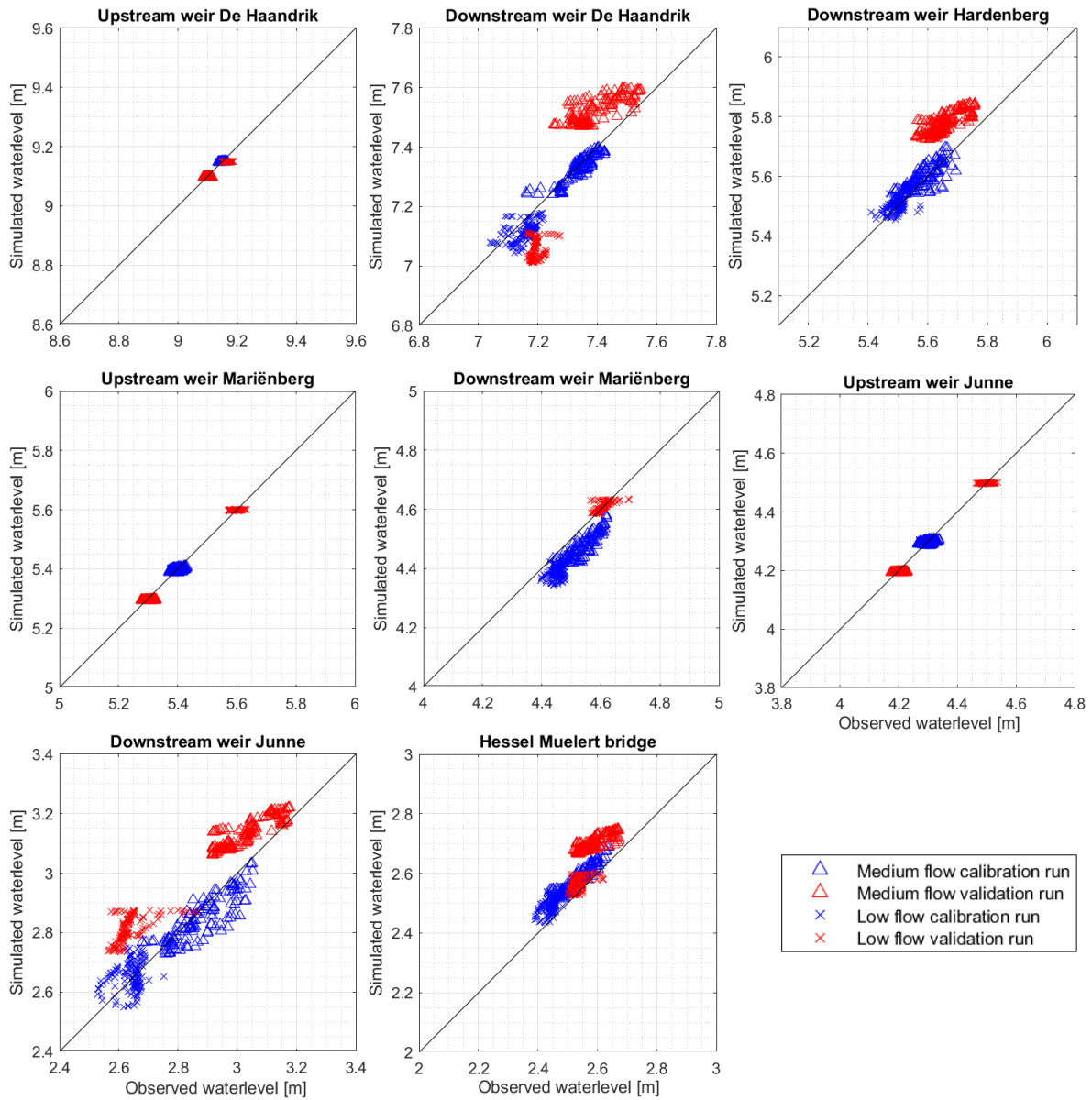
Figure G.2. *Observed vs. simulated water levels for calibration and validation of medium and low flow, diagonal black line representing perfect fit*